A STUDY OF BOX GIRDER BEHAVIOUR BASED ON EXTENSIONAL AND BENDING PLATE THEORIES

A thesis presented for the degree of

Ph.D (Engineering) in

the University of Lagos

by

O. A. SOMOLU, B.Sc. (Eng.)

Faculty of Engineering,
University of Lagos,
Lagos.

November, 1976.

A STUDY OF BOX GIRDER BEHAVIOUR BASED ON EXTENSIONAL AND BENDING PLATE THEORIES

A STUDY OF BOX GIRDER BEHAVIOUR BASED ON EXTENSIONAL AND BENDING PLATE THEORIES

ABSTRACT:

The thesis deals with the study of box girder behaviour under load and examines the deflexion and membrane stresses which arise as a consequence of loading. An extensive survey of the existing methods of analyses is carried out and two of them are outlined.

A composite concrete - steel box girder was used for the laboratory investigation.

A method of deriving the equation for transverse deflexion of a plate with its edges supported in any manner is outlined. This method does not seem to have been previously recorded in any text on plate bending theory.

The analysis of a closed trapezoidal (cross-section) box girder, employing both membrane and plate bending theories is then fully discussed. A computer programme is used to solve the resulting system of equations and the results obtained finally seem to agree with physical conjecture. Effective width factors obtained from the analysis are compared with existing recommendations for box girder bridges. The validity or otherwise of using effective width concept for the design of box girders is also discussed in the light of theoretical results. An in-depth study of the effect of side inclination of the box section is undertaken.

ACKNOWLEDGEMENTS

The work described in this thesis was carried out in the Civil Engineering Department of the University of Lagos. The author wishes to record her deep appreciation to her supervisor, Professor A.O. ADEKOLA, to whom the author is greatly indebted for his constant encouragement and interest throughout the project. His useful suggestions in respect of both the experimental and theoretical parts of the project are also acknowledged.

The experimental work, which was conducted in the Structural Engineering Laboratory, would not have been possible without the assistance of the Laboratory Staff and in particular Mr. S.O. ADEYEMI. Their help is gratefully acknowledged.

The author is also deeply grateful to Dr. K.A. ADEROGBA for his constant advice and valuable suggestions as the work progressed.

Finally, the author thanks the University of Lagos for the post-graduate studentship that supported her during the course of this work and all those who helped in typing the manuscript, tracing the drawings and in binding the thesis.

CHAPTER I

INTRODUCTION

1-1 General Introduction and History of Box Girders

The analysis of thin-walled boxes subjected to the action of applied loads is important in the design and construction of such structural members as aircraft wing sections, deep-sea vessel compartments, box girders used in bridges, modern cargo containers, and various other types of structural boxes which are subjected to either internal or external loads.

One of the first recorded attempts on the application of box girder configuration to bridges is the construction of the Brittania and Conway tubular bridges around 1849. This application posed some rather unusual problems and prompted extensive research, particularly with respect to the buckling of thin plates subjected to combined shear and bending moment.

In the wake of the large scale destruction of bridges in World War II, bridge building experienced a renaissance in post-war Europe. Many of the new bridges were of steel box girder construction. In recent years this form of bridge construction, either in steel or in concrete as pre-stressed beams, has gained popularity all over the world.

The cross-section of a box girder bridge may be of a variety of shapes (Fig. 1-1). It may consist of a single-cell, two separate but interconnected cells each supporting a roadway, multiple cells, or two deep inter-connected plate girders. These are only a few of the many

possible configurations which can be, and have been, used.

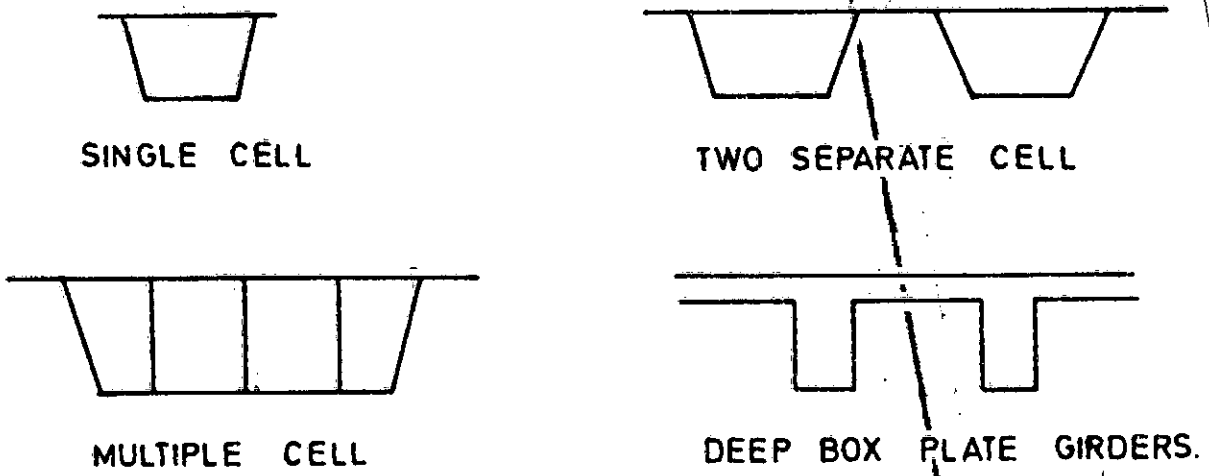

FIG 1-1

Box girder construction lends itself to various forms of prefabrication. In steel, large sections are rivetted or welded on a shop floor before transportation and assembly on site, thereby reducing the amount of in-situ welding or rivetting. In concrete, short lengths of the box section are cast in a yard and transported to construction site where they are assembled, joined and made monolithic by pre-stressing, again reducing the amount of in-situ concreting.

The deck of the box girders may be concrete as in a concrete box girder section or as a concrete element acting compositely with the thin steel plated box section, or it may be an orthotropic steel deck. In most cases, steel box girders are fabricated by welding from relatively thin plates, and details include stiffeners of a variety of shapes to

minimise the risk of buckling of the thin plates when the structure is subjected to normal loading.

An advantage of the box girder construction besides any structural merit is the fact that the space within the section (i.e. space within the box or boxes) can and is often used to accommodate various services.

1-2 Previous Methods of Analysis:

The types of loading encountered in box girder bridges can generally be represented as shown below:

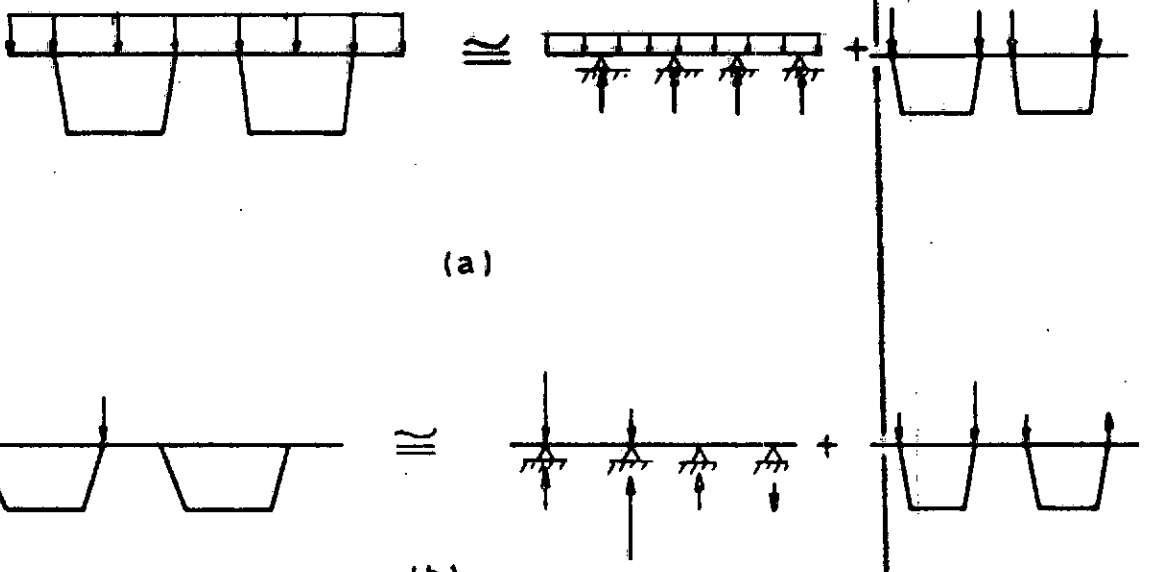

FIG 1-2

Fig. (1-2) (a) represents distributed load such as the dead load of the deck.

Fig. (1-2) (b) consists of localised forces such as vehicle wheel loads.

A general loading as shown below has components which bend, twist and deform the cross-section.

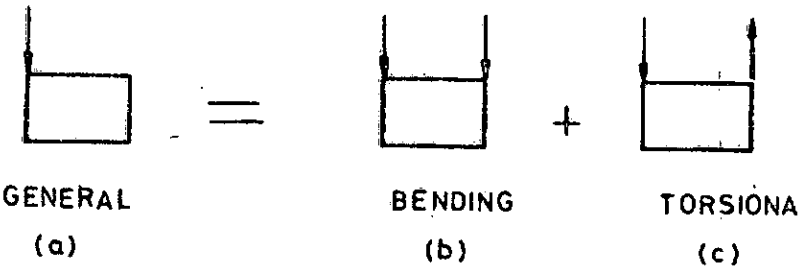

FIG 1-3

Thin-walled closed section girders are so stiff and strong in torsion that the torsional component of loading (in Fig. 1-3) might be assumed to have negligible effect on box girder response i.e. that the section will twist very little and deflect nearly uniformly vertically.

Now if the torsional component of the loading is applied as shears on the plate elements the section is twisted without deformation of the cross-section (Fig. 1-4) (b)

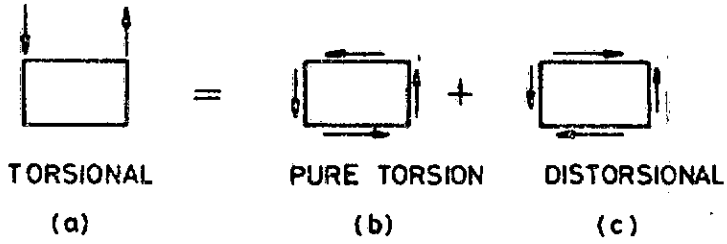

FIG 1-4

The resulting longitudinal warping stresses are small and no transverse flexural stresses are induced. But if the torsional loading is applied as shown in Fig. (1-4) (a) then there exist forces which also tend to deform the cross-section.

The subdivision of box girder response into deck plate action and girder action as well as the subdivision of the latter into flexural, torsional and distortional response is vital for a designer who must understand the behaviour of the structure that he is trying to create and utilize.

However, modern analytic methods do permit direct analysis of the total response for any arbitrary distribution of loading and can be valuable in checking a nearly completed design.

1-3 A Review of Analytical Tools Used in Solving Box Girder Problems:

The "Finite Element" method of analysis permits consideration of very realistic models of box girders; that is, it permits the treatment of arbitrary loading, end support conditions and flexible interior diaphragms. This great advantage in flexibility of application is achieved at the cost of substantial computing time on a very large computer, in view of the large sizes of the matrices resulting from the subdivision of the box girder into small elements.

A large number of analytic procedures for box girders are based on thin-walled beam theory. The "Plate Element" method of analysis and the "Generalised Coordinate" methods are refined analysis which have been developed, following basic concepts of thin-walled beam behaviour (4).

The major assumptions of the theory are that plate shears and moments in the longitudinal direction can be neglected and that longitudinal stresses vary linearly between joints of the cross-section.

Goldberg and Leve formulated a theory[14], presented later in this thesis, which considers the box girder configuration as an assemblage of plates. It is an 'exact' solution but is limited in its applicability to straight, prismatic box girders composed of isotropic plate elements with no interior diaphragms but with simple end support conditions, i.e. there is no deformation of the cross-section and no axial stresses at the ends.

Goldberg's formulation for folded plates considers the simultaneous plate bending and membrane actions of several plates joined together to form a folded plate system. The forces at the longitudinal edges of each plate are expressed as fixed-edge forces corrected or modified by the effect of displacement of the joints.

Scordelis, Johnston and Mattock have applied this theory to the analysis of box girder bridges. The inability of this analysis to account for effects of interior diaphragms and anisotropic plate elements such as transversely stiffened web plates limits its application to steel box girder but the theory may be found valuable for assessing the accuracy of more flexible but exact analyses.

Lacher applied thin-walled beam theory to box girders with flexible or rigid interior diaphragms. The solution is limited to simple support conditions. Scordelis and Lo used thin-walled beam theory to develop a finite segment analysis for isotropic plate elements and a use of transfer matrix solution that can treat flexible interior

diaphragms and continuous girders.

A number of investigators have considered analysis of box girders as orthotropic plates. Massonet and Gandolfi explored this formulation for box girders with contiguous cells and no interior diaphragms and reported that an orthotropic plate theory accounting for shearing deformation is required to account for deformation of the cross-section.

If a box girder is subjected to fixed loads, diaphragms or cross frames can be provided at all sections of load application. Deformation of the cross-section is thereby reduced to a negligible amount and the distortional component of load need be considered only in design of the diaphragms.

Although not directly relevant to the formulation presented in this work, mention must be made of the 'Beam on Elastic foundation Analysis of Box Girders' by R. Robinson et al[1]. The remarks which preceed the analysis can be summarised as follows:

Analytical studies have shown that a box girder subjected to transversely non-uniform loading undergoes deformation of the cross-section. This behaviour usually gives rise to non-uniform warping and hence to longitudinal stresses as well as deformation of the cross-section which in turn gives rise to transverse flexural stresses. These stresses tend to reduce the advantages anticipated from the high torsional stiffness of the box girder.

The authors made an attempt to present a simplified analytical procedure for box girders that accounts for the important characteristics of their behaviour. Their formulation resulted in a governing equation for transverse deflexion, using some empirical relations obtained from the AISC manual, and it was argued that this formulation was analogous to the beam on elastic foundation theory. According to the authors the BEF analogy provides an analytical procedure which accounts for deformation of the cross-section, for the effects of rigid or deformable interior diaphragms, longitudinally and transversely stiffened plate elements, non-prismatic section, continuity over intermediate supports, and for arbitrary end support conditions.

The authors' procedure however, suffers the limitation that it is not easily understood as to be applied by non-specialists and does not make apparent the interaction between bending and membrane theories of classical elasticity in the solution of this class of problems. A brief outline of the analogy is now presented.

BEF Analogy:

When a box girder has a torsional load acting on it, deformation of the cross-section occurs and this produces motions in the plane of the cross-section (see Fig. 1-5)..

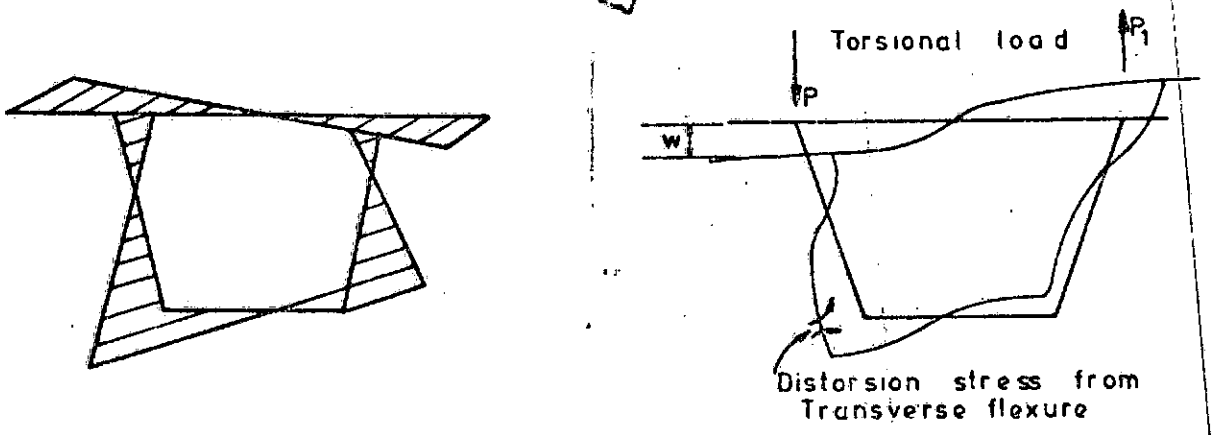

(b) WARPING STRESS PATTERN (a) DEFORMATION OF CROSS SECTION

FIG 1-5

To develop an approximate theory of the deformation of the cross-section the authors borrowed one basic assumption regarding this in plane motion from the theory of thin-walled beams of open section. It is assumed that the distortions are accompanied by sufficient warping to annul the average shear strains in the plates which form the cross-section.

In general, the warping displacements are not constant along the axis of the box cell. Longitudinal stresses arise from constraint of warping. If, in turn, these warping stresses vary along the girder, shearing forces are required by consideration of longitudinal equilibrium. These shears in the planes of plates also change from section to section, resulting in a net resistance to deformation of the cross-section which adds to the resistance caused by the flexural stiffness of the cross-section in its own plane.

The measure of distortion 'w' shown in Fig. 1-5 leads to warping displacements proportional to the slope 'w'. Warping stresses depend on the second derivatives of distortion w" and shears on the third

derivatives of the distortion w''''.

The forces per unit length which have their origin in warping and resist deformation are then proportional to w''''. These considerations suggested a governing differential equation for a w in the form:

$$E\,C_d w'''' + kw = P \qquad \ldots\ldots\ldots\ldots\ldots\ldots \quad (1)$$

where

C_d is a cross-sectional property related to warping, and apparently similar, at least dimensionally to a second moment of area,

k is a measure of the deformation stiffness of a unit length of the box cell and similar to a foundation modulus, whilst

P is the applied general distortional load per unit length.

From this it was observed that the equation representing the response of a box cell to a loading that causes deformation of the cross-section was analogous to that for beams on elastic foundation which is of the form:

$$EI\,\frac{\partial^4 \gamma}{\partial x^4} + \kappa\gamma = q, \text{ or } \frac{\partial^4 \gamma}{\partial x^4} + \beta^4\gamma = \frac{q}{EI} \qquad \ldots\ldots\ldots \quad (2)$$

where

EI = flexural rigidity of beam

γ = deflexion of beam

κ = modulus of subgrade reaction

q = intensity of lateral load

$\beta = \sqrt[4]{\frac{\kappa}{4EI}}$ characteristic of the system.

The analogy between the box cell subjected to torsional laoding and the BEF is summarised in Fig. 1-6.

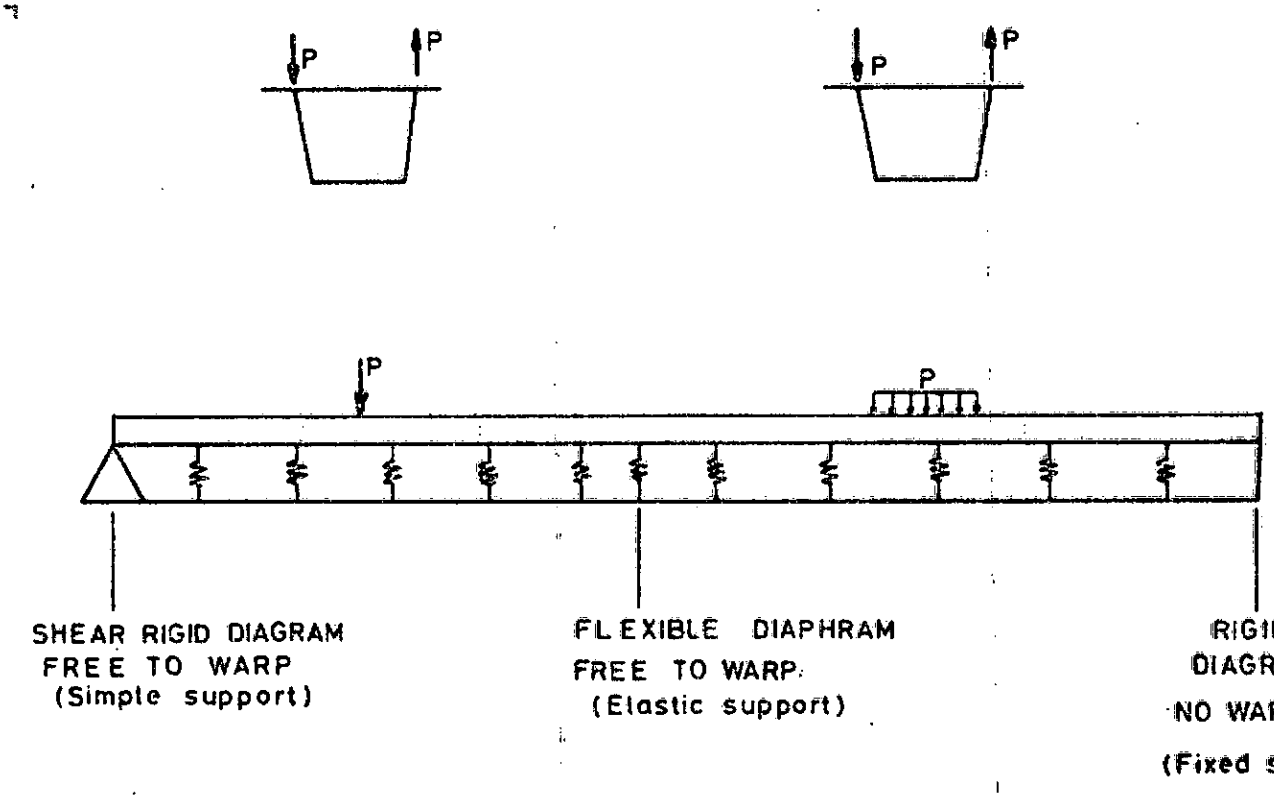

FIG 1-6

BEF Deflection $\propto$ Distortion Stress in Box Girder

BEF Moment $\propto$ Warping Stress in Box Girder

The resistance to torsional loading provided by the frame action of the cross-section of box girder is analogous to the effect of the foundation modulus k of the BEF. In other words, the resistance of the box girder cross-section to deformation corresponds to the BEF foundation modulus k.

The resistance to torsional load generated by restraint of warping in the box cell is related to the BEF moment of inertia I_b. Transverse diaphragms or cross-bracing of the box cell correspond to intermediate supports for the BEF.

Diaphragms or cross-braces in a box girder restrain deformation of the cross-section just as intermediate supports restrain transverse deflection of a beam on elastic foundation. The effect of diaphragm flexibility on box girder behaviour is determined by evaluating the corresponding support flexibility for the analogous BEF.

Experimental Verification:

There have been experimental studies of box girders and attempts have always been made to see how much agreement there is between results predicted by theory and actual experimental results. One of the most thorough experimental study is that of Mattock and Johnston on 1/4 and 1/5 scale models of simple-span steel box girder bridges. There were no interior diaphragms and all plate elements were isotropic so that the theory of Goldberg and Leve was applicable. Their results indicate that the Goldberg and Leve theory is reliable for box girders and they suggest that the reliability of other theories can be evaluated by comparison with the results predicted by this theory.

Results of comparative analyses reported by DeFries-Skene and Scordelis give a clear picture of the accuracy of thin-walled beam analyses.

There is a good agreement between results of Goldberg and Leve and the thin-walled beam theory, except in the vicinity of concentrated loads where peak stresses, by thin-walled beam theory, are low by about 25%.

However, this is also a characteristic of ordinary beam theory used for open section girders and should not inhibit engineering application of thin-walled beam theory for analysis of box girders.

Economics Of The Box Girder:

Box Girder bridge cross-sections are more stream-lined and more slender than other types and are often selected over other possible solutions because of their pleasing appearance (aesthetics).

They are particularly adaptable to prefabrication and to the standardisation of details. Relatively large segments can be prefabricated in the shop and transported and erected with relative ease on site in a short time. The main economic restraint will be the haulage distance from prefabrication shop floor to erection site and the cost of maintenance.

Although economic studies of a limited nature show cost advantages for box girders, it has been shown that in the comparative design of a bridge for a specific location that the box configuration is now necessarily the most economical.

Maintenance:

It can be argued that a smaller percentage of the total box girder bridge is exposed to the elements of the atmosphere (some of which are corrosive) than for other types of bridges, and thus maintenance costs are reduced.

However, there are still unanswered questions about the effect of condensation moisture and leakage of water through concrete deck. It is hoped that with welded construction, box girders can be fully sealed and such bridges should be free of internal corrosion once the oxygen is used up.

CHAPTER II

SOME BASIC EQUATIONS OF ELASTICITY AND PLATE BENDING

2-1 BASIC EQUATIONS OF PLATE BENDING THEORY:

The figure below shows the forces acting on a two-diamensional plate element of thickness t with the coordinate system as shown in the diagram.

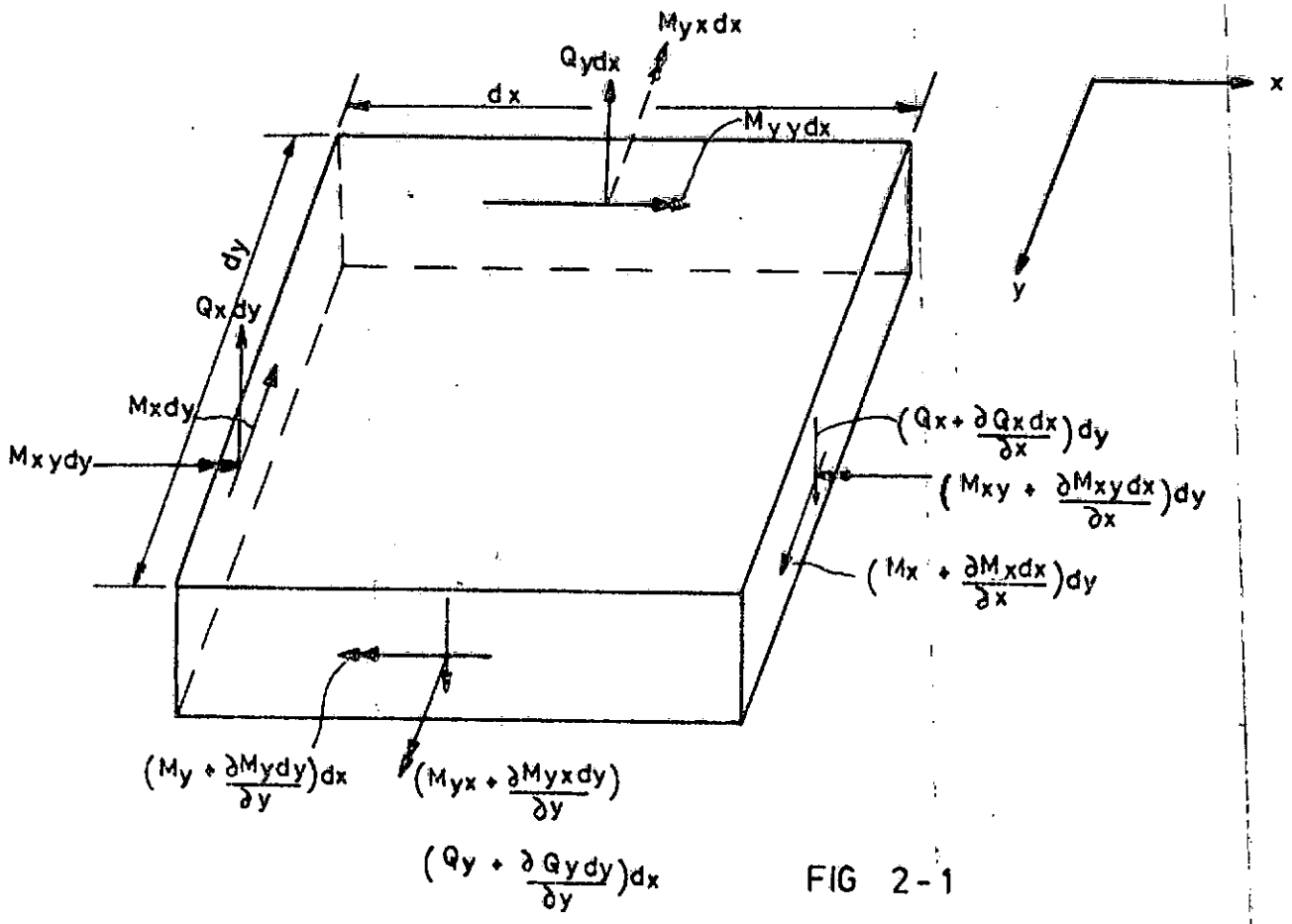

FIG 2-1

From the moment curvature relationship in pure bending of plates, (19) the moment and transverse deflexions are connected by the relations given in 2.1 below.

$$\left.\begin{aligned} M_{xx} &= -D\left\{\frac{\partial^2 w}{\partial x^2} + \nu\frac{\partial^2 w}{\partial y^2}\right\}, \\ M_{yy} &= -D\left\{\frac{\partial^2 w}{\partial y^2} + \nu\frac{\partial^2 w}{\partial x^2}\right\}, \\ M_{xy} &= D(1-\nu)\frac{\partial^2 w}{\partial x \partial y} = -M_{yx} \end{aligned}\right\} \quad 2.1$$

The magnitudes of the shearing forces per unit length, parallel to the y and x axes, are Q_x and Q_y. The intensity of load per unit area distributed over the upper surface is q. Projecting all the forces acting on the element on to the z- axis, we obtain,

$$\frac{\partial Q_x}{\partial x}.dxdy + \frac{\partial Q_y}{\partial y}.dydx + qdxdy = 0$$

$$\frac{\partial Q_x}{\partial x} + \frac{\partial Q_y}{\partial y} + q = 0 \qquad 2.2a$$

Taking moments of all forces acting on the element with respect to the x- axis, we obtain the equation of equilibrium:

$$\frac{\partial M_{xy}}{\partial x}.dxdy - \frac{\partial M_y}{\partial y}.dydx + Q_y.dxdy = 0$$

$$\frac{\partial M_{xy}}{\partial x} - \frac{\partial M_y}{\partial y} + Q_y = 0 \qquad 2.2b$$

The moments due to load q and δQ_y are neglected since they are small quantities of a higher order than those retained.

From 2.2b we deduce from a consideration of the moment equilibrium of forces acting on element, with respect to y- axis, the corresponding relation:

$$\frac{\partial M_{yx}}{\partial y} + \frac{\partial M_x}{\partial x} - Q_x = 0 \qquad 2.2c$$

Since there are no forces in the x and y directions, and no moments with respect to the z- axis, the equations 2.2a to 2.2c completely define the equilibrium of the element.

Eliminating Q_y and Q_x from equations 2.2a, 2.2b and 2.2c we arrive at:

$$\frac{\partial^2 M_x}{\partial x^2} + \frac{\partial^2 M_{yx}}{\partial x \partial y} + \frac{\partial^2 M_y}{\partial y^2} - \frac{\partial^2 M_{xy}}{\partial x \partial y} = -q$$

Since $M_{yx} = -M_{xy}$, the above equation can be written as:

$$\frac{\partial^2 M_x}{\partial x^2} + \frac{\partial^2 M_y}{\partial y^2} - 2\frac{\partial^2 M_{xy}}{\partial x \partial y} = -q \qquad 2.2d$$

Substituting equation 2.1 into equation 2.2d we have,

$$\frac{\partial^4 w}{\partial x^4} + \frac{2\,\partial^4 w}{\partial x^2 \partial y^2} + \frac{\partial^4 w}{\partial y^4} = \frac{q}{D} \qquad 2.3$$

The problem of the bending of a plate reduces to the integration of this equation to obtain the solution of w and can be written in the form:

$$\Delta^2 w = \frac{q}{D} \qquad 2.3a$$

where $\Delta^2 w = \Delta\Delta w$ and $\Delta w = \frac{\partial^2 w}{\partial x^2} + \frac{\partial^2 w}{\partial y^2}$

From equations 2.2b and 2.2c the shears are expressible in terms of w as:

$$\left.\begin{aligned} Q_x &= \frac{\partial M_{yx}}{\partial y} + \frac{\partial M_x}{\partial x} = -D\frac{\partial}{\partial x}\left\{\frac{\partial^2 w}{\partial x^2} + \frac{\partial^2 w}{\partial y^2}\right\} \\ Q_y &= \frac{\partial M_y}{\partial y} - \frac{\partial M_{xy}}{\partial x} = -D\frac{\partial}{\partial y}\left\{\frac{\partial^2 w}{\partial x^2} + \frac{\partial^2 w}{\partial y^2}\right\} \end{aligned}\right\} \qquad 2.4$$

Kirchoff showed that the twisting moment M_{xy} or M_{yx} and the shear force Q_x or Q_y can be combined at an edge to arrive at shear forces V_{xx} or V_{yy}, usually referred to as Kirchoff's shears.

$$V_x = \left(Q_x - \frac{\partial M_{xy}}{\partial y} \right)$$

$$= \left\{ \frac{\partial^3 w}{\partial x^2} + (2-\nu) \frac{\partial^3 w}{\partial x \partial y^2} \right\}$$

Likewise $$V_y = \left\{ \frac{\partial^3 w}{\partial y^3} + (2-\nu) \frac{\partial^3 w}{\partial y \partial x^2} \right\} \qquad 2.4a$$

2-2 BASIC EQUATIONS OF THE EXTENSIONAL THEORY:

Consider a two-dimensional element of a plate with the forces acting as shown in figure 2.2

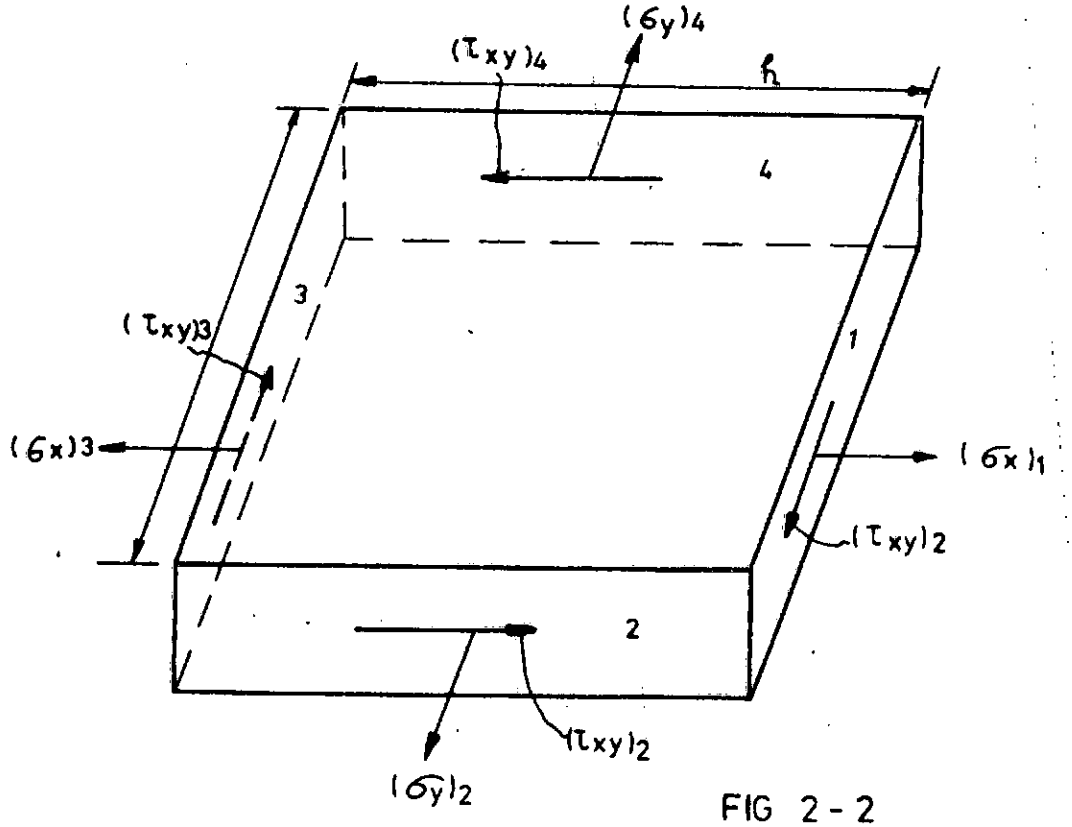

FIG 2 - 2

The problem in the theory of elasticity usually is to determine the state of stress in a body subjected to the action of external forces. It is only necessary to solve the derived differential equations of equilibrium such that the solutions satisfy the associated boundary conditions of a particular configuration.

In discussing the deformation of an elastic body, it is generally assumed that there are enough constraints to prevent the body moving as a rigid body so that no displacements of particles of the body are possible without a deformation of the body. The small displacements of particles of a deformed body are usually resolved into components u, v, w in the direction of the certesian coordinate axes x, y, z respectively.

Let h and k be the lengths of the sides of the element parallel to the x and y directions respectively.

If X and Y denote the components of body force intensity per unit volume, the condition of equilibrium for forces in the x-direction is:

$$(\sigma_x)_1 k - (\sigma_x)_3 k + (\tau_{xy})_2 h - (\tau_{xy})_4 h + Xhk = 0$$

$$\frac{(\sigma_x)_1 - (\sigma_x)_3}{k} + \frac{(\tau_{xy})_2 - (\tau_{xy})_4}{k} + X = 0$$

As h, k $\rightarrow$ o, this equation becomes,

$$\frac{\partial \sigma_x}{\partial x} + \frac{\partial \tau_{xy}}{\partial y} + X = 0 \qquad 2.5a$$

Similarly we obtain for forces in the y- direction,

$$\frac{\partial \sigma_y}{\partial y} + \frac{\partial \tau_{xy}}{\partial x} + Y = 0 \qquad 2.5b$$

The stresses are connected with the displacement u through

$$\sigma_{ij} = \mu \left\{ u_{i,j} + u_{j,i} + \frac{2\nu}{1-2\nu} u_{k,k} \delta_{ij} \right\} \qquad 2.6$$

where μ is the shear modulus, δ_{ij} the Kronecker delta, $u_1 = u$, $u_2 = v$, and i and j are ranging over the values 1, 2 only. The usual Einstein's summation convention over repeated indices is also implied. A comma before a suffix denotes differentiation with respect to the corresponding variable. The substitution of equation 2.6 into equation 2.5 gives:

$$u_{i,jj} + \frac{1}{1-2\nu} u_{j,ji} = 0 \quad , \qquad 2.7$$

which is the equilibrium equation in terms of the displacements, assuming that X and Y are equal to zero.

According to Papkovitch and Neuber, the complete general solution of the above equation is of the form:

$$u_i = \frac{\partial}{\partial x_i} (\phi_0 + x_k . \phi_k) - 4(1-\nu) . \phi_i ,$$

provided that:

$$\Delta(\phi_0, \phi_i) = (o, o) \qquad 2.8$$

Written in full this equation yields the following expressions for plane strain deformation:

$$\left.\begin{aligned} u &= \frac{\partial}{\partial x} (\phi_0 + x \phi_1 + y \phi_2) - 4(1-\nu) \phi_2 \\ v &= \frac{\partial}{\partial y} (\phi_0 + x \phi_1 + y \phi_2) - 4(1-\nu) \phi_2 \end{aligned}\right\} \qquad 2.9$$

For plane stress deformation, the corresponding expressions are obtained by replacing ν in equation 2.9 with $\frac{\nu}{1+\nu}$

2-3 DERIVATION OF HARMONIC COMPONENT OF A POINT LOAD ACTING ON A RECTANGULAR PLATE

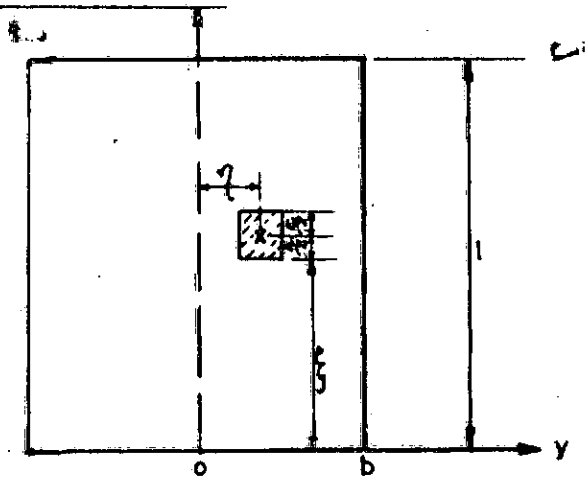

FIG 2 - 3

Let the plate be simply supported and let the point load P act over an infinitesimal interval ($\xi - {}^{e}/_{2}, \xi + {}^{e}/_{2}$)

$$f(x) = \frac{P}{e} \quad \text{for } \xi - {}^{e}/_{2} < x < \xi + {}^{e}/_{2} \qquad 2.10$$

$$= 0 \quad \text{for all others.}$$

Since the plate is to be simply supported at x = o and , structural consistence with support conditions suggests defining the load functions, f (x), in the form:

$$f(x) = \frac{P}{e} = \sum_{n=1}^{\infty} \sin \frac{n\pi x}{\ell} \; A_n \qquad 2.11$$

where A_n are as yet unknown superposition coefficients. Multiplying both sides of equation 2.11 by $\sin \frac{m\pi x}{\ell}$ and integrating between the limits o and ℓ we have

$$\int_0^{\ell} f(x) \sin \frac{m\pi x}{\ell}.dx = \sum_{n=1}^{\infty} \int_0^{\ell} A_n \sin \frac{n\pi x}{\ell} \sin \frac{m\pi x}{\ell}.dx$$

The left hand side of the equation becomes

$$\frac{P}{e} \int_{\xi-{}^{e}/_{2}}^{\xi+{}^{e}/_{2}} \sin \frac{m\pi x}{\ell}.dx = \left\{ -\frac{P}{e}\frac{\ell}{m\pi} \cos \frac{m\pi x}{\ell} \right\}_{\xi-{}^{e}/_{2}}^{\xi+{}^{e}/_{2}}$$

$$= \frac{2P}{e}.\frac{\ell}{m\pi}.\sin \frac{m\pi}{\ell} \; \xi.\sin \frac{m\pi e}{2\ell} \qquad 2.12$$

In the limit as $\epsilon \to 0$,

$$P \sin \frac{m\pi}{\ell}\xi \; \frac{\sin \frac{m\pi\epsilon}{2\ell}}{\frac{m\pi\epsilon}{\ell}} = P \sin \frac{m\pi}{\ell}\xi$$

The right hand side of the equation takes the form

$$\tfrac{1}{2} \sum_{n=1}^{\infty} A_n \int_0^{\ell} \{\cos \tfrac{\pi x}{\ell}(n-m) - \cos \tfrac{\pi x}{\ell}(n+m)\}.dx$$

$$= \tfrac{1}{2} A_n \left\{ \frac{\sin \frac{\pi x}{\ell}(n-m)}{\frac{\pi}{\ell}(n-m)} - \frac{\sin \frac{\pi x}{\ell}(n+m)}{\frac{\pi}{\ell}(n+m)} \right\}_0^{\ell}$$

$$= \tfrac{1}{2} \sum_{n=1}^{\infty} A_n \left\{ \frac{\sin \pi (n-m)}{\frac{\pi}{\ell}(n-m)} - \frac{\sin \pi (n+m)}{\frac{\pi}{\ell}(n+m)} \right\} \qquad 2.13$$

This expression is zero for all values of n and m except when n = m, when it becomes $\frac{\ell}{2}.A_m$

From this solution of equation 2.11 we have

$$P \sin \frac{m\pi}{\ell}\xi = \frac{\ell}{2}.A_m$$

or $$A_m = \frac{2P}{\ell} \sin \frac{m\pi}{\ell}\xi$$

and hence

$$f(x) = \sum_{n=1}^{\infty} \frac{2P}{\ell} \sin \frac{m\pi}{\ell}\xi \sin \frac{n\pi x}{\ell} \qquad 2.14$$

2-4 DERIVATION OF THE EQUATION FOR TRANSVERSE DEFLEXION OF A PLATE WITH ALL ITS EDGES SIMPLY SUPPORTED

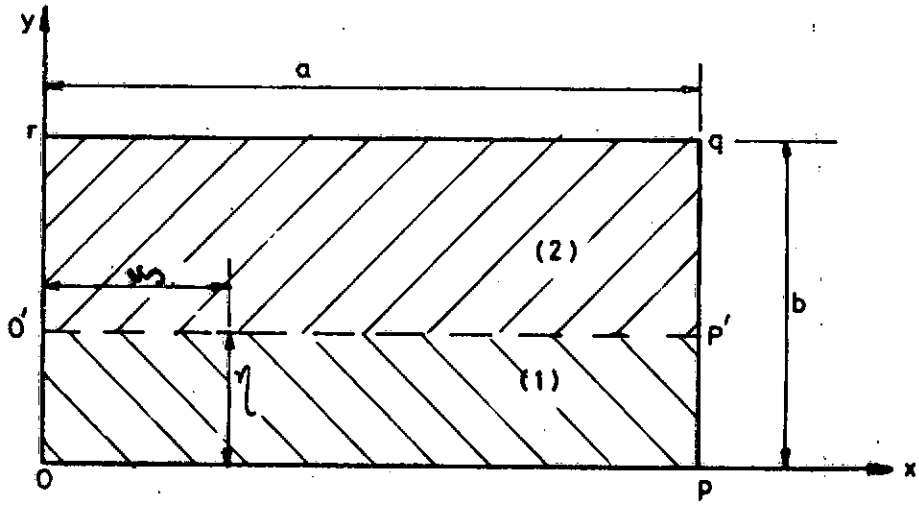

FIG 2-4

The coordinate axes are as shown in Fig. (2-4).

Let the imaginary line o'p' divide the plate opqr into two parts so that the plate opqr will now be considered as two plates having the common interface o'p'.

Let the deflexion field for plate (1) be given by the equation

$$w^{(1)} = A_n^{(1)} \text{ch}\lambda y + B_n^{(1)} \text{sh}\lambda y + C_n^{(1)} y\text{ch}\lambda y + D_n^{(1)} y\text{sh}\lambda y \qquad 2.15$$

and that for plate (2) by

$$w^{(2)} = A_n^{(2)} \text{ch}\lambda(b-y) + B_n^{(2)} \text{sh}\lambda(b-y) + C_n^{(2)} (b-y)\text{ch}\lambda(b-y) + D_n^{(2)} (b-y)\text{sh}\lambda(b-y) \qquad 2.16$$

where for brevity, the summation sign Σ has been ommitted.

The boundary conditions are

$$\left.\begin{aligned} \{w^{(1)}\}_{y=o} &= \{w^{(2)}\}_{y=b} = 0 \\ \{M_y^{(1)}\}_{y=o} &= \{M_y^{(2)}\}_{y=b} = 0 \end{aligned}\right\} \qquad 2.17$$

$$\text{At } y = 0,\ w^{(1)} = 0,\ \therefore A_n^{(1)} = 0$$

$$\text{At } y = b,\ w^{(2)} = 0,\ \therefore A_n^{(2)} = 0$$

$$\text{At } y = 0,\ M_y^{(1)} = 0,\ \therefore D_n^{(1)} = 0$$

$$\text{At } y = b,\ M_y^{(2)} = 0,\ \therefore D_n^{(2)} = 0$$

At the imaginary interface, the continuity conditions are as follows:

$$\text{(i)} \quad \left\{ \frac{\partial w^{(1)}}{\partial y} \right\}_{y=\eta} = \left\{ \frac{\partial w^{(2)}}{\partial y} \right\}_{y=b-\eta}$$

$$\text{(ii)} \quad \left\{ M_y^{(1)} \right\}_{y=\eta} = \left\{ M_y^{(2)} \right\}_{y=b-\eta}$$

$$\text{(iii)} \quad \left\{ w^{(1)} \right\}_{y=\eta} = \left\{ w^{(2)} \right\}_{y=b-\eta}$$

$$\text{(iv)} \quad \left\{ V_y^{(2)} \right\}_{y=b-\eta} - \left\{ V_y^{(1)} \right\}_{y=\eta} = P_u$$

Now, the equations 2.15 and 2.16 now reduce to:

$$w^{(1)} = B_n^{(1)} sh\lambda y + C_n^{(1)} y ch\lambda y \qquad 2.18$$

$$w^{(2)} = B_n^{(2)} sh\lambda(b-y) + C_n^{(2)} (b-y)\, ch\lambda(b-y) \qquad 2.19$$

Applying the first of the common interface conditions we obtain

$$B_n^{(1)} \lambda ch\lambda\eta + C_n^{(1)} (ch\lambda\eta + \lambda\eta sh\lambda\eta) = -B_n^{(2)} \eta ch\lambda(b-\eta)$$

$$- C_n^{(2)} \{ch\lambda(b-\eta) + \lambda(b-\eta) sh\lambda(b-\eta)\} \qquad 2.20$$

The second of the interface conditions relating to moments also yield

$$B_n^{(1)} sh\lambda\eta + C_n^{(1)}\{\lambda\eta ch\lambda\eta + \frac{2}{1-\nu} sh\lambda\eta\} = \lambda B_n^{(2)} sh\lambda(b-\eta) + C_n^{(2)}\{\lambda(b-\eta)ch\lambda(b-\eta) + \frac{2}{1-\nu} sh\lambda(b-\eta)\} \quad 2.21$$

whilst the interface deflexion continuity condition gives

$$B_n^{(1)} sh\lambda\eta + C_n^{(1)}\eta ch\lambda\eta = B_n^{(2)} sh\lambda(b-\eta) + C_n^{(2)}(b-\eta)ch\lambda(b-\eta) \quad 2.22$$

By suitable manipulation of equations 2.21 and 2.22 we obtain

$$C_n^{(2)} = C_n^{(1)} \frac{sh\lambda\eta}{sh\lambda(b-\eta)} \quad 2.23$$

Now, invoking the last of the interface conditions, namely $V_{y_2} - V_{y_1} = P$, we have,

$$(1-\nu)\lambda B_n^{(2)} ch\lambda(b-\eta) + C_n^{(2)}\{(1-\nu)\lambda(b-\eta)sh\lambda(b-\eta) - (1+\nu)ch\lambda(b-\eta)\} + (1-\nu)\lambda B_n^{(1)} ch\lambda\eta + C_n^{(1)}\{(1-\nu)\lambda\eta sh\lambda\eta - (1+\nu)ch\lambda\eta\} = \frac{P_u}{\lambda^2 D} \quad 2.24$$

Eliminating $B_n^{(1)}$ and $B_n^{(2)}$ from equations 2.20 and 2.24 we obtain

$$-2\lambda^2 ch\lambda(b-\eta)\, C_n^{(2)} - 2\lambda^2 ch\lambda\eta\, C_n^{(1)} = \frac{P_u}{D} \quad 2.25$$

Substituting for $C_n^{(2)}$ in equation 2.25 using the relation in 2.23 and using well known relations in hyperbolic functions we deduce that

$$C_n^{(1)} = -\frac{P_u}{2\lambda^2 D}.\frac{sh\lambda(b-\eta)}{sh\lambda b} \qquad 2.26$$

and similarly

$$C_n^{(2)} = -\frac{P_u}{2\lambda^2 D}.\frac{sh\lambda\eta}{sh\lambda b} \qquad 2.27$$

Eliminating B_{n_2} from 2.20 and 2.22 we arrive at

$$B_n^{(1)}\lambda sh\lambda b + C_n^{(1)}\{\lambda\eta ch\lambda b + ch\lambda\eta sh\lambda(b-\eta)\} =$$

$$- C_n^{(2)}\{ch\lambda(b-\eta)sh\lambda(b-\eta) - \lambda(b-\eta)\}$$

Substituting for $C_n^{(1)}$ and $C_n^{(2)}$ in this relation we obtain

$$B_n^{(1)} = \frac{P_u sh\lambda(b-\eta)}{2\lambda^3 D.sh\lambda b}\left\{\lambda b coth\lambda b + 1 - \lambda(b-\eta)coth\lambda(b-\eta)\right\} \qquad 2.28$$

By back substitution into 2.20 or 2.22 we have

$$B_n^{(2)} = \frac{-P_u sh\lambda\eta}{2\lambda^3 D.sh\lambda b}\left\{1 + \lambda b coth\lambda b - \lambda\eta coth\lambda\eta\right\} \qquad 2.29$$

Hence the deflexion fields are given as

$$w^{(1)} = \Sigma\frac{P_u}{2\lambda^3 D}\{-(1+\lambda b coth\lambda b) + \lambda(b-\eta)coth\lambda(b-\eta) + \lambda y coth\lambda y\}\frac{sh\lambda(b-\eta)\ sh\lambda y}{sh\lambda b} \qquad 2.30a$$

and

$$w^{(2)} = \Sigma \frac{P_u}{2\lambda^3 D} \left\{ - (1+\lambda b \coth\lambda b) + \lambda\eta\coth\lambda\eta + \lambda(b-y)\coth\lambda(b-y) \right\} \frac{sh\lambda\eta sh\lambda(b-y)}{sh\lambda b} \qquad 2.30b$$

Noting that $P_u = \frac{2P}{a}\Sigma \sin\lambda x \sin\lambda\xi$, with

$\lambda = \frac{m\pi}{a}$, we have

$$w_1 = \sum_{n=1}^{\infty} \frac{Pa^2}{m^3\pi^3 D} \left\{ - (1+\lambda b\coth\lambda b) + \lambda(b-\eta)\mathrm{cth}\lambda(b-\eta) + \lambda y\,\mathrm{cth}\lambda y \right\} \frac{sh\lambda(b-\eta)sh\lambda y.\sin\lambda x \sin\lambda\xi}{sh\lambda b} \qquad 2.31a$$

$$w_2 = \sum_{n=1}^{\infty} \frac{Pa^2}{m^3\pi^3 D} \left\{ - (1+\lambda b\,\mathrm{cth}\lambda b) + \lambda\eta\,\mathrm{cth}\lambda\eta + \lambda(b-y)\mathrm{cth}\lambda(b-y) \right\} \frac{sh\lambda\eta sh\lambda(b-y)\sin\lambda x.\sin\lambda\xi}{sh\lambda b} \qquad 2.31b$$

Although the solution desired is known {19}, the method of derivation employed here does not appear to have been previously recorded in standard texts on plate bending.

The expression found in standard texts {19} for the deflexion of a plate carrying a single load P at some given point $x = \xi$, $y = \eta$, is of the form:

$$w = \frac{Pa^2}{\pi^3 D} \sum_{m=1}^{\infty} \left\{ 1+\beta m\coth\beta m - \frac{\beta m}{b}.y_1\coth\frac{\beta m}{b}.y_1 - \frac{\beta m}{b}\eta\coth\frac{\beta m}{b}\eta \right\} \frac{sh\frac{\beta m}{b}\eta.\ sh\frac{\beta m}{b}.y_1 \sin\frac{m\pi}{a}\xi \sin\frac{m\pi x}{a}}{m^3 sh\beta m} \qquad 2.32$$

in which $\beta m = \frac{m\pi b}{a}$, $y_1 = b-y$ and $y \geqslant \eta$ (figure 2-4)

In the case where $y < \eta$, the quantity y_1 must be replaced by y and the quantity η by $\eta_1 = b-\eta$.

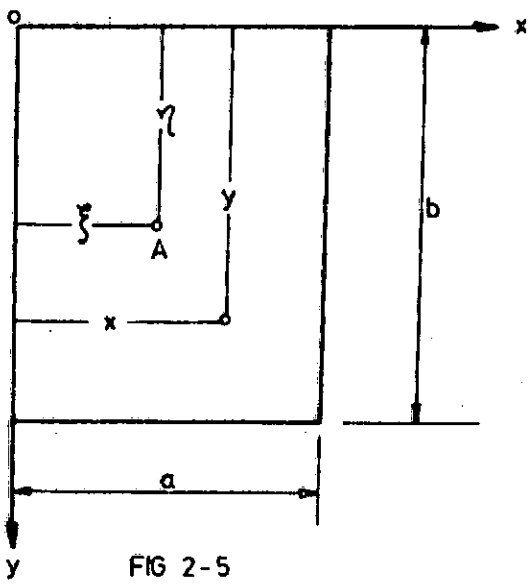

FIG 2-5

The case of $y < \eta$ corresponds to the region 1 of the method described in this work, whilst that of $y \geqslant \eta$ corresponds to region 2.

Equation 2.32 is therefore identical with deflexion fields defined by equations 2.31a and 2.31b provided for region 2, when $y > \eta$, y_1 is replaced by b-y and for region 1, when $y < \eta$, y_1 is replaced by y and η by b-η.

This method will be used throughout this work for obtaining the equations of the deflexion fields for a transversely loaded plate with any desired boundary conditions.

2-5 DERIVATION OF AN ALTERNATIVE FORM OF THE EQUATIONS FOR THE TRANSVERSE DEFLEXION OF A PLATE WITH ALL ITS FOUR EDGES SIMPLY SUPPORTED

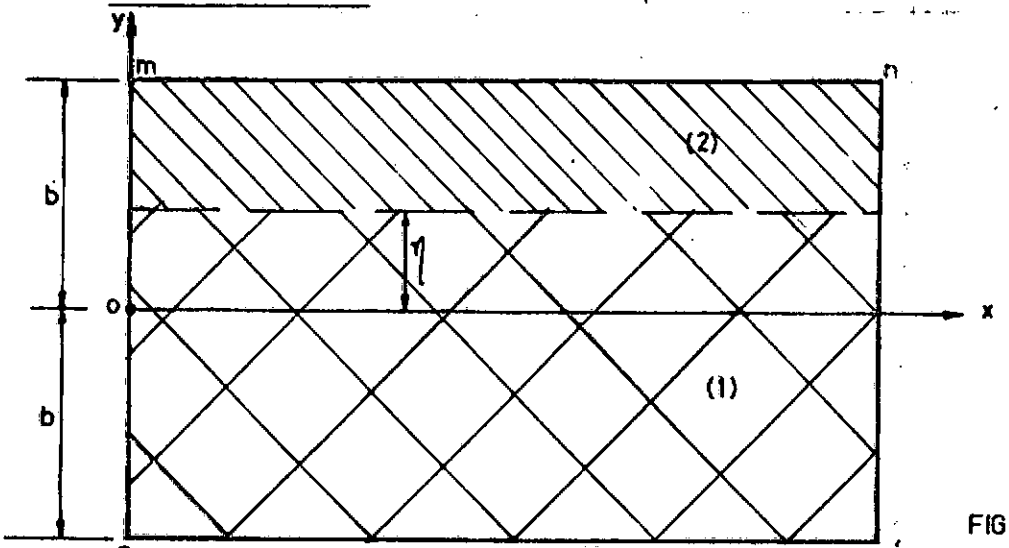

FIG 2 - 6

Let the coordinate axes be as in figure 2-6 which shows the plate o'nmp with all its four edges, mn, no', o'p and pm simply supported.

Let $w^{(1)}$ be the deflexion equation of plate (1) and $w^{(2)}$ that of plate (2).

$$\text{Let } w^{(1)} = A_n^{(1)} ch\lambda(y+b) + B_n^{(1)} sh\lambda(y+b) + C_n^{(1)}(y+b)ch\lambda(y+b) + D_n^{(1)}(y+b)sh\lambda(y+b) \qquad 2.33$$

$$w^{(2)} = A_n^{(2)} ch\lambda(b-y) + B_n^{(2)} sh\lambda(b-y) + C_n^{(2)}(b-y)ch\lambda(b-y) + D_n^{(2)}(b-y)sh\lambda(b-y) \qquad 2.34$$

The boundary conditions are:

$$w^{(1)} = w^{(2)} = M_x = 0 \text{ at } x = 0 \text{ and } \ell$$

$$\text{and } w^{(1)}\big|_{y=-b} = w^{(2)}\big|_{y=b} = 0$$

$$M_y^{(1)}\big|_{y=-b} = M_y^{(2)}\big|_{y=b} = 0$$

The choice of a suitable eigenvalue will enable the first set of conditions to be satisfied whilst our choice of the structure of equations 2.33 and 2.34 ensures automatic satisfaction of the second sets of conditions.

At the interface, i.e. at $y = \eta$, the continuity conditions to be satisfied are, as before:

(i) $w^{(1)} = w^{(2)}$

(ii) $\frac{\partial w^{(1)}}{\partial y} = \frac{\partial w}{\partial y}^{(2)}$

(iii) $M_{yy}^{(1)} = M_{yy}^{(2)}$

(iv) $V_{yy}^{(1)} = V_{yy}^{(2)} = P_u$

Applying these conditions using equations 2.33 and 2.34 and employing certain standard mathematical techniques we obtain explicitly the values of the superposition coefficients as

$$A_n^{(1)} = A_n^{(2)} = D_n^{(1)} = D_n^{(2)} = 0$$

$$C_n^{(1)} = \frac{P_u}{2\lambda^2 D} \cdot \frac{sh\lambda(b-\eta)}{sh2\lambda b} \qquad 2.35$$

$$C_n^{(2)} = \frac{P_u}{2\lambda^2 D} \cdot \frac{sh\lambda(b+\eta)}{sh2\lambda b} \qquad 2.36$$

$$B_n^{(1)} = \frac{P_u}{2\lambda^3 D} \cdot \frac{sh\lambda(b-\eta)}{sh2\lambda b} \{\lambda(b-\eta)cth\lambda(b-\eta) - (1+2\lambda b cth2\lambda b)\} \qquad 2.37$$

$$B_n^{(2)} = \frac{P_u}{2\lambda^3 D} \cdot \frac{sh\lambda(b+\eta)}{sh2\lambda b} \{\lambda(b+\eta)cth\lambda(b+\eta) - (1+2\lambda b cth2\lambda b)\} \qquad 2.38$$

The deflexion fields now take the form

$$w^{(1)} = \frac{P'}{2\lambda^3 D} \cdot \frac{sh\lambda(b-\eta)}{sh2\lambda b} \left[\{\lambda(b-\eta)cth\lambda(b-\eta) - (1+2\lambda b cth2\lambda b)\}.sh\lambda(b+y) + \lambda(b+y)ch\lambda(b+y) \right].sin\lambda\xi.sin\lambda x \qquad 2.39$$

$$w^{(2)} = \frac{P'}{2\lambda^3 D} \cdot \frac{sh\lambda(b+\eta)}{sh2\lambda b} \left[\{\lambda(b+\eta)cth\lambda(b+\eta) - (1+2\lambda b cth2\lambda b)\}.sh\lambda(b-y) + \lambda(b-y)ch\lambda(b-y) \right].sin\lambda\xi.sin\lambda x \qquad 2.40$$

where

$$\lambda = \frac{n\pi}{\ell} \quad \text{and} \quad P' = \frac{2P}{\ell} \quad \text{for a point load } P.$$

2-6 DERIVATION OF THE EQUATION OF TRANSVERSE DEFLEXION OF A RECTANGULAR PLATE WITH TWO OPPOSITE EDGESSIMPLY SUPPORTED AND THE OTHER TWO FIXED

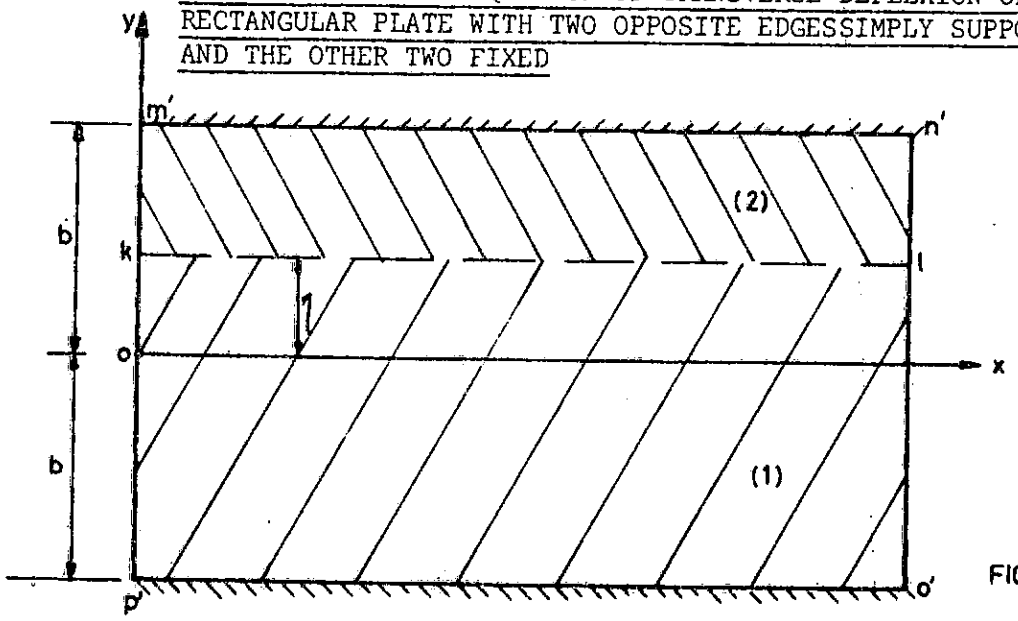

FIG 2-7

Edges m'n' and o'p' are fixed whilst edges n'o' and p'm' are both simply supported.

Let the imaginary interface of the plate be along kℓ.

We take the deflexion equation in the form:

$$w^{(1)} = A_n^{(1)} ch\lambda(y+b) + B_n^{(1)} sh\lambda(y+b) + C_n^{(1)}(y+b)ch\lambda(y+b) + D_n^{(1)}(y+b)sh\lambda(y+b) \qquad 2.41$$

$$w^{(2)} = A_n^{(2)} ch\lambda(b-y) + B_n^{(2)} sh\lambda(b-y) + C_n^{(2)}(b-y)ch\lambda(b-y) + D_n^{(2)}(b-y)sh\lambda(b-y) \qquad 2.42$$

The boundary conditions are:

$$\left.\begin{aligned} &\text{(i)} \quad \{w\}_{y=b} = \{w\}_{y=-b} = 0 \\ &\text{(ii)} \quad \left\{\frac{\partial w}{\partial y}\right\}_{y=b} = \left\{\frac{\partial w}{\partial y}\right\}_{y=-b} = 0 \end{aligned}\right\} \qquad 2.43$$

At the interface, the continuity conditions to be satisfied are:

(1) $w^{(1)} = w^{(2)}$

(2) $\frac{\partial w^{(1)}}{\partial y} = \frac{\partial w^{(2)}}{\partial y}$

(3) $M_{yy}^{(1)} = M_{yy}^{(2)}$

(4) $V_{yy}^{(1)} - V_{yy}^{(2)} = \frac{P_u}{D}$

As in the previous cases, these conditions are applied using the equations 2.41 and 2.42, and employing certain standard mathematical techniques, to obtain the superposition coefficients.

$$A_n^{(1)} = A_n^{(2)} = 0$$

$$B_n^{(1)} = -Cl.\ (Kl-Hl)$$

$$C_n^{(1)} = Cl.(-Hl + Kl)$$

$$D_n^{(1)} = Cl.(2\lambda^2 b(b-\eta)sh\lambda(b+\eta) - \lambda(b+\eta)sh\lambda(b-\eta)sh2\lambda b)$$

$$B_n^{(2)} = -Cl\ (Gl - G2)$$

$$C_n^{(2)} = Cl\ (Gl - G2)$$

$$D_n^{(2)} = Cl.(2\lambda^2 b(b+\eta)sh\lambda(b-\eta) - \lambda(b-\eta)sh\lambda(b+\eta)sh2\lambda b)$$

where $$C1 = \frac{P_u}{2\lambda^2 D}(sh^2 2\lambda b - 4\lambda^2 b^2)^{-1}$$

$$H1 = \lambda(b-\eta)\{sh\lambda(b+\eta) + 2\lambda b ch\lambda(b+\eta)\}$$

$$K1 = sh\lambda(b-\eta)(sh2\lambda b + \lambda(b+\eta)ch2\lambda b)$$

$$G1 = sh\lambda(b+\eta)(sh2\lambda b + 2\lambda b ch2\lambda b)$$

$$G2 = \lambda(b+\eta)\{ch\lambda(b+\eta)sh2\lambda b + 2\lambda b ch\lambda(b-\eta)\}$$

Hence the complete expression for $w^{(1)}$ and $w^{(2)}$ can be written out by substituting into 2.42 and 2.43 the expressions for the superposition coefficients.

For a superimposed load of intensity q on a plate simply supported on all four edges the displacement field is as follows:

$$W = \frac{4\lambda^{-5}q}{\ell D}\left[1 - \frac{2 + \lambda b th\lambda b}{2ch\lambda b}.ch\lambda y + \frac{\lambda y sh\lambda y}{2ch\lambda b}\right]sin\lambda x$$

$$\theta_{y=b} = \frac{2\lambda^{-4}q}{\ell D}(\lambda b sech^2\lambda b - tanh\lambda b)$$

$$\theta_{y=-b} = -\frac{2\lambda^{-4}q}{\ell D}(\lambda b sech^2\lambda b - tanh\lambda b)$$

$$V_{yy|y=b} = -V_{yy|y=-b} = 2(1-\nu)\frac{\lambda^{-2}q}{\ell}(\lambda b sech^2\lambda b - \frac{3+\nu}{1-\nu}tanh\lambda b)$$

CHAPTER III

3-1 METHOD OF ANALYSIS OF BOX GIRDER

This analysis is of a closed box girder with a single-cell trapezoidal cross-section as shown in Fig. (3-1). The plates are rigidly connected along their common edges and closed off at the ends by integral diaphragms. This analysis considers both extensional and bending actions of the plates.

Eight continuity conditions are written for each joint (there are four joints in this system). Therefore, there are 8n simultaneous equations to be solved, where n is the number of joints with unknown forces and displacements.

Essentially, the thirty-two resulting equations of this analysis are written in terms of superposition coefficients. After solving the set of equations, the thirty-two superposition coefficients are obtained and these are used to determine forces and displacements at any point of cross-section using the appropriate expressions.

3-2

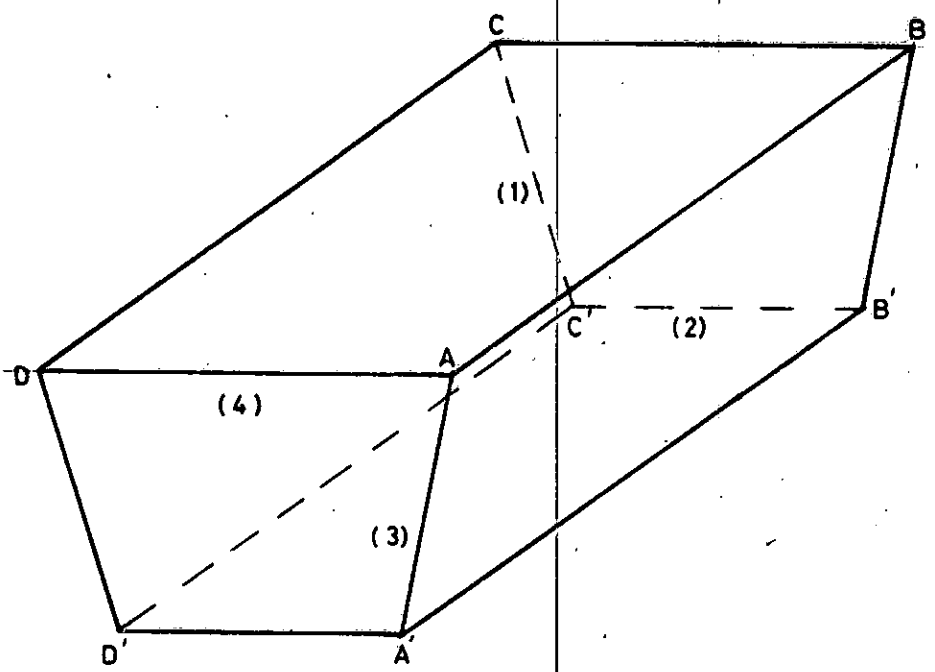

FIG 3-1

Figure (3-1) shows the system to be analysed. The system consists of four plates ABCD, ABB'A', A'B'C'D' and DCC'D' which are joined rigidly along AB, A'B', D'C' and DC. Each plate is rectangular and coordinate systems are chosen as shown in Figure (3-2).

It is further assumed that:

$$AB = DC = A'B' = D'C' = \ell = \text{span} \qquad (3.1)$$

$$\left.\begin{aligned} AD &= BC = 2b \\ AA' &= BB' = CC' = DD' = 2c \\ D'A' &= C'B' = 2d \end{aligned}\right] \qquad (3.2)$$

$$\hat{DAA} = \hat{ADD'} = 2\alpha \qquad (3.3)$$

3-3 SYSTEM OF CO-ORDINATE AXES

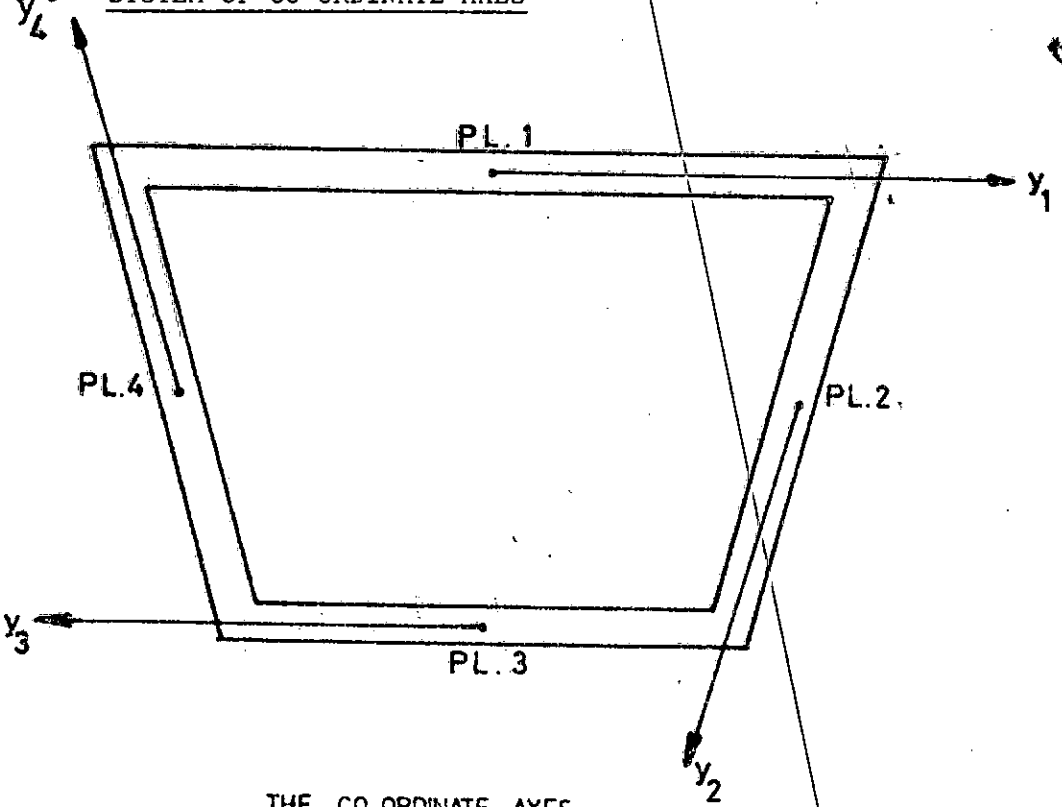

THE CO ORDINATE AXES
USED FOR THE ANALYSIS

FIG 3 - 2

The figure above shows the directions of the coordinate axes of the plates which make up the box girder. In all cases, the x-direction is normal to the paper.

At a first attempt at this analysis the coordinate axes were taken as shown in figure below

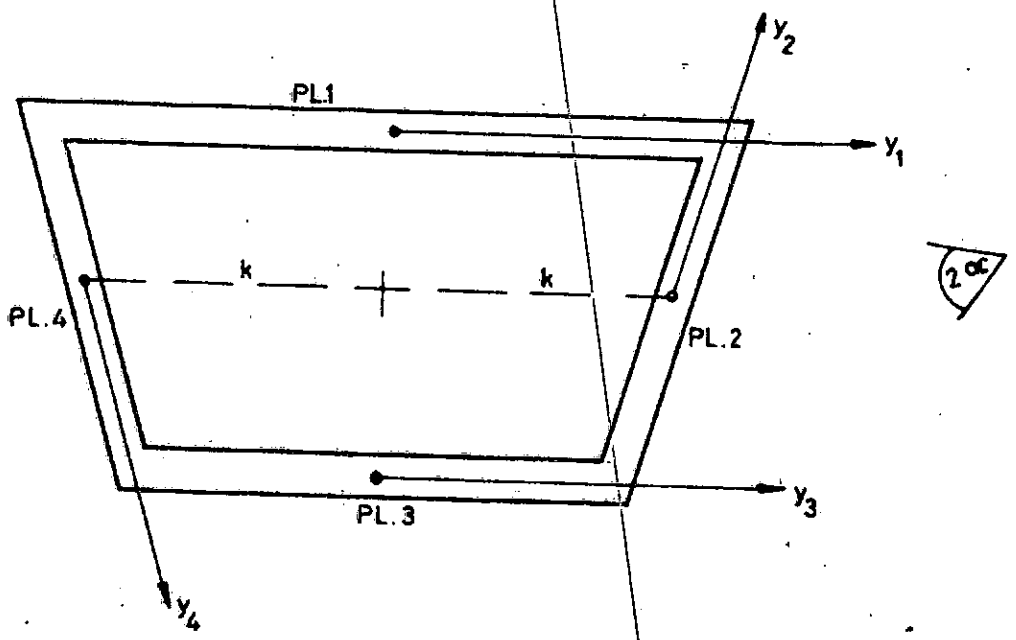

FIG 3-3

Here it was discovered that although the results exhibited symmetry the signs of the longitudinal stresses did not conform with those anticipated from a physical conjecture. However, with this cyclic order of orientation of the y-axes, the trend of the results would seem to conform with physical conjecture.

The figures below show the assumed directions of the forces and displacements of the system to be analysed.

Figure (3-4) Diagram showing directions of forces.

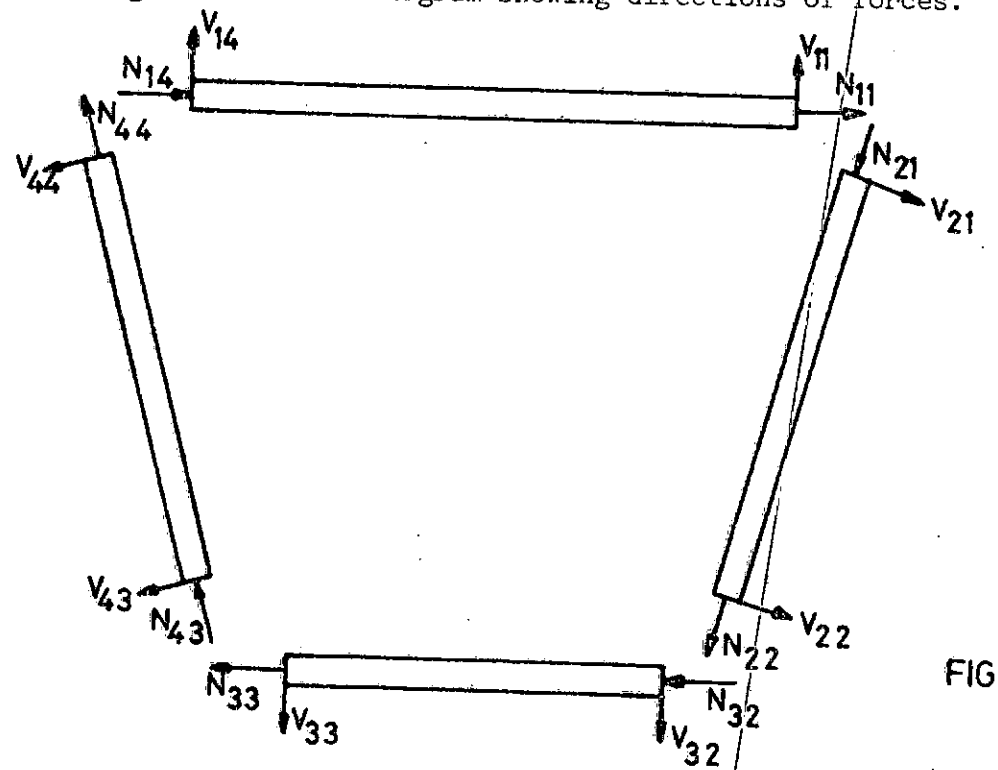

FIG 3-4

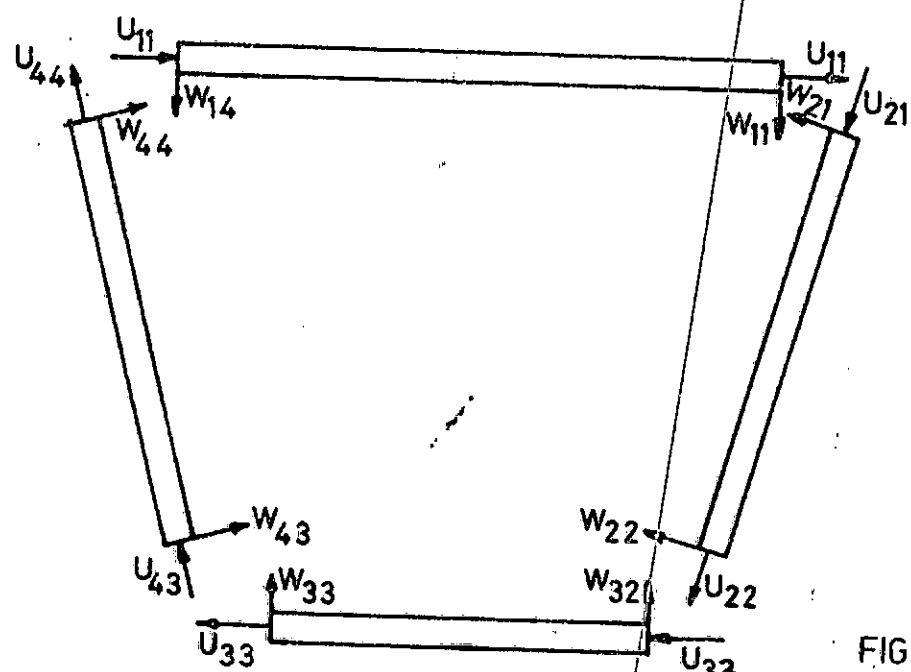

FIG 3-5

Figure (3-5) Diagram showing direction of displacements

3-4.1 DERIVATION OF EQUATIONS TO BE USED IN THE ANALYSIS

BENDING CONSIDERATIONS:

The previously derived equation for the deflection surface of a plate simply supported on all four edges with a concentrated load P acting at $x = \xi$, $y = \eta$ is given by:

$$Wo = \frac{P\,sh\lambda(b-\eta)}{2\lambda^3 D.sh(2\lambda b)}\Big[-\{\lambda(b-\eta)cth\lambda(b-\eta) - \{1+2\lambda b\,cth(2\lambda b)\}\}sh\lambda(y+b) + \lambda(y+b)ch\lambda(y+b)\Big].\sin(\lambda x)\sin(\lambda\xi)$$

which is valid for the range $-\eta > y > -b$ (3.4)

and $$Wo = \frac{P\,sh\lambda(b+\eta)}{2\lambda^3 D.sh(2\lambda b)}\Big[-\{\lambda(b+\eta)cth\lambda(b+\eta) - \{1+2\lambda b\,cth(2\lambda b)\}\}sh\lambda(b-y) + \lambda(b-y)ch\lambda(b-y)\Big].\sin(\lambda\xi)\sin(\lambda x)$$

which is valid for the range $-\eta < y < b$ (3.5)

These equations can be written in the form:

$$Wo = F_1\{G_1 sh\lambda(y+b) + \lambda(y+b)ch\lambda(y+b)\}\sin(\lambda x)$$

for $-\eta > y > -b$ (3.6)

$$Wo = F_0\{G_0 sh\lambda(b-y) + \lambda(b-y)ch\lambda(b-y)\}\sin(\lambda x)$$

for $-\eta < y < b$ (3.7)

where

$$F_1 = \frac{P}{2\lambda^3 D}.\frac{sh\lambda(b-\eta).\sin(\lambda\xi)}{sh(2\lambda b)}$$

$$G_1 = \{\lambda(b-\eta)cth\lambda(b-\eta) - (1+2\lambda b cth(2\lambda b))\}$$

$$F_0 = \frac{P}{2\lambda^3 D}.\frac{sh\lambda(b+\eta).\sin(\lambda\xi)}{sh(2\lambda b)}$$

$$G_0 = \{\lambda(b+\eta)cth\lambda(b+\eta) - (1+2\lambda b cth(2\lambda b))\}$$

At junction 1 of the box girder configuration y = b.

Wo will take the form:

$$Wo = F_0\{G_0 sh\lambda(b-y) + \lambda(b-y)ch\lambda(b-y)\}\sin(\lambda x)$$

$$\frac{\partial w_0}{\partial y} = -\lambda F_0\{G_0 ch\lambda(b-y) + \lambda(b-y)sh\lambda(b-y) + ch\lambda(b-y)\}\sin(\lambda x)$$

Now $M_{yyo} = -D\{\nabla^2 w_0 - (1-\nu)\frac{\partial^2 w_0}{\partial x^2}\}$

$$\nabla^2 w_0 = 2\lambda^2 sh\lambda(b-y).F_0$$

$$\frac{\partial^2 w_0}{\partial x^2} = -\lambda F_0\{G_0 sh\lambda(b-y) + \lambda(b-y)ch\lambda(b-y)\}\sin(\lambda x)$$

$$\therefore M_{yyo} = -D\Big[2\lambda^2 sh\lambda(b-y).F_0 + \lambda^2 F_0.\{G_0(1-\nu)sh\lambda(b-y) + (1-\nu)\lambda(b-y)ch\lambda(b-y)\}\Big]\sin(\lambda x) \qquad (3.8)$$

$$V_{yyo} = -D\frac{\partial}{\partial y}\{\nabla^2 w_0 + (1-\nu)\frac{\partial^2 w_0}{\partial x^2}$$

$$= -D\Big[-2\lambda^3 ch\lambda(b-y)F_0 + \lambda^3 F_0(1-\nu)\{G_0 ch\lambda(b-y) + ch\lambda(b-y) + \lambda(b-y)sh\lambda(b-y)\}\Big]\sin(\lambda x) \qquad (3.9)$$

At junction 4, $y = -b$

$$\therefore \quad Wo = F_1\{G_1 sh\lambda(y+b) + \lambda(y+b)ch\lambda(y+b)\}sin(\lambda x)$$

$$\frac{\partial w_0}{\partial y} = \lambda F_1\{G_1 ch\lambda(y+b) + ch\lambda(y+b) + \lambda(y+b)sh\lambda(y+b)\}sin(\lambda x)$$

$$\frac{\partial^2 w_0}{\partial x^2} = -\lambda^2 F_1\{G_1 sh\lambda(y+b) + \lambda(y+b)ch\lambda(y+b)\}sin(\lambda x)$$

$$\nabla^2 w_0 = 2\lambda^2 sh\lambda(y+b)F_1$$

$$M_{yyo} = -D\Big[2\lambda^2 sh\lambda(y+b).F_1 + \lambda^2 F_1\{G_1(1-\nu)sh\lambda(y+b) + (1-\nu)\lambda(y+b)ch\lambda(y+b)\}\Big]sin(\lambda x) \quad (3.10)$$

$$V_{yyo} = -D\Big[2\lambda^3 ch\lambda(y+b).F_1 - \lambda^3(1-\nu)F_1\{G_1 ch\lambda(y+b) + ch\lambda(y+b) + \lambda(y+b)sh\lambda(y+b)\}\Big]sin(\lambda x) \quad (3.11)$$

In this analysis, a superposition scheme for the deflection field will be used. A deflection field denoted by w^* will be superimposed on Wo (the known deflection field) and from the resulting total deflection $w = wo + w^*$ we will derive the slopes, moments and shears.

Now; guided by the trigonometric dependence of wo, we take w^* in the form:

$$w^* = \lambda\{A_n^{(i)}ch(\lambda y) + B_n^{(i)}sh(\lambda y) + C_n^{(i)}(\lambda y)ch(\lambda y) + D_n^{(i)}(\lambda y)sh(\lambda y)\}sin(\lambda x) \quad (3.12)$$

where superscripts in round brackets are used in reference to the plates. It will be observed that w^* satisfies the biharmonic equation

$$\frac{\partial^4 w}{\partial x^4} + \frac{2\partial^4 w}{\partial x^2 \partial y^2} + \frac{\partial^4 w}{\partial y^4} = 0 \quad (3.13)$$

$$\frac{\partial w^*}{\partial y} = \lambda^2\Big[A_n^{(i)}sh(\lambda y) + B_n^{(i)}ch(\lambda y) + C_n^{(i)}\{ch(\lambda y) + (\lambda y)sh(\lambda y)\} + D_n^{(i)}\{sh(\lambda y) + (\lambda y)ch(\lambda y)\}\Big]sin(\lambda x) \qquad (3.14)$$

$$\nabla^2 w = 2\lambda^3\{C_n^{(i)}sh(\lambda y) + D_n^{(i)}ch(\lambda y)\}sin(\lambda x)$$

$$\frac{\partial^2 w}{\partial x^2} = -\lambda^3\{A_m^{(i)}ch(\lambda y) + B_n^{(i)}sh(\lambda y) + C_n^{(i)}(\lambda y)ch(\lambda y) + D_n^{(i)}(\lambda y)sh(\lambda y)\}sin(\lambda x$$

$$M_{yy} = -D\{\nabla^2 w - (1-\nu)\frac{\partial^2 w}{\partial x^2}\}$$

$$= -D\lambda^3\Big[A_n^{(i)}(1-\nu)ch(\lambda y) + B_n^{(i)}(1-\nu)sh(\lambda y) + C_n^{(i)}\{2sh(\lambda y) + (1-\nu)(\lambda y)ch(\lambda y)\} + D_n^{(i)}\{2ch(\lambda y) + (1-\nu)(\lambda y)sh(\lambda y)\}\Big]sin(\lambda x) \qquad (3.15)$$

$$V_{yy} = -D\frac{\partial}{\partial y}\{\nabla^2 w + (1-\nu)\frac{\partial^2 w}{\partial x^2}\}$$

$$= -D\lambda^4\Big[-A_n^{(i)}(1-\nu)sh(\lambda y) - B_n^{(i)}(1-\nu)ch(\lambda y) + C_n^{(i)}\Big\{2ch(\lambda y) - (1-\nu)\{ch(\lambda y) + (\lambda y)sh(\lambda y)\}\Big\} + D_n^{(i)}\{2sh(\lambda y) - (1-\nu)\{sh(\lambda y) + (\lambda y)ch(\lambda y)\}\Big]sin(\lambda x$$

(3.16

Using the expressions for moment and shears in equations 3.10, 3.11, 3.15 and 3.16, the edge forces arising from consideration of bending only are readily determined.

3-4.2 IN-PLANE STRESS CONSIDERATIONS

The application of fourier transform together with the continuity conditions for plane stress suggest that the stress functions applicable to this problem should be constructed as follows:

$$\left.\begin{aligned} \phi_0 &= \{\bar{A}_n^{(i)}\,sh(\lambda y) + \bar{B}_n^{(i)}\,ch(\lambda y)\}\sin(\lambda x) \\ \phi_1 &= 0 \\ \phi_2 &= \lambda\{\bar{C}_n^{(i)}\,sh(\lambda y) + \bar{D}_n^{(i)}\,ch(\lambda y)\}\sin(\lambda x) \end{aligned}\right\} \qquad (3.17)$$

Where here and henceforth, a bar, placed over a quantity, is used to distinguish the extensional field from the deflexion field.

From previous definition of u_i,

$$\left.\begin{aligned} U_x &= \frac{\partial}{\partial x}(\phi_0 + y\phi_2) = \frac{\partial \phi_0}{\partial x} + y\frac{\partial \phi_2}{\partial x} \\ U_y &= \frac{\partial \phi_0}{\partial y} + y\frac{\partial \phi_2}{\partial y} + (1-2\kappa)\phi_2 \end{aligned}\right\} \qquad (3.18)$$

Where $\kappa = 2/(1+\nu)$

$$\therefore\ U_x^{(i)} = \lambda\{\bar{A}_n^{(i)}\,sh(\lambda y) + \bar{B}_n^{(i)}\,ch(\lambda y) + (\lambda y).\bar{C}_n^{(i)}\,sh(\lambda y) + (\lambda y).\bar{D}_n^{(i)}\,ch(\lambda y)\}\cos(\lambda x) \qquad (3.19)$$

$$U_y^{(i)} = \lambda\Big[\bar{A}_n^{(i)}\,ch(\lambda y) + \bar{B}_n^{(i)}\,sh(\lambda y) + \bar{C}_n^{(i)}\{(\lambda y)ch(\lambda y) + (1-2\kappa)sh(\lambda y)\} + \bar{D}_n^{(i)}\{(\lambda y)sh(\lambda y) + (1-2\kappa)ch(\lambda y)\}\Big]\sin(\lambda x) \qquad (3.20)$$

Now,

$$\sigma_{ij} = \mu\left(u_{i,j} + u_{j,i} + \frac{2\nu}{1-2\nu} U_{\kappa,\kappa}\ \delta_{ij}\right)$$

$$U_i = \frac{\partial}{\partial x_i}(\phi_0 + x_\kappa \phi_\kappa) - \frac{4}{1+\nu}\cdot\phi_i$$

$$= \frac{\partial}{\partial x_i}(\phi_0 + x_\kappa \phi_\kappa) - 2\kappa\phi_i$$

$$= \phi_{0,i} + (x_\kappa \phi_\kappa)_{,i} - 2\kappa\phi_i$$

$$= \phi_{0,i} + x_\kappa \phi_{\kappa,i} + x_{\kappa,i}\phi_\kappa - 2\kappa\phi_i$$

$$= \phi_{0,i} + x_\kappa \phi_{\kappa,i} + \delta_{i\kappa}\phi_\kappa - 2\kappa\phi_i$$

$$= \phi_{0,i} + x_\kappa \phi_{\kappa,i} + (1-2\kappa)\phi_i$$

$$U_{i,j} = \phi_{0,ij} + x_{\kappa,j}\phi_{\kappa,i} + x_\kappa \phi_{\kappa,ij} + (1-2\kappa)\phi_{i,j}$$

$$= \phi_{0,ij} + \phi_{j,i} + x_\kappa \phi_{\kappa,ij} + (1-2\kappa)\phi_{i,j}$$

$$= \phi_{0,ij} + \phi_{i,j} + x_\kappa \phi_{\kappa,ij} + (1-2\kappa)\phi_{j,i} \qquad (3.21)$$

$$\therefore \quad \sigma_{ij} = \mu\{2\phi_{0,ij} + 2(1-\kappa)\phi_{j,i} + 2(1-\kappa)\phi_{i,j}$$

$$+ 2x_\kappa \phi_{\kappa,ij} + 2(1-\kappa)\phi_{\kappa,\kappa}\delta_{ij}\}$$

$$= 2\mu\{\phi_{0,ij} + (1-2\kappa)(\phi_{i,j} + \phi_{j,i}) + x_\kappa \phi_{\kappa,ij}$$

$$+ (\kappa-2)\phi_{\kappa,\kappa}\ \delta_{ij}\} \qquad (3.22)$$

$$\therefore \quad \left.\begin{aligned} \sigma_{xx} &= 2\mu\{\frac{\partial^2\phi_0}{\partial x^2} + y\frac{\partial^2\phi_2}{\partial x^2} + (\kappa-2)\frac{\partial\phi_2}{\partial y}\} \\ \sigma_{yy} &= 2\mu\{\frac{\partial^2\phi_0}{\partial y^2} + y\frac{\partial^2\phi_2}{\partial y^2} - \kappa\frac{\partial\phi_2}{\partial y}\} \\ \sigma_{xy} &= 2\mu\{\frac{\partial^2\phi_0}{\partial x\partial y} + y\frac{\partial^2\phi_2}{\partial x\partial y} + (1-\kappa)\frac{\partial\phi_2}{\partial x}\} \end{aligned}\right\} \qquad (3.23)$$

$$\sigma_{xx} = 2\mu\lambda^2\Big[-\bar{A}_n^{(i)}sh(\lambda y) - \bar{B}_n^{(i)}ch(\lambda y) + \bar{C}_n^{(i)}\{(\kappa-2)ch(\lambda y) - (\lambda y)sh(\lambda y)\} + \bar{D}_n^{(i)}\{(\kappa-2)sh(\lambda y) - (\lambda y)ch(\lambda y)\}\Big]sin(\lambda x) \qquad (3.24)$$

$$\sigma_{yy} = 2\mu\lambda^2\Big[\bar{A}_n^{(i)}sh(\lambda y) + \bar{B}_n^{(i)}ch(\lambda y) + \bar{C}_n^{(i)}\{(\lambda y)sh(\lambda y) - \kappa ch(\lambda y)\} + \bar{D}_n^{(i)}\{(\lambda y)ch(\lambda y) - \kappa sh(\lambda y)\}\Big]sin(\lambda x) \qquad (3.25)$$

$$\sigma_{xy} = 2\mu\lambda^2\Big[\bar{A}_m^{(i)}ch(\lambda y) + \bar{B}_n^{(i)}sh(\lambda y) + \bar{C}_n^{(i)}\{(\lambda y)ch(\lambda y) + (1-\kappa)sh(\lambda y)\} + \bar{D}_n^{(i)}\{(\lambda y)sh(\lambda y) + (1-\kappa)ch(\lambda y)\}\Big]cos(\lambda x) \qquad (3.26)$$

From these expressions we can obtain the edge forces

$$N_{11}^{(y)} = t\sigma_{yy}|_{y=b} \quad , \quad S_{11}^{(xy)} = t\sigma_{xy}|_{y=b}$$

$$N_{14}^{(y)} = t\sigma_{yy}|_{y=-b} \quad , \quad S_{14}^{(xy)} = t\sigma_{xy}|_{y=-b} \text{ etc.}$$

3-5 EQUILIBRIUM OF FORCES AND COMPATIBILITY OF DISPLACEMENTS AT JOINTS

The forces at each joint were resolved in the horizontal and vertical directions. So also were the displacements. We will now proceed to write out these resolutions at each joint. Taking junction 1 as an example,

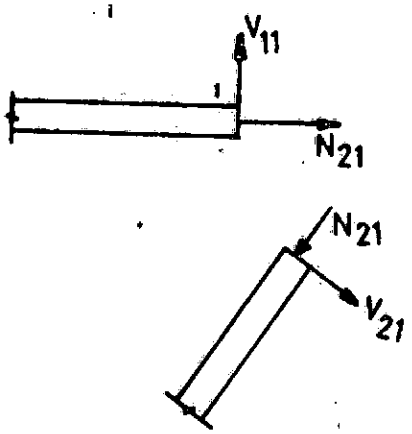

FORCES AT JOINT 1

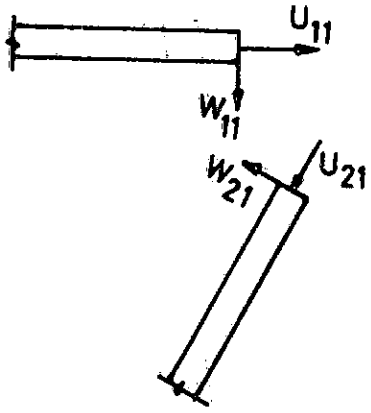

DISPLACEMENTS AT JOINT 1

Resolving the forces we have

1. $V_{11} - V_{21}\cos 2\alpha - N_{21}\sin 2\alpha = 0$

2. $N_{11} + V_{21}\sin 2\alpha - N_{21}\cos 2\alpha = 0$

Resolving the displacements we have,

3. $U_{11} + U_{21}\cos 2\alpha + W_{21}\sin 2\alpha = 0$

4. $W_{11} - U_{21}\sin 2\alpha + W_{21}\cos 2\alpha = 0$

Note: From henceforth two subscripts will be used. The first denotes the plate number, the second the joint number.

The other continuity conditions to be satisfied at the junction are:

5. $U_{x_{11}} - U_{x_{21}} = 0$

6. $\theta_{11} - \theta_{21} = 0$

7. $M_{y_{11}} - M_{y_{21}} = 0$

8. $N_{xy_{11}} + N_{xy_{21}} = 0$

In the same manner, the continuity conditions at the other three junctions are written.

JUNCTION 2

1. $V_{32} + V_{22}\cos 2\alpha + N_{22}\sin 2\alpha = 0$

2. $N_{32} + N_{22}\cos 2\alpha - V_{22}\sin 2\alpha = 0$

3. $U_{32} - W_{22}\sin 2\alpha - U_{22}\cos 2\alpha = 0$

4. $W_{32} + U_{22}\sin 2\alpha - W_{22}\cos 2\alpha = 0$

5. $U_{x_{22}} - U_{x_{32}} = 0$

6. $\theta_{22} - \theta_{32} = 0$

7. $M_{y_{22}} - M_{y_{32}} = 0$

8. $N_{xy_{22}} + N_{xy_{32}} = 0$

JUNCTION 3

1. $V_{33} + V_{43}\cos 2\alpha - N_{43}\sin 2\alpha = 0$

2. $N_{33} + N_{43}\cos 2\alpha + V_{43}\sin 2\alpha = 0$

3. $U_{33} - U_{43}\cos 2\alpha + W_{43}\sin 2\alpha = 0$

4. $W_{33} - W_{43}\cos 2\alpha - U_{43}\sin 2\alpha = 0$

5. $U_{x_{33}} - U_{x_{43}} = 0$

6. $\theta_{33} - \theta_{43} = 0$

7. $M_{y_{33}} - M_{y_{43}} = 0$

8. $N_{xy_{33}} + N_{xy_{43}} = 0$

JUNCTION 4

1. $V_{14} - V_{44}\cos 2\alpha + N_{44}\sin 2\alpha = 0$

2. $N_{14} - N_{44}\cos 2\alpha - V_{44}\sin 2\alpha = 0$

3. $U_{14} + U_{44}\cos 2\alpha - W_{44}\sin 2\alpha = 0$

4. $W_{14} + W_{44}\cos 2\alpha + U_{44}\sin 2\alpha = 0$

5. $U_{x_{44}} - U_{x_{14}} = 0$

6. $\theta_{44} - \theta_{14} = 0$

7. $M_{y_{44}} - M_{y_{14}} = 0$

8. $N_{xy_{44}} + N_{xy_{14}} = 0$

3-6 We now proceed to satisfy the joint equations taking the joints one by one. The equations are written out separately and explicitly in terms of the superposition coefficients.

1. $V_{11} - V_{21}\cos 2\alpha - N_{21}\cos 2\alpha = 0$

$$A_n^{(1)}P4.P8\,sh(\lambda b) + B_n^{(1)}P4.P8.ch(\lambda b) - C_n^{(1)}\{P5.P8ch(\lambda b) - P4.P8.(\lambda b)sh(\lambda b)\} - D_n^{(1)}\{P5.P8.sh(\lambda b) - P4.P8(\lambda b)ch(\lambda b)\}$$

$$+ A_n^{(2)}P4.P8.sh(\lambda c)\cos c - B_n^{(2)}P4.P8.ch(\lambda c)\cos c + C_n^{(2)}\{P5.P8.ch(\lambda c) - P4.P8(\lambda c)sh(\lambda c)\}\cos c - D_n^{(2)}\{P5.P8sh(\lambda c) - P4.P8(\lambda c)ch(\lambda c)\}\cos c$$

$$+ \bar{A}_n^{(2)}sh(\lambda c)\sin c - \bar{B}_n^{(2)}ch(\lambda c)\sin c - \bar{C}_n^{(2)}\{(\lambda c)sh(\lambda c) + P2ch(\lambda c)\}\sin c + \bar{D}_n^{(2)}\{(\lambda c)ch(\lambda c) + P2sh(\lambda c)\}\sin c = F_0.\lambda\{P4.G_0 - P5\}$$

2. $N_{11} + V_{21}\sin 2\alpha - N_{21}\cos 2\alpha = 0$

$$\bar{A}_n^{(1)}sh(\lambda b) + \bar{B}_n^{(1)}ch(\lambda b) + \bar{C}_n^{(1)}\{(\lambda b)sh(\lambda b) + P2ch(\lambda b)\} + \bar{D}_n^{(1)}\{(\lambda b)ch(\lambda b) + P2sh(\lambda b)\} + \bar{A}_n^{(2)}sh(\lambda c)\cos c - \bar{B}_n^{(2)}ch(\lambda c)\cos c - \bar{C}_n^{(2)}\{(\lambda c)sh(\lambda c) + P2ch(\lambda c)\}\cos c + \bar{D}_n^{(2)}\{(\lambda c)ch(\lambda c) + P2sh(\lambda c)\}\cos c - A_n^{(2)}P4.P8.sh(\lambda c)\sin c + B_n^{(2)}P4.P8.ch(\lambda c)\sin c - C_n^{(2)}\{P5.P8.ch(\lambda c) + P4.P8(\lambda c)sh(\lambda c)\}\sin c + D_n^{(2)}\{P5.P8.sh(\lambda c) - P4.P8.\lambda c.ch(\lambda c)\}\sin c = 0$$

3. $U_{11} + U_{21}\cos 2\alpha + W_{21}\sin 2\alpha = 0$

$$\overline{A}_n^{(1)}ch(\lambda b) + \overline{B}_n^{(1)}sh(\lambda b) + \overline{C}_n^{(1)}\{(\lambda b)ch(\lambda b) + Plsh(\lambda b)\} + \overline{D}_n^{(1)}\{(\lambda b)sh(\lambda b) + Plch(\lambda b)\} + \overline{A}_n^{(2)}ch(\lambda c)cosc - \overline{B}_n^{(2)}sh(\lambda c)cosc - \overline{C}_n^{(2)}\{(\lambda c)ch\lambda c + Plsh(\lambda c)cosc + \overline{D}_n^{(2)}\{(\lambda c)sh(\lambda c) + Plch(\lambda c)cosc + A_n^{(2)}ch(\lambda c)sinc - B_n^{(2)}sh(\lambda c)sinc - (\lambda c)C_n^{(2)}ch(\lambda c)sinc + D_n^{(2)}(\lambda c)sh(\lambda c)sinc = 0$$

4. $W_{11} - U_{21}\sin 2\alpha + W_{21}\cos 2\alpha = 0$

$$A_n^{(1)}ch(\lambda b) + B_n^{(1)}sh(\lambda b) + C_n^{(1)}(\lambda b)ch(\lambda b) + D_n^{(1)}(\lambda b)sh(\lambda b) + A_n^{(2)}ch(\lambda c)cosc - B_n^{(2)}sh(\lambda c)cosc - C_n^{(2)}(\lambda c)ch(\lambda c)cosc + D_n^{(2)}(\lambda c)sh(\lambda c)c - \overline{A}_n^{(2)}ch(\lambda c)sinc + \overline{B}_n^{(2)}sh(\lambda c)sinc + \overline{C}_n^{(2)}\{(\lambda c)ch(\lambda c) + Plsh(\lambda c)\}sinc - \overline{D}_n^{(2)}\{(\lambda c)sh(\lambda c) + Plch(\lambda c)\}sinc = 0$$

5. $U_{x_{11}} - U_{x_{21}} = 0$

$$\overline{A}_n^{(1)}sh(\lambda b) + \overline{B}_n^{(1)}ch(\lambda b) + (\lambda b)\overline{C}_n^{(1)}sh(\lambda b) + \overline{D}_n^{(1)}(\lambda b)ch(\lambda b) + \overline{A}_n^{(2)}sh(\lambda c) - \overline{B}_n^{(2)}ch(\lambda c) - (\lambda c)\overline{C}_n^{(2)}sh(\lambda c) + (\lambda c)\overline{D}_n^{(2)}ch(\lambda c) = 0$$

6. $\theta_{11} - \theta_{21} = 0$

$$A_n^{(1)}\lambda sh(\lambda b) + B_n^{(1)}\lambda ch(\lambda b) + C_n^{(1)}\lambda\{ch(\lambda b) + (\lambda b)sh(\lambda b)\} + D_n^{(1)}\lambda\{sh(\lambda b) + (\lambda b)ch(\lambda b)\} + A_n^{(2)}\lambda sh(\lambda c) - B_n^{(2)}\lambda ch(\lambda c) - C_n^{(2)}\lambda\{ch(\lambda c) + (\lambda c)sh(\lambda c)\} + \lambda D_n^{(2)}\{sh(\lambda c) + (\lambda c)ch(\lambda c)\} = F_0\{1 + G_0\}$$

7. $M_{y11} - M_{y21} = 0$

$$A_n^{(1)}ch(\lambda b) + B_n^{(1)}sh(\lambda b) + C_n^{(1)}\{P6sh(\lambda b) + (\lambda b)ch(\lambda b)\}$$
$$+ D_n^{(1)}\{P6ch(\lambda b) + (\lambda b)sh(\lambda b)\} - A_n^{(2)}ch(\lambda c) + B_n^{(2)}sh(\lambda c)$$
$$+ C_n^{(2)}\{P6sh(\lambda c) + (\lambda c)ch(\lambda c)\} - D_n^{(2)}\{P6ch(\lambda c) + (\lambda c)sh(\lambda c)\} = 0$$

8. $N_{xy11} + N_{xy21} = 0$

$$\overline{A}_n^{(1)}ch(\lambda b) + \overline{B}_n^{(1)}sh(\lambda b) + \overline{C}_n^{(1)}\{(\lambda b)ch(\lambda b) + P3sh(\lambda b)\}$$
$$+ \overline{D}_n^{(1)}\{(\lambda b)sh(\lambda b) + P3ch(\lambda b)\} + \overline{A}_n^{(2)}ch(\lambda c) - \overline{B}_n^{(2)}sh(\lambda c)$$
$$- \overline{C}_n^{(2)}\{(\lambda c)ch(\lambda c) + P3sh(\lambda c)\} + \overline{D}_n^{(2)}\{(\lambda c)sh(\lambda c) + P3ch(\lambda c)\} = 0$$

JUNCTION 2:

1. $V_{32} + V_{22}cos2\alpha + N_{22}sin2\alpha = 0$

$$-A_n^{(3)}P4.P8.sh(\lambda d) + B_n^{(3)}P4.P8.ch(\lambda d) - C_n^{(3)}\{-P4.P8(\lambda d)ch(\lambda d)$$
$$+ P5.P8.ch(\lambda d)\} + D_n^{(3)}\{-P4.P8.ch(\lambda d) + P5.P8.sh(\lambda d)\} + A_n^{(2)}P4.P8.sh(\lambda c)cos$$
$$+ B_n^{(2)}P4.P8.ch(\lambda c)cosc - C_n^{(2)}\{P5.P8.ch(\lambda c) - P4.P8.(\lambda c)sh(\lambda c)\}cosc$$
$$- D_n^{(2)}\{P5.P8.sh(\lambda c) - P4.P8.(\lambda c)ch(\lambda c)\}cosc + \overline{A}_n^{(2)}sh(\lambda c)sinc$$
$$+ \overline{B}_n^{(2)}ch(\lambda c)sinc + \overline{C}_n^{(2)}\{(\lambda c)sh(\lambda c) + P2ch(\lambda c)\}.sinc$$
$$+ \overline{D}_n^{(2)}\{(\lambda c)ch(\lambda c) + P2sh(\lambda c)\}.sinc = 0$$

2. $N_{32} + N_{22}\cos 2\alpha - V_{22}\sin 2\alpha = 0$

$$-\bar{A}_n^{(3)}\mathrm{sh}(\lambda d) + \bar{B}_n^{(3)}\mathrm{ch}(\lambda d) + \bar{C}_n^{(3)}\{(\lambda d)\mathrm{sh}(\lambda d) + P2\mathrm{ch}(\lambda d)\}$$
$$- D_n^{(3)}\{(\lambda d)\mathrm{ch}(\lambda d) + P2\mathrm{sh}(\lambda d)\} + \bar{A}_n^{(2)}\mathrm{sh}(\lambda c)\cos c + \bar{B}_n^{(2)}\mathrm{ch}(\lambda c)\cos c$$
$$+ \bar{C}_n^{(2)}\{(\lambda c)\mathrm{sh}(\lambda c) + P2\mathrm{ch}(\lambda c)\}\cos c + \bar{D}_n^{(2)}\{(\lambda c)\mathrm{ch}(\lambda c) + P2\mathrm{sh}(\lambda c)\}\cos c$$
$$- A_n^{(2)}P4.P8.\mathrm{sh}(\lambda d)\sin c - B_n^{(2)}P4.P8.\mathrm{ch}(\lambda d)\sin c + C_n^{(2)}\{P5.P8.\mathrm{ch}(\lambda d)$$
$$- P4.P8(\lambda d)\mathrm{sh}(\lambda d)\}\sin c + D_n^{(2)}\{P5.P8.\mathrm{sh}(\lambda d) - P4.P8(\lambda d)\mathrm{ch}(\lambda d)\sin c = 0$$

3. $U_{32} - W_{22}\sin 2\alpha - U_{22}\cos 2\alpha = 0$

$$\bar{A}_n^{(3)}\mathrm{ch}(\lambda d) - \bar{B}_n^{(3)}\mathrm{sh}(\lambda d) - \bar{C}_n^{(3)}\{(\lambda d)\mathrm{ch}(\lambda d) + P1\mathrm{sh}(\lambda d)\}$$
$$+ \bar{D}_n^{(3)}\{(\lambda d)\mathrm{sh}(\lambda d) + P1\mathrm{ch}(\lambda d)\} - \bar{A}_n^{(2)}\mathrm{ch}(\lambda c)\cos c - \bar{B}_n^{(2)}\mathrm{sh}(\lambda c)\cos c$$
$$- \bar{C}_n^{(2)}\{(\lambda c)\mathrm{ch}(\lambda c) + P1\mathrm{sh}(\lambda c)\}\cos c - \bar{D}_n^{(2)}\{(\lambda c)\mathrm{sh}(\lambda c) + P1\mathrm{ch}(\lambda c)\}\cos c$$
$$- A_n^{(2)}\mathrm{ch}(\lambda c)\sin c - B_n^{(2)}\mathrm{sh}(\lambda c)\sin c - C_n^{(2)}(\lambda c)\mathrm{ch}(\lambda c)\sin c$$
$$- D_n^{(2)}(\lambda c)\mathrm{sh}(\lambda c)\sin c = 0$$

4. $W_{32} + U_{22}\sin 2\alpha - W_{22}\cos 2\alpha = 0$

$$A_n^{(3)}\mathrm{ch}(\lambda d) - B_n^{(3)}\mathrm{sh}(\lambda d) - C_n^{(3)}(\lambda d)\mathrm{ch}(\lambda d) + D_n^{(3)}(\lambda d)\mathrm{sh}(\lambda d)$$
$$- A_n^{(2)}\mathrm{ch}(\lambda c)\cos c - B_n^{(2)}\mathrm{sh}(\lambda c)\cos c - C_n^{(2)}(\lambda c)\mathrm{ch}(\lambda c)\cos c - D_n^{(2)}(\lambda c)\mathrm{sh}(\lambda c)\cos$$
$$+ \bar{A}_n^{(2)}\mathrm{ch}(\lambda c)\sin c + \bar{B}_n^{(2)}\mathrm{sh}(\lambda c)\sin c + \bar{C}_n^{(2)}\{(\lambda c)\mathrm{ch}(\lambda c) + P1\mathrm{sh}(\lambda c)\}\sin c$$
$$+ \bar{D}_n^{(2)}\{(\lambda c)\mathrm{sh}(\lambda c) + P1\mathrm{ch}(\lambda c)\}\sin c = 0$$

5. $U_{x_{22}} - U_{x_{32}} = 0$

$$\bar{A}_n^{(2)}sh(\lambda c) + \bar{B}_n^{(2)}ch(\lambda c) + \bar{C}_n^{(2)}(\lambda c)sh(\lambda c) + \bar{D}_n^{(2)}(\lambda c)ch(\lambda c)$$
$$+ \bar{A}_n^{(3)}sh(\lambda d) - \bar{B}_n^{(3)}ch(\lambda d) - (\lambda d)\bar{C}_n^{(3)}sh(\lambda d) + \bar{D}_n^{(3)}(\lambda d)ch(\lambda d) = 0$$

6. $\theta_{22} - \theta_{32} = 0$

$$A_n^{(2)}sh(\lambda c) + B_n^{(2)}ch(\lambda c) + C_n^{(2)}\{ch(\lambda c) + (\lambda c)sh(\lambda c)\}$$
$$+ D_n^{(2)}\{sh(\lambda c) + (\lambda c)ch(\lambda c)\} + A_n^{(3)}sh(\lambda d) - B_n^{(3)}ch(\lambda d)$$
$$- C_n^{(3)}\{ch(\lambda d) + (\lambda d)sh(\lambda d)\} + D_n^{(3)}\{sh(\lambda d) + (\lambda d)ch(\lambda d)\} = 0$$

7. $M_{y_{22}} - M_{y_{32}} = 0$

$$A_n^{(2)}ch(\lambda c) + B_n^{(2)}sh(\lambda c) + C_n^{(2)}\{P6sh(\lambda c) + (\lambda c)ch(\lambda c)\}$$
$$+ D_n^{(2)}\{P6ch(\lambda c) + (\lambda c)sh(\lambda c)\} - A_n^{(3)}ch(\lambda d) + B_n^{(3)}sh(\lambda d)$$
$$+ C_n^{(3)}\{P6sh(\lambda d) + (\lambda d)ch(\lambda d)\} - D_n^{(3)}\{P6ch(\lambda d) + (\lambda d)sh(\lambda d)\} = 0$$

8. $N_{xy_{22}} + N_{xy_{32}} = 0$

$$\bar{A}_n^{(2)}ch(\lambda c) + \bar{B}_n^{(2)}sh(\lambda c) + \bar{C}_n^{(2)}\{(\lambda c)ch(\lambda c) + P1sh(\lambda c)\}$$
$$+ \bar{D}_n^{(2)}\{(\lambda c)sh(\lambda c) + P1ch(\lambda c)\} + \bar{A}_n^{(3)}ch(\lambda d) - \bar{B}_n^{(3)}sh(\lambda d)$$
$$- \bar{C}_n^{(3)}\{(\lambda d)ch(\lambda d) + P1sh(\lambda d)\} + \bar{D}_n^{(3)}\{(\lambda d)sh(\lambda d) + P1ch(\lambda d)\} = 0$$

JUNCTION 3:

1. $V_{33} + V_{43}\cos 2\alpha - N_{43}\sin 2\alpha = 0$

$$A_n^{(3)}P4.P8.sh(\lambda d) + B_n^{(3)}P4.P8.ch(\lambda d) - C_n^{(3)}\{P5.P8.ch(\lambda d) - P4.P8.(\lambda d)sh(\lambda d)\} - D_n^{(3)}\{P5.P8.sh(\lambda d) - P4.P8(\lambda d)ch(\lambda d)\} - A_n^{(4)}P4.P8.sh(\lambda c)\cos c + B_n^{(4)}P4.P8.ch(\lambda c)\cos c - C_n^{(4)}\{P5.P8.ch(\lambda c) - P4.P8(\lambda c)sh(\lambda c)\}\cos c + D_n^{(4)}\{P5.P8.sh(\lambda c) - P4.P8(\lambda c)ch(\lambda c)\}\cos c + \bar{A}_n^{(4)}sh(\lambda c)\sin c - \bar{B}_n^{(4)}ch(\lambda c)\sin c - \bar{C}_n^{(4)}\{(\lambda c)sh(\lambda c) + P2ch(\lambda c)\}\sin c + \bar{D}_n^{(4)}\{(\lambda c)ch(\lambda c) + P2sh(\lambda c)\}\sin c = 0$$

2. $N_{33} + N_{43}\cos 2\alpha + V_{43}\sin 2\alpha = 0$

$$\bar{A}_n^{(3)}sh(\lambda d) + \bar{B}_n^{(3)}ch(\lambda d) + \bar{C}_n^{(3)}\{(\lambda d)sh(\lambda d) + P2ch(\lambda d)\} + \bar{D}_n^{(3)}\{(\lambda d)ch(\lambda d) + P2sh(\lambda d)\} - \bar{A}_n^{(4)}sh(\lambda c)\cos c + \bar{B}_n^{(4)}ch(\lambda c)\cos c + \bar{C}_n^{(4)}\{(\lambda c)sh(\lambda c) + P2ch(\lambda c)\}\cos c - \bar{D}_n^{(4)}\{(\lambda c)ch(\lambda c) + P2sh(\lambda c)\}\cos c - A_n^{(4)}P4.P8.sh(\lambda c)\sin c + B_n^{(4)}P4.P8.ch(\lambda c)\sin c - C_n^{(4)}\{P5.P8.ch(\lambda c) - P4.P8.(\lambda c)sh(\lambda c)\}\sin c + D_n^{(4)}\{P5.P8.sh(\lambda c) - P4.P8(\lambda c)ch(\lambda c)\}\sin c =$$

3. $U_{33} - U_{43}\cos 2\alpha + W_{43}\sin 2\alpha = 0$

$$A_n^{(3)}ch(\lambda d) + \bar{B}_n^{(3)}sh(\lambda d) + \bar{C}_n^{(3)}\{(\lambda d)ch(\lambda d) + P1sh(\lambda d)\} + \bar{D}_n^{(3)}\{(\lambda d)sh(\lambda d) + P1ch(\lambda c)\} - \bar{A}_n^{(4)}ch(\lambda c)\cos c + \bar{B}_n^{(4)}sh(\lambda c)\cos c + \bar{C}_n^{(4)}\{(\lambda c)ch(\lambda c) + P1sh(\lambda c)\}\cos c - \bar{D}_n^{(4)}\{(\lambda c)sh(\lambda c) + P1ch(\lambda c)\}\cos c + A_n^{(4)}ch.(\lambda c)\sin c - B_n^{(4)}sh(\lambda c)\sin c - C_n^{(4)}(\lambda c)ch(\lambda c)\sin c + D_n^{(4)}(\lambda c)sh(\lambda c)\sin c = 0$$

4. $W_{33} - W_{43}\cos 2\alpha - U_{43}\sin 2\alpha = 0$

$$A_n^{(3)}ch(\lambda d) + B_n^{(3)}sh(\lambda d) + C_n^{(3)}(\lambda d)ch(\lambda d) + D_n^{(3)}(\lambda d)sh(\lambda d)$$
$$- A_n^{(4)}ch(\lambda c)\cos c + B_n^{(4)}sh(\lambda c)\cos c + C_n^{(4)}(\lambda c)ch(\lambda c)\cos c$$
$$- D_n^{(4)}(\lambda c)sh(\lambda c)\cos c - \bar{A}_n^{(4)}ch(\lambda c)\sin c + \bar{B}_n^{(4)}sh(\lambda c)\sin c$$
$$+ \bar{C}_n^{(4)}\{(\lambda c)ch(\lambda c) + Plsh(\lambda c)\}\sin c - \bar{D}_n^{(4)}\{(\lambda c)sh(\lambda c)$$
$$+ Plch(\lambda c)\}\sin c = 0$$

5. $U_{x_{33}} - U_{x_{43}} = 0$

$$\bar{A}_n^{(3)}sh(\lambda d) + \bar{B}_n^{(3)}ch(\lambda d) + \bar{C}_n^{(3)}(\lambda d)sh(\lambda d) + \bar{D}_n^{(3)}(\lambda d)ch(\lambda d)$$
$$+ \bar{A}_n^{(4)}sh(\lambda c) - \bar{B}_n^{(4)}ch(\lambda c) - (\lambda c)\bar{C}_n^{(4)}sh(\lambda c) + \bar{D}_n^{(4)}(\lambda c)ch(\lambda c) = 0$$

6. $\theta_{33} - \theta_{43} = 0$

$$A_n^{(3)}sh(\lambda d) + B_n^{(3)}ch(\lambda d) + C_n^{(3)}\{ch(\lambda d) + (\lambda d)sh(\lambda d)\}$$
$$+ D_n^{(3)}\{sh(\lambda d) + (\lambda d)ch(\lambda d)\} - A_n^{(4)}sh(\lambda c) - B_n^{(4)}ch(\lambda c)$$
$$- C_n^{(4)}\{ch(\lambda c) + (\lambda c)sh(\lambda c)\} - D_n^{(4)}\{sh(\lambda c) + (\lambda c)ch(\lambda c)\} = 0$$

7. $M_{y_{33}} - M_{y_{43}} = 0$

$$A_n^{(3)}ch(\lambda d) + B_n^{(3)}sh(\lambda d) + C_n^{(3)}\{P6sh(\lambda d) + (\lambda d)ch(\lambda d)\}$$
$$+ D_n^{(3)}\{P6ch(\lambda d) + (\lambda d)sh(\lambda d)\} - A_n^{(4)}ch(\lambda d) + B_n^{(4)}sh(\lambda c)$$
$$+ C_n^{(4)}\{P6sh(\lambda c) + (\lambda c)ch(\lambda c)\} - D_n^{(4)}\{P6.ch(\lambda c) + (\lambda c)sh(\lambda c)\} = 0$$

8. $N_{xy_{33}} + N_{xy_{43}} = 0$

$$\overline{A}_n^{(3)}ch(\lambda d) + \overline{B}_n^{(3)}sh(\lambda d) + \overline{C}_n^{(3)}\{(\lambda d)ch(\lambda d) + P1sh(\lambda d)\}$$
$$+ \overline{D}_n^{(3)}\{(\lambda d)sh(\lambda d) + P1ch(\lambda d)\} + \overline{A}_n^{(4)}ch(\lambda c) - \overline{B}_n^{(4)}sh(\lambda c)$$
$$- \overline{C}_n^{(4)}\{(\lambda c)ch(\lambda c) + P1sh(\lambda d)\} + \overline{D}_n^{(4)}\{(\lambda c)sh(\lambda c) + P1ch(\lambda c)\} = 0$$

JUNCTION 4

1. $V_{14} - V_{44}\cos 2\alpha + N_{44}\sin 2\alpha = 0$

$$- A_n^{(1)}P4.P8.sh(\lambda b) + B_n^{(4)}P4.P8.ch(\lambda b) - C_n^{(4)}\{P5.P8.ch(\lambda b)$$
$$- P4.P8(\lambda b).sh(\lambda b)\} + D_n^{(1)}\{P5.P8.sh(\lambda b) - P4.P8.(\lambda b)ch(\lambda b)\}$$
$$- A_n^{(4)}P4.P8.sh(\lambda c)\cos c - B_n^{(4)}P4.P8.ch(\lambda c)\cos c + C_n^{(4)}\{P5.P8.ch(\lambda c)$$
$$- P4.P8(\lambda c)sh(\lambda c)\}\cos c + D_n^{(4)}\{P5.P8.sh(\lambda c) - P4.P8(\lambda c)ch(\lambda c)\}\cos c$$
$$+ \overline{A}_n^{(4)}sh(\lambda c)\sin c + \overline{B}_n^{(4)}ch(\lambda c)\sin c + \overline{C}_n^{(4)}\{(\lambda c)sh(\lambda c) + P2ch(\lambda c)\sin c$$
$$+ \overline{D}_n^{(4)}\{(\lambda c)ch(\lambda c) + P2sh(\lambda c)\sin c = -\lambda F_1\{P4G_1 - P5\}$$

2. $N_{14} - N_{44}\cos 2\alpha - V_{44}\sin 2\alpha = 0$

$$- \overline{A}_n^{(1)}sh(\lambda b) + \overline{B}_n^{(1)}ch(\lambda b) + \overline{C}_n^{(1)}\{(\lambda b)sh(\lambda b) + P2ch(\lambda b)\}$$
$$- \overline{D}_n^{(1)}\{(\lambda b)ch(\lambda b) + P2sh(\lambda b)\} - \overline{A}_n^{(4)}sh(\lambda c)\cos c - \overline{B}_n^{(4)}ch(\lambda c)\cos c$$
$$- \overline{C}_n^{(4)}\{(\lambda c)sh(\lambda c) + P2ch(\lambda c)\}\cos c - \overline{D}_n^{(4)}\{(\lambda c)ch(\lambda c) + P2sh(\lambda c)\}\cos c$$
$$- A_n^{(4)}P4.P8.sh(\lambda c)\sin c - B_n^{(4)}P8.P4.ch(\lambda c)\sin c + C_n^{(4)}\{P5.P8.ch(\lambda c)$$
$$- P4.P8(\lambda c)sh(\lambda c)\}\sin c + D_n^{(4)}\{P5.P8.sh(\lambda c) - P4.P8(\lambda c)ch(\lambda c)\}\sin c =$$

3. $U_{14} + U_{44}\cos 2\alpha - W_{44}\sin 2\alpha = 0$

$$- A_n^{(1)}ch(\lambda b) - B_n^{(1)}sh(\lambda b) - C_n^{(1)}(\lambda b)ch(\lambda b) - D_n^{(1)}(\lambda b)sh(\lambda b)$$
$$+ A_n^{(4)}ch(\lambda c)\cos c - B_n^{(4)}sh(\lambda c)\cos c - C_n^{(4)}(\lambda c)ch(\lambda c)\cos c$$
$$+ D_n^{(4)}(\lambda c)sh(\lambda c)\cos c + \overline{A}_n^{(4)}ch(\lambda c)\sin c + \overline{B}_n^{(4)}sh(\lambda c)\sin c$$
$$+ \overline{C}_n^{(4)}\{(\lambda c)ch(\lambda c) + Plsh(\lambda c)\}\sin c + \overline{D}_n^{(4)}\{(\lambda c)sh(\lambda c)$$
$$+ Plch(\lambda c)\}\sin c = 0$$

4. $W_{14} + W_{44}\cos 2\alpha + U_{44}\sin 2\alpha = 0$

$$\overline{A}_n^{(1)}ch(\lambda b) + \overline{B}_n^{(1)}sh(\lambda b) + \overline{C}_n^{(1)}\{(\lambda b)ch(\lambda b) + Plsh(\lambda b)\}$$
$$+ \overline{D}_n^{(1)}\{(\lambda b)sh(\lambda b) + Plch(\lambda b)\} + \overline{A}_n^{(4)}ch(\lambda c)\cos c$$
$$+ \overline{B}_n^{(4)}sh(\lambda c)\cos c + \overline{C}_n^{(4)}\{(\lambda c)ch(\lambda c) + Plsh(\lambda c)\}\cos c$$
$$+ \overline{D}_n^{(4)}\{(\lambda c)sh(\lambda c) + Plch(\lambda c)\}\cos c + A_n^{(4)}ch(\lambda c)\sin c$$
$$- B_n^{(4)}sh(\lambda c)\sin c - C_n^{(4)}(\lambda c)ch(\lambda c)\sin c + D_n^{(4)}(\lambda c)sh(\lambda c)\sin c = 0$$

5. $U_{x_{44}} - U_{x_{14}} = 0$

$$\overline{A}_n^{(4)}sh(\lambda c) + \overline{B}_n^{(4)}ch(\lambda c) + \overline{C}_n^{(4)}(\lambda c)sh(\lambda c) + \overline{D}_n^{(4)}(\lambda c)ch(\lambda c)$$
$$+ \overline{A}_n^{(1)}sh(\lambda b) - \overline{B}_n^{(1)}ch(\lambda b) - \overline{C}_n^{(1)}(\lambda b)sh(\lambda b) + \overline{D}_n^{(1)}(\lambda b)ch(\lambda b) = 0$$

6. $\theta_{44} - \theta_{14} = 0$

$$- A_n^{(1)}\lambda sh(\lambda b) + B_n^{(1)}\lambda ch(\lambda b) + C_n^{(1)}\lambda\{ch(\lambda b) + (\lambda b)sh(\lambda b)\}$$
$$- D_n^{(1)}\lambda\{sh(\lambda b) + (\lambda b)ch(\lambda b)\} - A_n^{(4)}\lambda sh(\lambda c) - B_n^{(4)}\lambda ch(\lambda c)$$
$$- C_n^{(4)}\lambda\{ch(\lambda c) + (\lambda c)sh(\lambda c)\} - D_n^{(4)}\lambda\{sh(\lambda c) + (\lambda c)ch(\lambda c)\}$$
$$= -F_1\{1+G_1\}$$

7. $M_{y_{44}} - M_{y_{14}} = 0$

$$- A_n^{(1)}ch(\lambda b) + B_n^{(1)}sh(\lambda b) + C_n^{(1)}\{P6.sh(\lambda b) + (\lambda b)ch(\lambda b)\}$$
$$- D_n^{(1)}\{P6.ch(\lambda b) + (\lambda b)sh(\lambda b)\} + A_n^{(4)}ch(\lambda c) + B_n^{(4)}sh(\lambda c)$$
$$+ C_n^{(4)}\{P6.sh(\lambda c) + (\lambda c)ch(\lambda c)\} + D_n^{(4)}\{P6.ch(\lambda c) + (\lambda c)sh(\lambda c)\} = 0$$

8. $N_{xy_{44}} + N_{xy_{14}} = 0$

$$+ \overline{A}_n^{(1)}ch(\lambda b) - \overline{B}_n^{(1)}sh(\lambda b) - \overline{C}_n^{(1)}\{(\lambda b)ch(\lambda b) + Plsh(\lambda b)\}$$
$$+ \overline{D}_n^{(1)}\{(\lambda b)sh(\lambda b) + Plch(\lambda b)\} + A_n^{(4)}ch(\lambda c) + B_n^{(4)}sh(\lambda c)$$
$$+ \overline{C}_n^{(4)}\{(\lambda c)ch(\lambda c) + Plsh(\lambda c)\} + \overline{D}_n^{(4)}\{(\lambda c)sh(\lambda c) + Plch(\lambda c)\} = 0$$

In satisfying these joint continuity conditions, we arrive at thirty-two equations. The expressions for the non-zero elements of the resulting matrix and the non-zero elements of the resulting right-hand column matrix are given in the Appendix.

These equations were written out in matrix form for computational purposes on the IBM 370/145 computer at the University of Lagos Computer Centre. The method of solution and the computer programme used are given in the Appendix.

3-6 THEORY OF GOLDBERG AND LEVE

The method of analysis due to Goldberg and Leve is now presented because of the similarity of its theoretical basis with the formulation presented in this work, namely extensional and bending theories of plates.

Goldberg's formulation for folded plates considers the simultaneous plate bending and membrane action of several plates. The forces at the longitudinal edges of each plate are expressed as fixed-edge forces corrected or modified by the effect of displacement of the joints. The displacements to be determined are visualised as being four in number at each point of the joint, thus yielding a total number of 4n simultaneous equations, 'n' being the number of joints.

In this thesis however, a uniformity of method is maintained by using Papkovitch - Neuber potentials for the extensional theory. Apart from completeness and familiarisation with the harmonic functions, this approach has the added advantage of avoiding Goldberg's trial substitution from which success can be expected only if one is sufficiently experienced on the solution of boundary-value problems of elasticity.

Besides, the main advantage of Goldberg's formulation, namely the reduction of the number of equations to be solved from 8n to 4n, where n is the number of joints, is achieved at the expense of simplicity of approach in formulation. His general formulation does not sufficiently reveal the physics of the problem, especially to the

uninitiated. In any event, with the existence of computers capable of solving a large number of equations, particularly when the finite difference or the finite element approach is used in solving this class of problems, little would appear to be gained from this reduction in the number of equations, when it is realised that the complicated form of the equations resulting from Goldberg's formulation may occasion many human errors in a large system.

GOLDBERG and LEVE'S FORMULATION

The four displacements at an edge are as follows:

Two components of translation and a rotation all lying in the plane normal to the joint i.e.,

(i) Translation of edges i and j) "w" Normal to slab
(ii) Rotation of edges i and j) "θ"
(iii) Translations normal to edges i and j) "v" In plane of slab
(iv) Translation tangential to edges i and j) "u" In direction of joint

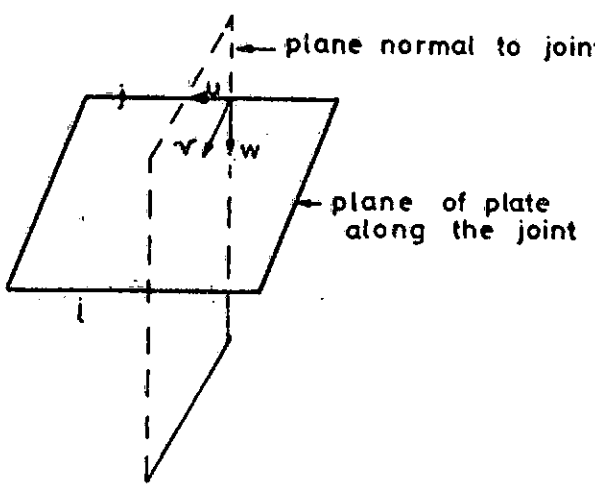

FIG 3-6

EDGE DISPLACEMENTS AND EDGE FORCE RELATIONS

First a single slab is considered and formulae are developed for the internal forces resulting from the various generalised edge displacements. These edge displacements are of two types:

Displacement normal to the slab, arising from plate bending, and displacement in the plane of the slab arising from membrane stresses.

DISPLACEMENTS NORMAL TO THE SLAB

The displacement normal to the slab 'w' was taken in the form suggested by Levy as

$$w(x,y) = \Sigma w_m(y)\sin.\frac{m\pi x}{a} \qquad 3.27$$

The m^{th} term must satisfy the homogeneous differential equation of the form

$$\frac{\partial^4 w}{\partial x^4} + \frac{2\partial^4 w}{\partial x^2 \partial y^2} + \frac{\partial^4 w}{\partial y^4} \qquad 3.28$$

For Wm to satisfy equation (3.26), $W_m(y)$ must be of the form:

$$Wm = A_1 m.\sinh.\frac{m\pi y}{a} + A_2 m.\cosh.\frac{m\pi y}{a} + A_3 m.\frac{m\pi y}{a},\sinh.\frac{m\pi y}{a} + A_4 m.\frac{m\pi y}{a}.\cosh.\frac{m\pi y}{a} \qquad 3.29$$

The plate problem may now be resolved into the following two edge-displacement cases for a typical slab i-j.

CASE A ROTATIONS OF EDGES i and j

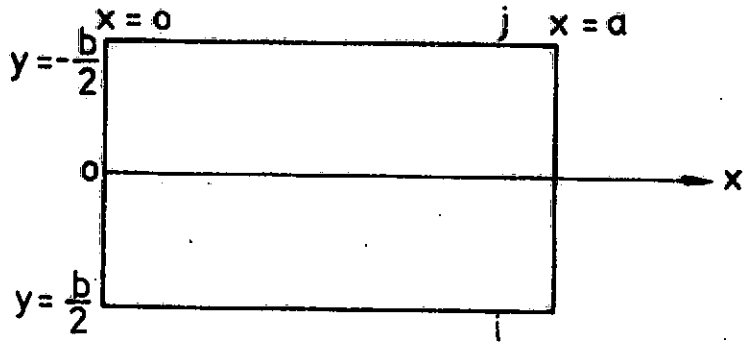

Boundary conditions:

$$\left.\begin{aligned} &\left(Wm = 0 \;,\; \frac{\partial^2 w_m}{\partial x^2} = 0\right)_{x=o,x=a} \\ &\left(Wm = 0\right)_{y=\pm b/2} \end{aligned}\right] \qquad 3.30$$

$$\left(\frac{\partial w_m}{\partial y}\right)_{y=b/2} = \theta_{im}.\sin.\frac{m\pi x}{a}, \left(\frac{\partial w_m}{\partial y}\right)_{y=-b/2} = \bar{\theta}_{jm}.\sin.\frac{m\pi x}{a} \qquad 3.31$$

It can be seen that the expressions for w_m satisfies the boundary conditions w_m and Mx at x = o and x = a.

The problem is further simplified by considering the plate edge rotations in two parts:

(i) Symmetrical case in which the rotations of plate ij at its edges i and j (i.e. $y=\pm\frac{b}{2}$) are equal but oposite in sign.

$$\theta'_{ijm} = -\theta'_{jim} = \overline{\theta}'_{im}.\sin.\frac{m\pi x}{a}$$

Since the rotation must be an odd function of y to achieve anti-symmetry in rotation at the plate edges, it follows that the form of w_m must be an even function of y thereby making the superposition coefficients A_{1m} and A_{4m} to assume zero values.

Applying these stated edge conditions to the residual form of w_m and satisfying the additional boundary condition $w_m = o$ at $y = \pm\frac{b}{2}$, we deduce that

$$A_{2m} = -\alpha_m A_{3m} \tanh\alpha_m \qquad \text{where } \alpha_m = \frac{m\pi b}{a}$$

$$A_{3m} = \frac{b\,\overline{\theta}'_{im}}{\alpha_m(\alpha_m \operatorname{sech}\alpha_m + \sinh\alpha_m)}$$

and hence

$$w_m = \frac{b\,\overline{\theta}'_{im}}{\alpha_m(\alpha_m \operatorname{sech}\alpha_m + \sinh\alpha_m)}\left[\frac{\alpha_m y}{b}.\operatorname{sh}\left(\frac{\alpha_m y}{b}\right) - \alpha_m \operatorname{th}\alpha_m \operatorname{ch}\left(\frac{\alpha_m y}{b}\right)\right]$$

..... 3.32

(ii) Anti-symmetric case in which the rotations of plate ij at its edges i and j are equal,

$$\theta''_{ijm} = \theta''_{jim} = \overline{\theta}''_{im}.\sin.\frac{m\pi x}{a}$$

Since the edge rotations are the same, the form of displacement w_m must be an odd function of y, thereby making A_{3m} and A_{2m} to assume zero values. Applying the edge conditions as stated under (ii) above to the residual form of w_m and satisfying the condition of zero transverse displacement at $y = \pm b$ we establish that

$$A_{1m} = -\alpha_m A_{4m} \coth\alpha_m$$

$$A_{4m} = \frac{-b\bar{\theta}''_{im}}{\alpha_m(\alpha_m \operatorname{csch}\alpha_m - \operatorname{ch}\alpha_m)}$$

and hence

$$w_m = \frac{-b\bar{\theta}''_{im}.\sin(\frac{m\pi x}{a})}{\alpha_m(\alpha_m \operatorname{csch}\alpha_m - \operatorname{ch}\alpha_m)}\left[\frac{\alpha_m y}{b}.\operatorname{ch}\left(\frac{\alpha_m y}{b}\right) - \alpha_m \operatorname{cth}\alpha_m \operatorname{sh}\left(\frac{\alpha_m y}{b}\right)\right] \quad \ldots\ldots\ldots \quad 3.33$$

If it is assumed that a positive rotation occurs at the positive end of our y- coordinate axis, i.e. at i, then

$$\theta_{ijm} = \theta'_{ijm} + \theta''_{ijm} = \bar{\theta}'_{im} + \bar{\theta}''_{im}$$

and $$\theta_{jim} = \theta'_{jim} + \theta''_{jim} = -\bar{\theta}'_{im} + \bar{\theta}''_{im}$$

from which we deduce that for the symmetrical part

$$\bar{\theta}'_{im} = \tfrac{1}{2}(\theta_{im} - \theta_{jm})$$

where θ_{ijm} and θ_{jim} are respectively the m^{th} term of the θ_{ij} and θ_{ji} half-range series and

for the anti-symmetric part

$$\bar{\theta}''_{im} = \tfrac{1}{2}(\theta_{im} + \theta_{jm})$$

The complete solution for w_m incorporating the odd and even parts now takes the form

$$w_m = \frac{b}{2}\sin\left(\frac{m\pi x}{a}\right)\Bigg[\theta_{im}\left\{(\alpha_m\text{sech}\alpha_m + \sinh\alpha_m)^{-1}\left\{\frac{y}{b}\text{sh}\left(\frac{\alpha_m y}{b}\right) - \tanh\alpha_m\text{ch}\left(\frac{\alpha_m y}{b}\right)\right\}\right.$$

$$\left. - (\alpha_m\text{cosech}\alpha_m - \cosh\alpha_m)^{-1}\left\{\frac{y}{b}\text{ch}\left(\frac{\alpha_m y}{b}\right) - \coth\alpha_m\text{sh}\left(\frac{\alpha_m y}{b}\right)\right\}\right\}$$

$$- \theta_{jm}\left\{(\alpha_m\text{sech}\alpha_m + \sinh\alpha_m)^{-}\ \frac{y}{b}\text{sh}\left(\frac{\alpha_m y}{b}\right) - \tan\alpha_m\text{ch}\left(\frac{\alpha_m y}{b}\right)\right.$$

$$\left. + (\alpha_m\text{cosech}\alpha_m - \cosh\alpha_m)^{-1}\left\{\frac{y}{b}\text{ch}\left(\frac{\alpha_m y}{b}\right) - \coth\alpha_m\text{sh}\left(\frac{\alpha_m y}{b}\right)\right\}\right\}\Bigg]$$

..... 3.34

CASE B TRANSLATION OF THE EDGES

The boundary conditions at the simply supported edges x = o and x = a remain the same; the other edge conditions are

$$\frac{\partial w_m}{\partial y} = 0 \text{ at } y = \pm b$$

The problem is treated in a manner similar to case A; that is a division of the problem into

(i) symmetric , in which $w_{ijm} = w_{jim} = \bar{w}'_{im}\sin\frac{m\pi x}{a}$

and (ii) anti-symmetric , in which $w_{ijm} = -w_{jim} = \bar{w}''_{im}\sin\frac{m\pi x}{a}$

The structure of w_m for the symmetric case is $w_m = \left[A_{2m}\cosh\left(\frac{m\pi y}{a}\right)\right.$

$$\left. + A_{3m}\left(\frac{m\pi y}{a}\right)\sinh\left(\frac{m\pi y}{a}\right)\right]\sin\left(\frac{m\pi x}{a}\right)$$

From the boundary conditions at the edges, we find

$$A_{2m} = -A_{3m}(1 + \alpha_m\coth\alpha_m)$$

and so

$$W_m = A_{3m}\left[\frac{m\pi y}{a}.\sinh\left(\frac{m\pi y}{a}\right) - (1 + \alpha_m \coth\alpha_m)\cosh\left(\frac{m\pi y}{a}\right)\right]\sin\frac{m\pi x}{a}$$

Noting that the displacement at the edges is $\overline{W}'_{im}\sin\frac{m\pi x}{a}$

then $$A_{3m} = \frac{-\overline{W}'_{im}}{\alpha_m \operatorname{csch}\alpha_m + \cosh\alpha_m}$$

For the anti-symmetric case

$$W_m = \left(A_{1m}\sinh\left(\frac{m\pi y}{a}\right) + A_{4m}\frac{m\pi y}{a}.\cosh\left(\frac{m\pi y}{a}\right)\right)\sin\frac{m\pi x}{a}$$

From which we deduce that

$$A_{1m} = -A_{4m}(1 + \alpha_m \tanh\alpha_m)$$

$$A_{4m} = \frac{\overline{W}''_{im}}{\alpha_m \operatorname{sech}\alpha_m - \sinh\alpha_m}$$

Noting as in the previous case A that

$$\overline{W}'_{im} = \tfrac{1}{2}(w_{im} - w_{jm})$$

and $$\overline{W}''_{im} = \tfrac{1}{2}(w_{im} + w_{jm})$$

then the complete form of W_m is given by

$$W_m = \tfrac{1}{2}\sin\frac{m\pi x}{a}\Bigg[w_{im}\Big((\alpha_m \operatorname{csch}\alpha_m + \cosh\alpha_m)^{-1}\Big\{-\frac{\alpha_m y}{b}.\sinh\left(\frac{\alpha_m y}{b}\right) + (1 + \alpha_m \coth\alpha_m)\cosh\left(\frac{\alpha_m y}{b}\right)\Big\} + (\alpha_m \operatorname{sech}\alpha_m - \sinh\alpha_m)^{-1}$$

$$\Big\{-(1 + \alpha_m \tanh\alpha_m)\sinh\left(\frac{\alpha_m y}{b}\right) + \frac{\alpha_m y}{b}.\cosh\left(\frac{\alpha_m y}{b}\right)\Big\}\Big)$$

$$- w_{jm}\Big((\alpha_m \mathrm{csch}\alpha_m + \mathrm{ch}\alpha_m)^{-1}\{-\frac{\alpha_m y}{b}\mathrm{sh}\Big(\frac{\alpha_m y}{b}\Big) + (1+\alpha_m \mathrm{coth}\alpha_m)\mathrm{ch}\Big(\frac{\alpha_m y}{b}\Big)\}$$

$$- (\alpha_m \mathrm{sech}\alpha_m - \mathrm{sh}\alpha_m)^{-1}\{-(1+\alpha_m \tanh\alpha_m)\mathrm{sh}\Big(\frac{\alpha_m y}{b}\Big) + \frac{\alpha_m y}{b}\mathrm{ch}\Big(\frac{\alpha_m y}{b}\Big)\}\Big)\Big] \qquad (3.35)$$

The total displacement field in terms of the edge rotation and edge displacements W can now be written in the form:

$$W_m = \sin\frac{m\pi x}{a}.\Big[\theta_{im}\{\gamma_{1m}F_1(y) - \gamma_{2m}F_2(y)\} - \theta_{jm}\{\gamma_{1m}F_1(y) + \gamma_{2m}F_2(y)\}$$

$$- w_{im}\{\gamma_{3m}F_3(y) - \gamma_{4m}F_4(y)\} + w_{jm}.\{\gamma_{3m}F_3(y) + \gamma_{4m}F_4(y)\}\Big]$$

where $\gamma_{1m} = \frac{b}{2}(\alpha_m \mathrm{sech}\alpha_m + \mathrm{sh}\alpha_m)^{-1}$

$\gamma_{2m} = \frac{b}{2}(\alpha_m \mathrm{cosech}\alpha_m - \mathrm{ch}\alpha_m)^{-1}$

$\gamma_{3m} = \frac{1}{2}(\alpha_m \mathrm{cosech}\alpha_m + \mathrm{ch}\alpha_m)^{-1}$

$\gamma_{4m} = \frac{1}{2}(\alpha_m \mathrm{sech}\alpha_m - \mathrm{sh}\alpha_m)^{-1}$

$F_1(y) = \frac{y}{b}.\sinh(\frac{\alpha_m y}{b}) - \tanh\alpha_m \cosh(\frac{\alpha_m y}{b})$

$F_2(y) = \frac{y}{b}.\cosh(\frac{\alpha_m y}{b}) - \coth\alpha_m \sinh(\frac{\alpha_m y}{b})$

$F_3(y) = \frac{\alpha_m y}{b}.\sinh(\frac{\alpha_m y}{b}) - (1+\alpha_m \coth\alpha_m)\cosh(\frac{\alpha_m y}{b})$

$F_4(y) = \frac{\alpha_m y}{b}.\cosh(\frac{\alpha_m y}{b}) - (1+\alpha_m \tanh\alpha_m)\sinh(\frac{\alpha_m y}{b})$

These expressions will be used later to determine moments and shears at the edges of plates joined in such a way at their adjacent edges to form a system of folded plate to any given geometrical form.

In-plane displacements or membrane forces

If we assume u_1 and u_2 to be the in-plane displacements in the x and y directions respectively. It can be easily demonstrated that the structures of u_1 and u_2 that satisfy the equilibrium equations in plane stress without body forces are

$$u_1 = \left[A_{1m} ch\left(\frac{\alpha_m y}{b}\right) + A_{2m} sh\left(\frac{\alpha_m y}{b}\right) + A_{3m} \cdot \frac{\alpha_m y}{b} ch\left(\frac{\alpha_m y}{b}\right) + A_{4m} \cdot \frac{\alpha_m y}{b} sh\left(\frac{\alpha_m y}{b}\right) \right] \sin\left(\frac{m\pi x}{b}\right)$$

$$u_2 = \left[B_{1m} ch\left(\frac{\alpha_m y}{b}\right) + B_{2m} sh\left(\frac{\alpha_m y}{b}\right) + B_{3m} \cdot \frac{\alpha_m y}{b} ch\left(\frac{\alpha_m y}{b}\right) + B_{4m} \cdot \frac{\alpha_m y}{b} sh\left(\frac{\alpha_m y}{b}\right) \right] \sin\left(\frac{m\pi x}{a}\right)$$

where the B_{im}'s are related to A_{im}'s in the following manner:

$$B_{1m} = A_{2m} - \frac{3-\nu}{1+\nu} \cdot A_{3m}, \quad B_{2m} = A_{1m} - \frac{3-\nu}{1+\nu} \cdot A_{4m}$$

$$B_{3m} = A_{4m}, \quad B_{4m} = A_{3m}$$

Case A Translation Normal to the edges i and j

Considering now the translations of the edges i and j of plate ij in the direction of y only. If the solution is split into (i) symmetrical case in which $(u_{2m})_{y=b} = -(u_{2m})_{y=-b}$ and (ii) anti-symmetrical case in which $(u_{2m})_{y=b} = (u_{2m})_{y=-b}$ and applying the implied boundary condition that $u_1 = 0$ at $y = \pm b$, the complete solutions using the techniques of the earlier analysis are as follows:

$$u_{1m} = \tfrac{1}{2}\cos\frac{m\pi x}{a}\Big[u_{2im}\{(\alpha_m \operatorname{sech}\alpha_m - \tfrac{3-\nu}{1+\nu}\operatorname{sh}\alpha_m)^{-1}\alpha_m F_1(y)$$

$$- (\alpha_m \operatorname{cosech}\alpha_m + \tfrac{3-\nu}{1+\nu}\operatorname{ch}\alpha_m)^{-1}\alpha_m F_2(y)\}$$

$$- u_{2jm}\{(\alpha_m \operatorname{sech}\alpha_m - \tfrac{3-\nu}{1+\nu}\operatorname{sh}\alpha_m)^{-1}\alpha_m F_1(y)$$

$$+ (\alpha_m \operatorname{cosech}\alpha_m + \tfrac{3-\nu}{1+\nu}\operatorname{ch}\alpha_m)^{-1}\alpha_m F_2(y)\}\Big]$$

$$u_{2m} = \tfrac{1}{2}\sin\frac{m\pi x}{a}\Big[u_{2im}\{(\alpha_m \operatorname{sech}\alpha_m - \tfrac{3-\nu}{1+\nu}\operatorname{sh}\alpha_m)^{-1}\alpha_m F_5(y)$$

$$- (\alpha_m \operatorname{cosech}\alpha_m + \tfrac{3-\nu}{1+\nu}\operatorname{sh}\alpha_m)^{-1}\alpha_m F_6(y)\}$$

$$- u_{2jm}(\alpha_m \operatorname{sech}\alpha_m - \tfrac{3-\nu}{1+\nu}\operatorname{sh}\alpha_m)^{-1}\alpha_m F_5(y)$$

$$+ (\alpha_m \operatorname{cosech}\alpha_m + \tfrac{3-\nu}{1+\nu}\operatorname{ch}\alpha_m)^{-1}\alpha_m F_6(y)$$

where $F_5(y) = \frac{y}{b}\operatorname{ch}(\frac{\alpha_m y}{b}) - \{\frac{3-\nu}{1+\nu}.\alpha_m^{-1} + \tanh\alpha_m\}\operatorname{sh}(\frac{\alpha_m y}{b})$

$F_6(y) = \frac{y}{b}\operatorname{sh}(\frac{\alpha_m y}{b}) - \{\frac{3-\nu}{1+\nu}.\alpha_m^{-1} + \coth\alpha_m\}\operatorname{ch}(\frac{\alpha_m y}{b})$

Case B. Translations Tangential to the edges i and j

In this case translations take place in the direction of x whilst at the edges i and j translations in the direction of y are completely restrained i.e. $u_2 = 0$ for $y = \pm b$.

Again, following the procedure adopted in the preceding analysis and noting that

$$(u_1)_{y=b} = u_{1im}\cos(\frac{m\pi x}{a}), (u_1)_{y=-b} = u_{1jm}\cos(\frac{m\pi x}{a})$$

and further splitting the translations into

(i) symmetrical, in which $(u_{1m})_{y=b} = (u_{1m})_{y=-b}$

and (ii) anti-symmetrical, in which $(u_{1m})_{y=b} = -(u_{1m})_{y=-b}$

we arrive at the following equations for u_1 and u_2

$$u_{1m} = \tfrac{1}{2}\cos(\frac{m\pi x}{a})\Big[u_{1im}\{-(\alpha_m \operatorname{cosech}\alpha_m - \frac{3-\nu}{1+\nu}\operatorname{ch}\alpha_m)^{-1}\alpha_m F_7(y) + (\alpha_m \operatorname{sech}\alpha_m + \frac{3-\nu}{1+\nu}\operatorname{sh}\alpha_m)^{-1}\alpha_m F_8(y)\} - u_{1jm}\{(\alpha_m \operatorname{cosech}\alpha_m - \frac{3-\nu}{1+\nu}\operatorname{ch}\alpha_m)^{-1}\alpha_m F_7(y) + (\alpha_m \operatorname{sech}\alpha_m + \frac{3-\nu}{1+\nu}\operatorname{sh}\alpha_m)^{-1}\alpha_m F_8(y)\}\Big]$$

$$u_{2m} = \tfrac{1}{2}\sin(\frac{m\pi x}{a})\Big[u_{1im}\{(\alpha_m \operatorname{sech}\alpha_m + \frac{3-\nu}{1+\nu}\operatorname{sh}\alpha_m)^{-1}\alpha_m F_1(y) - (\alpha_m \operatorname{cosech}\alpha_m - \frac{3-\nu}{1+\nu}\operatorname{ch}\alpha_m)^{-1}\alpha_m F_2(y)\} - u_{1jm}\{(\alpha_m \operatorname{sech}\alpha_m + \frac{3-\nu}{1+\nu}\operatorname{sh}\alpha_m)^{-1}\alpha_m F_1(y) + (\alpha_m \operatorname{cosech}\alpha_m - \frac{3-\nu}{1+\nu}\operatorname{ch}\alpha_m)^{-1}\alpha_m F_2(y)\}\Big]$$

where $F_7(y) = \frac{y}{b}\operatorname{sh}(\frac{\alpha_m y}{b}) + \{\frac{3-\nu}{1+\nu}\alpha_m^{-1} - \coth\alpha_m\}\operatorname{ch}(\frac{\alpha_m y}{b})$

$F_8(y) = \frac{y}{b}\operatorname{ch}(\frac{\alpha_m y}{b}) + \{\frac{3-\nu}{1+\nu}\alpha_m^{-1} - \tanh\alpha_m\}\operatorname{sh}(\frac{\alpha_m y}{b})$

The total in-plane displacement fields now become

$$u_{1m} = \tfrac{1}{2}\cos\left(\frac{m\pi x}{a}\right)\Big[u_{2im}\{\beta_{1m}F_1(y) - \beta_{2m}F_2(y)\} - u_{2jm}\{\beta_{1m}F_1(y) + \beta_{2m}F_2(y)\} + u_{1im}\{-\beta_{3m}F_7(y) + \beta_{4m}F_8(y)\} - u_{1jm}\{\beta_{3m}F_1(y) + \beta_{4m}F_2(y)\}\Big] \quad \ldots\ldots\ldots (3.36)$$

$$u_{2m} = \tfrac{1}{2}\sin\left(\frac{m\pi x}{a}\right)\Big[u_{2im}\{\beta_{1m}F_5(y) - \beta_{2m}F_6(y)\} - u_{2jm}\{\beta_{1m}F_5(y) + \beta_{2m}F_6(y)\} + u_{1im}\{\beta_{4m}F_1(y) - \beta_{3m}F_2(y)\} - u_{1jm}\{\beta_{4m}F_1(y) + \beta_{3m}F_2(y)\}\Big] \quad \ldots\ldots\ldots (3.37)$$

where $\beta_{1m} = (\alpha_m \operatorname{sech}\alpha_m - \frac{3-\nu}{1+\nu}\operatorname{sh}\alpha_m)^{-1}\alpha_m$

$\beta_{2m} = (\alpha_m \operatorname{cosech}\alpha_m + \frac{3-\nu}{1+\nu}\operatorname{ch}\alpha_m)^{-1}\alpha_m$

$\beta_{3m} = (\alpha_m \operatorname{cosech}\alpha_m - \frac{3-\nu}{1+\nu}\operatorname{ch}\alpha_m)^{-1}\alpha_m$

$\beta_{4m} = (\alpha_m \operatorname{sech}\alpha_m + \frac{3-\nu}{1+\nu}\operatorname{sh}\alpha_m)^{-1}\alpha_m$

Having determined the transverse and in-plane displacement fields, it now only remains to evaluate moments, shears and stress resultants needed for ensuring equilibrium at the junctions. These are M_{yy}, V_{yy}, N_{yy} and N_{xy} at junctions i and j.

The expressions that define these moments and forces in terms of displacements are as follows:

$$M_{yy} = -D\left(\frac{\partial^2 w_m}{\partial y^2} + \nu\frac{\partial^2 w_m}{\partial x^2}\right)$$

$$V_{yy} = -D\left(\frac{\partial^3 w_m}{\partial y^3} + (2-\nu)\frac{\partial^3 w_m}{\partial x^2 \partial y}\right)$$

$$N_{yy} = \frac{Eh}{1-\nu^2}\left(\frac{\partial u_2}{\partial y} + \frac{\partial u_1}{\partial x}\right)$$

$$N_{xy} = \frac{Eh}{2(1+\nu)}\left(\frac{\partial u_1}{\partial y} + \frac{\partial u_2}{\partial x}\right)$$

where $D = \frac{Eh^3}{12(1-\nu^2)}$

Applying these relations to the equations of displacements already derived we find that the edge forces are as follows: at end i

$$M_{yy}^{ij} = \frac{Eh^3}{12(1-\nu^2)} \sin\frac{m\pi x}{a}\left[C_1\theta_{im} + C_2\theta_{jm} - C_3 w_{im} + C_4 w_{jm}\right]$$

$$V_{yy}^{ij} = \frac{Eh^3}{12(1-\nu^2)} \sin\frac{m\pi x}{a}\left[C_5\theta_{im} + C_6\theta_{jm} - C_7 w_{im} + C_8 w_{jm}\right]$$

$$N_{yy}^{ij} = \frac{Eh}{(1+\nu)^2} \sin\frac{m\pi x}{a}\left[-C_9 u_{2im} + C_{10} u_{2jm} - C_{11} u_{1im} + C_{12} u_{1jm}\right]$$

$$N_{xy}^{ij} = \frac{Eh}{(1+\nu)^2} \cos\frac{m\pi x}{a}\left[-C_{13} u_{2im} - C_{14} u_{2jm} - C_{15} u_{1im} + C_{16} u_{1jm}\right] \quad 3.38$$

and at end j

$$M_{yy}^{ji} = \frac{Eh^3}{12(1-\nu^2)} \sin\frac{m\pi x}{a}\left[C_1\theta_{jm} + C_2\theta_{im} + C_3 w_{jm} - C_4 w_{im}\right]$$

$$V_{yy}^{ji} = \frac{Eh^3}{12(1-\nu^2)} \sin\frac{m\pi x}{a}\left[-C_5\theta_{jm} - C_6\theta_{im} - C_7 w_{jm} + C_8 w_{im}\right]$$

$$N_{yy}^{ji} = \frac{Eh}{(1+\nu)^2} \sin\frac{m\pi x}{a}\left[-C_9 u_{2jm} + C_{10} u_{2im} + C_{11} u_{1jm} - C_{12} u_{1im}\right]$$

$$N_{xy}^{ji} = \frac{Eh}{(1+\nu)^2} \cos\frac{m\pi x}{a}\left[C_{13} u_{2jm} + C_{14} u_{2jm} - C_{15} u_{1jm} + C_{16} u_{1im}\right] \quad 3.39$$

where

$$C_1 = \frac{\alpha_m}{b}\left[\frac{\cosh\alpha_m}{(\alpha_m\operatorname{sech}\alpha_m + \sinh\alpha_m)} - \frac{\sinh\alpha_m}{(\alpha_m\operatorname{cosech}\alpha_m - \cosh\alpha_m)}\right]$$

$$C_2 = -\frac{\alpha_m}{b}\left[\frac{\cosh\alpha_m}{(\alpha_m\operatorname{sech}\alpha_m + \sinh\alpha_m)} + \frac{\sinh\alpha_m}{(\alpha_m\operatorname{cosech}\alpha_m - \cosh\alpha_m)}\right]$$

$$C_3 = C_5 = \left(\frac{\alpha_m}{b}\right)^2\left[\frac{\cosh\alpha_m}{(\alpha_m\operatorname{cosech}\alpha_m + \cosh\alpha_m)} - \frac{\sinh\alpha_m}{(\alpha_m\operatorname{sech}\alpha_m - \sinh\alpha_m)} - (1-\nu)\right]$$

$$C_4 = C_6 = -\left(\frac{\alpha_m}{b}\right)^2\left[\frac{\cosh\alpha_m}{(\alpha_m\operatorname{cosech}\alpha_m + \cosh\alpha_m)} + \frac{\sinh\alpha_m}{(\alpha_m\operatorname{sech}\alpha_m - \sinh\alpha_m)}\right]$$

$$C_7 = \left(\frac{\alpha_m}{b}\right)^3\left[\frac{\sinh\alpha_m}{(\alpha_m\operatorname{cosech}\alpha_m + \cosh\alpha_m)} - \frac{\cosh\alpha_m}{(\alpha_m\operatorname{sech}\alpha_m - \sinh\alpha_m)}\right]$$

$$C_8 = -\left(\frac{\alpha_m}{b}\right)^3\left[\frac{\sinh\alpha_m}{(\alpha_m\operatorname{cosech}\alpha_m + \cosh\alpha_m)} + \frac{\cosh\alpha_m}{(\alpha_m\operatorname{sech}\alpha_m - \sinh\alpha_m)}\right]$$

$$C_9 = \frac{\alpha_m}{b}\left[-\frac{\cosh\alpha_m}{(\alpha_m\operatorname{sech}\alpha_m - \frac{3-\nu}{1+\nu}\sinh\alpha_m)} + \frac{\sinh\alpha_m}{(\alpha_m\operatorname{csch}\alpha_m + \frac{3-\nu}{1+\nu}\cosh\alpha_m)}\right]$$

$$C_{10} = -\frac{\alpha_m}{b}\left[\frac{\cosh\alpha_m}{(\alpha_m\operatorname{sech}\alpha_m - \frac{3-\nu}{1+\nu}\sinh\alpha_m)} + \frac{\sinh\alpha_m}{(\alpha_m\operatorname{csch}\alpha_m + \frac{3-\nu}{1+\nu}\cosh\alpha_m)}\right]$$

$$C_{11} = C_{13} = \frac{\alpha_m}{b}\left[\frac{\cosh\alpha_m}{(\alpha_m\operatorname{csch}\alpha_m - \frac{3-\nu}{1+\nu}\cosh\alpha_m)} - \frac{\sinh\alpha_m}{(\alpha_m\operatorname{sech}\alpha_m + \frac{3-\nu}{1+\nu}\sinh\alpha_m)} + (1+\nu)\right]$$

$$C_{12} = C_{14} = -\frac{\alpha_m}{b}\left[\frac{\cosh\alpha_m}{(\alpha_m \operatorname{csch}\alpha_m - \frac{3-\nu}{1+\nu}\cosh\alpha_m)} + \frac{\sinh\alpha_m}{(\alpha_m \operatorname{sech}\alpha_m + \frac{3-\nu}{1+\nu}\sinh\alpha_m)}\right]$$

$$C_{15} = \frac{\alpha_m}{b}\left[-\frac{\sinh\alpha_m}{(\alpha_m \operatorname{csch}\alpha_m - \frac{3-\nu}{1+\nu}\cosh\alpha_m)} + \frac{\cosh\alpha_m}{(\alpha_m \operatorname{sech}\alpha_m + \frac{3-\nu}{1+\nu}\sinh\alpha_m)}\right]$$

$$C_{16} = \frac{\alpha_m}{b}\left[\frac{\sinh\alpha_m}{(\alpha_m \operatorname{csch}\alpha_m - \frac{3-\nu}{1+\nu}\cosh\alpha_m)} + \frac{\cosh\alpha_m}{(\alpha_m \operatorname{sech}\alpha_m + \frac{3-\nu}{1+\nu}\sinh\alpha_m)}\right]$$

To these edges, forces given in equations 3.38 & 39 must be added the fixed edge forces arising from the initially loaded plates clamped at their opposite edges $y = \pm b$.

Since the direction of joint forces and joint displacements of two slabs meeting at a point do not in general have a common orientation, it is convenient to refer these quantities to the same of axes through a transformation process. The joint forces and joint displcements are therefore transformed from the changing (y,z) directions at each edge to fixed (ξ,η) directions.

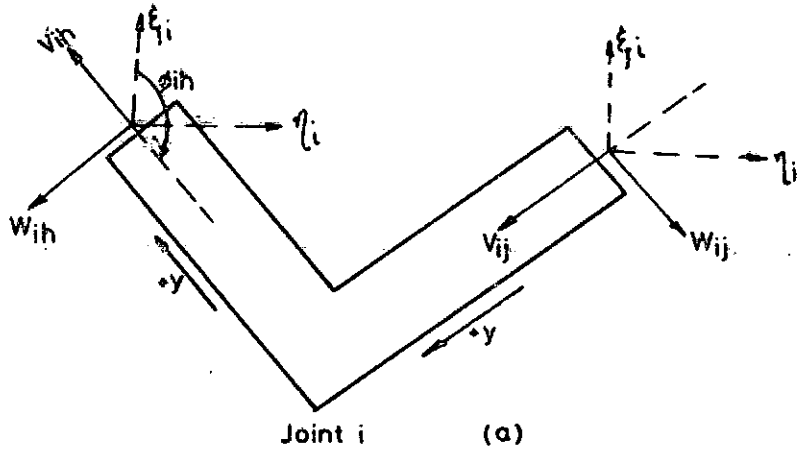

TRANSFORMATION OF JOINT DISPLACEMENTS

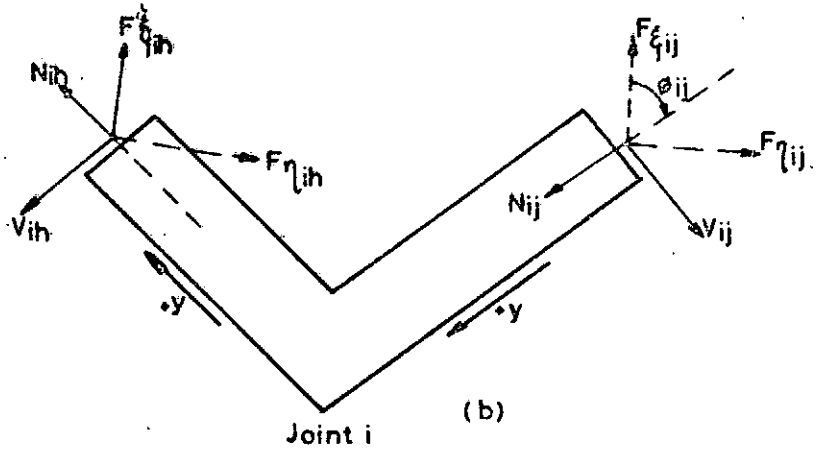

TRANSFORMATION OF JOINT FORCES.

FIG 3-7

Using this technique the joint displacement transform to

$$w_{ijm} = \eta_{im}\cos\phi_{ij} - \xi_{im}\sin\phi_{ij}$$

$$u_{2ijm} = -\eta_{im}\sin\phi_{ij} - \xi_{im}\cos\phi_{ij}$$

$$w_{ihm} = \eta_{im}\cos\phi_{ih} - \xi_{im}\sin\phi_{ih}$$

$$u_{2ihm} = -\eta_{im}\sin\phi_{ih} - \xi_{im}\cos\phi_{ih} \qquad 3.40$$

whilst the joint forces transform to:

$$F_{\eta ijm} = V_{ijm}\cos\phi_{ij} - N_{ijm}\sin\phi_{ij}$$

$$F_{\xi ijm} = -V_{ijm}\sin\phi_{ij} - N_{ijm}\cos\phi_{ij}$$

$$F_{\eta ihm} = V_{ihm}\cos\phi_{ih} - N_{ihm}\sin\phi_{ih}$$

$$F_{\xi ihm} = -V_{ihm}\sin\phi_{ih} - N_{ihm}\cos\phi_{ih} \qquad 3.41$$

These being the relations a joint i of two slabs hi and ij joined at i. The first set of equations, that is equations 3.40, ensure the satisfaction of compatibility of displacements at the joint whilst the second set, equations 3.41, together with equations of moments and membrane shears are used to satisfy the quilibrium conditions of forces at the joint thus:

$$M_{ijm} + M_{ihm} = 0$$

$$F_{\eta ijm} + F_{\eta ihm} = 0$$

$$F_{\xi ijm} + F_{\xi ihm} = 0$$

$$S_{ijm} + S_{ihm} = 0$$

All the transformed joint forces and moments at joint i are now expressible in terms of the joint roations θ_h, θ_i and θ_j, the joint displacements η_h, η_i, η_j, ξ_h, ξ_i, ξ_j, and u_{1h}, u_{1i}, u_{1j}.

It is immediately seen that there are four unkown displacements at each joint which will completely define the state of shears in any system of folded slab.

When applied to a single cell box girder with four corners, there will therefore be sixteen equations with sixteen unkown displacements. The mean advantage of the method is the reduction in the number of equations for a single cell box girder from thrity-two equations with thirty-two unknowns to one of sixteen by sixteen.

Goldberg derived the fixed edge forces which are given below:

$$M_{ijm} = -M_{jim} = \frac{4qa^2}{m^3\pi^3}\left[\frac{2\cosh\alpha_m}{\alpha_m \operatorname{csch}\alpha_m + \cosh\alpha_m} - 1\right]\sin\frac{m\pi x}{a}$$

$$V_{ijm} = V_{jim} = \frac{8qa}{m^2\pi^2}\,\frac{\sinh\alpha_m}{(\alpha_m \operatorname{csch}\alpha_m + \cosh\alpha_m)}\sin\frac{m\pi x}{a}$$

TABLE 1

2B/L	(β) ANALYSIS	(β) MOFFATT
0.00	1.0	1.00
0.10	0.95	0.80
0.20	0.88	0.67
0.40	0.71	0.49
0.60	0.59	0.38
0.80	0.50	0.30
1.00	0.43	0.28

NOTE: Merrison's recommendations have been derived from table given by Moffatt.

3-7 DISCUSSIONS OF THEORETICAL RESULTS

GENERAL COMMENTS:

The method of analysis presented lends itself to application as a design tool and as a means of checking almost completed designs. Although this work is limited to isotropic plates, the analysis for an orthotropic plate system is not of a higher degree of complexity. The choice of an isotropic plate system is deliberate in order to obtain theoretical results which may be an aid in the design proposals for an orthotropic system. As a design tool the method is less cumbersome for computer application than the finite element approach of analysing this type of structure. The displacement method of analysis of folded plates due to Goldberg and Leve certainly has the merit of solving fewer equations but, as has been observed elsewhere, it does not lend itself to ready application by the practitioner without the involvement of a specialist. It also has the disadvantage of a large number of back substitutions, with possible attendant computational errors, whereas this method is more direct for obtaining stresses and displacements in one operation. The resulting equations from a consideration of equilibrium and compatibility of displacements at the joints were solved using the Gauss-Jordan complete elimination method for varieties of single cell box girder cross-sectional geometry.

DISPLACEMENTS

Attention was paid to deflexions as the dominant displacement for transverse loading. The deflexions are in general small for the transverse loading of 200KN adopted for purposes of computation,

especially considering that one of the sections considered was wide and shallow, the depth to width ratio being one to four. The element of the box section that suffers greatest in terms of deflexion is the top compression flange to which the load is directly applied. This is in accord with St. Venant's principle. The conclusion drawn from this is that the transition from a single cell section to a double or multiple cell section should be partly governed by a consideration of limitation on deflexions. Figure 3·8 shows the trend of central deflexion with top and bottom box girder widths. It should be noted that the deflexion of the bottom plate is upward, that is, hogging. However, a quantitative discussion of the deflexion cannot be done since the section was not subjected to normal HA loading.

STRESSES

For symmetrical loading the stresses exhibit shear lag phenomenon in both top and bottom flanges. Effective widths based on an average stress equal to the maximum theoretical flange stress were computed for a rectangular section and a symmetrical trapezoidal section.

Top and bottom flanges of both the rectangular and the trapezoidal box sections exhibit shear lag. In the case of rectangular section, where top and bottom flange widths are the same, shear lag effects are about the same. In the trapezoidal box section however, the bottom flange which is comparatively smaller in width exhibits shear lag to a lesser extent. It is therefore obvious that the aspect ratio is the dominant factor in effective width variation in both top and bottom flange plates regardless of the fact that one is in compression and the

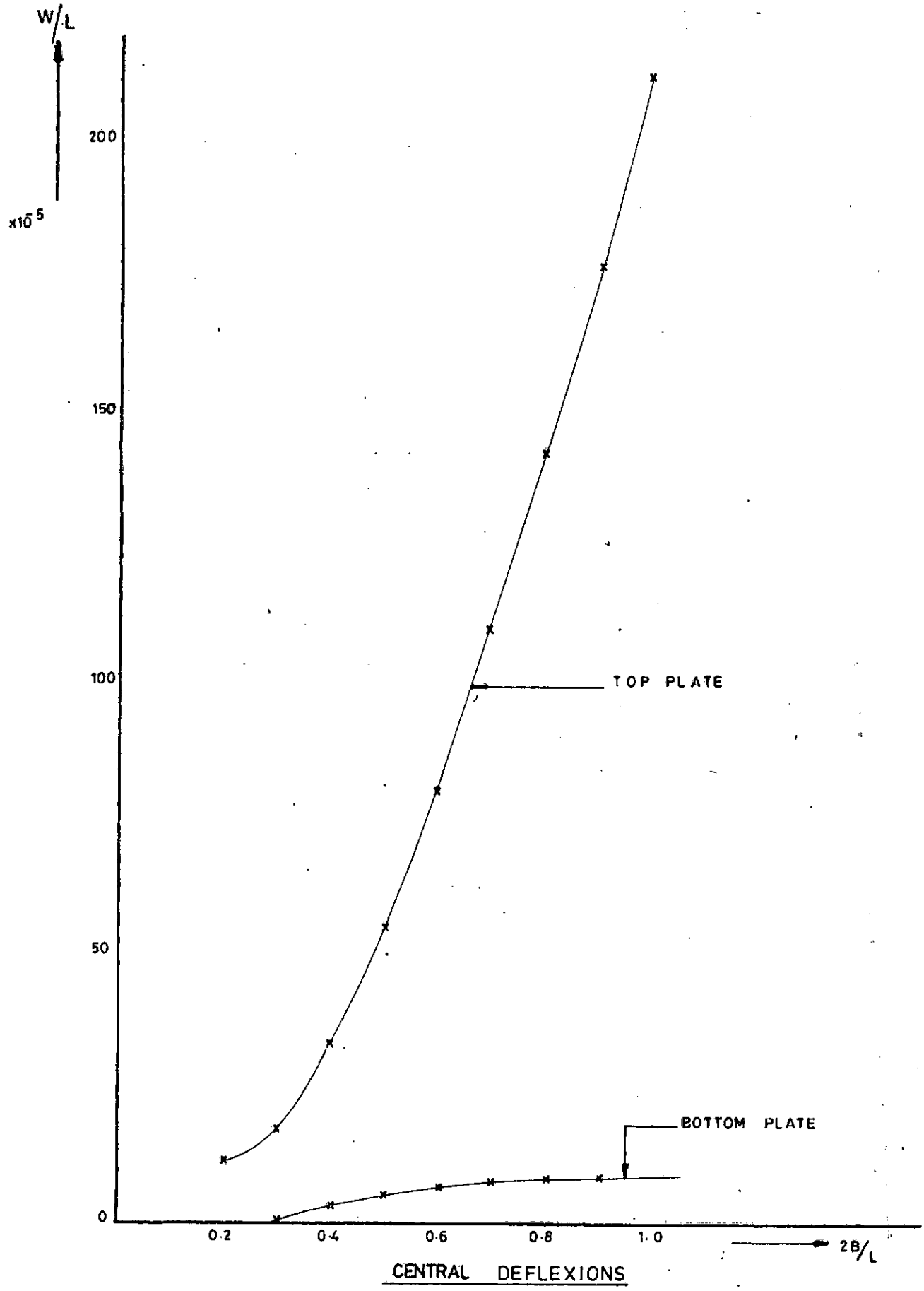
W/L
x10⁻⁵
200
150
100
50
0
TOP PLATE
BOTTOM PLATE
0·2
0·4
0·6
0·8
1·0
2B/L
CENTRAL DEFLEXIONS

FIG. 3—8

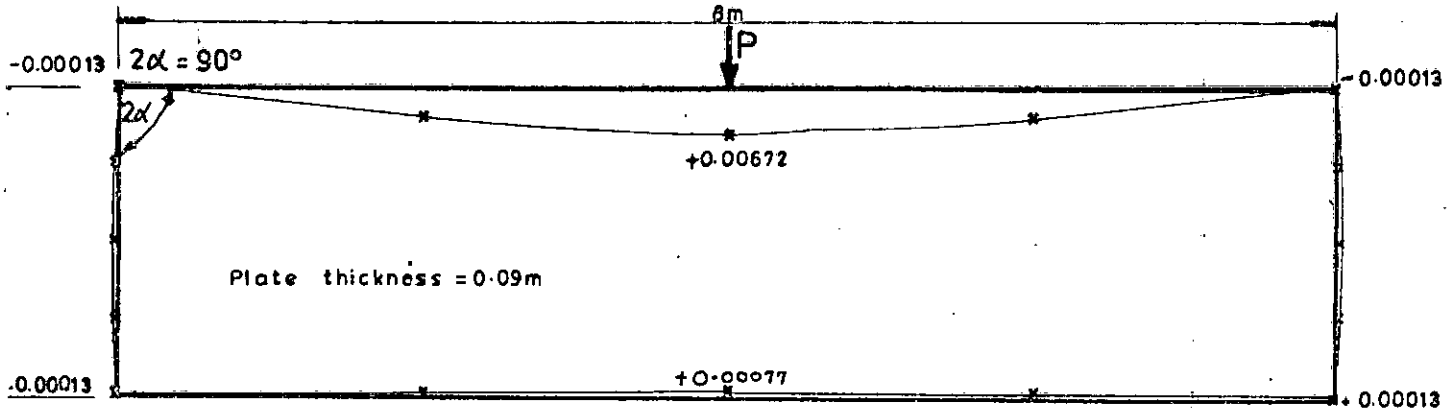

W

(a) TRANSVERSE DEFLEXIONS

UNITS

DEFLECTION IN METRE

STRESS IN KN/M²

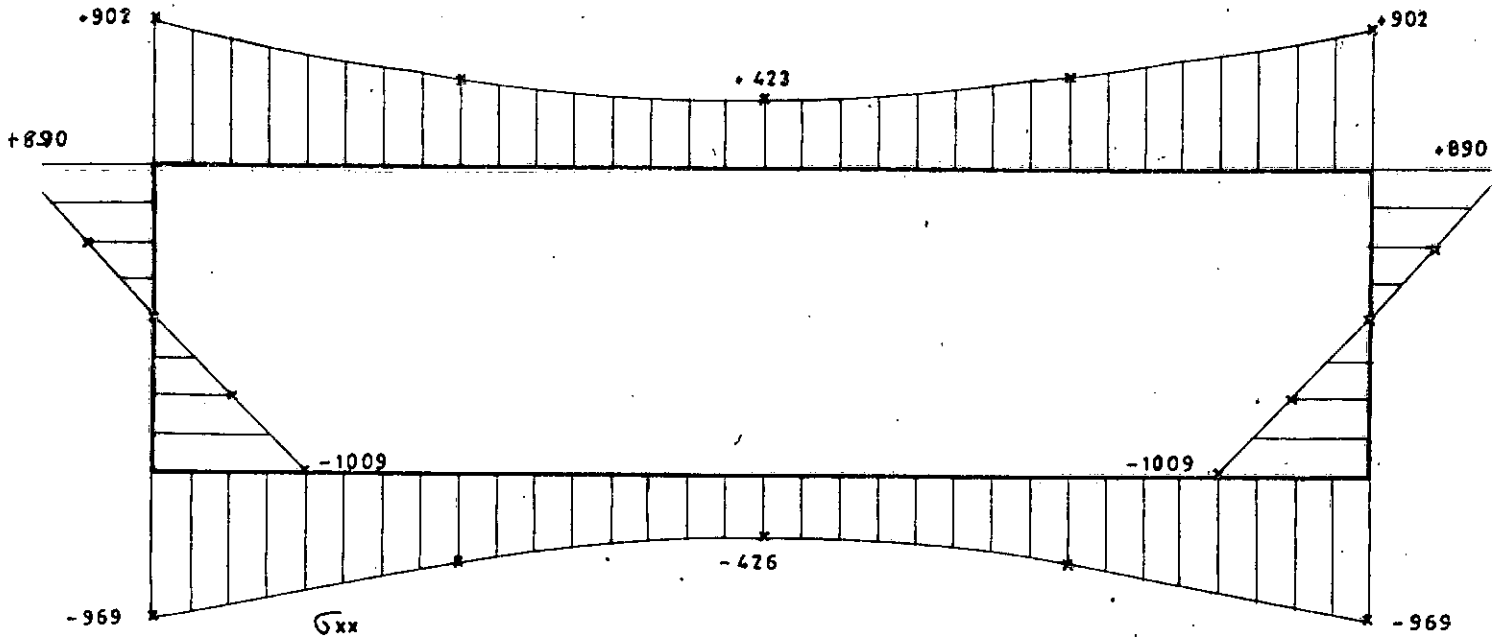

(b) LONGITUDINAL STRESS PATTERN

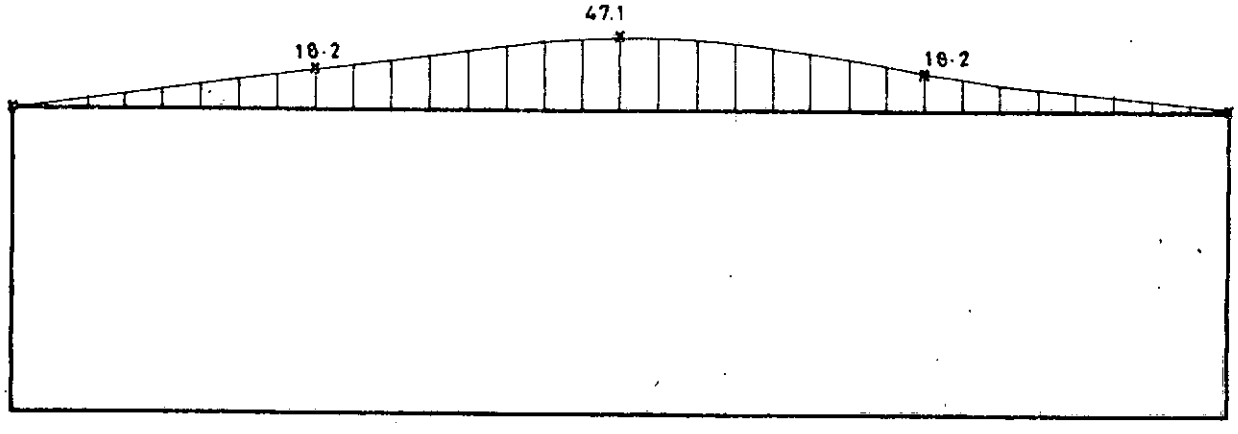

M_{yy} BENDING MOMENT PATTERN

(c)

FIG. 3–9

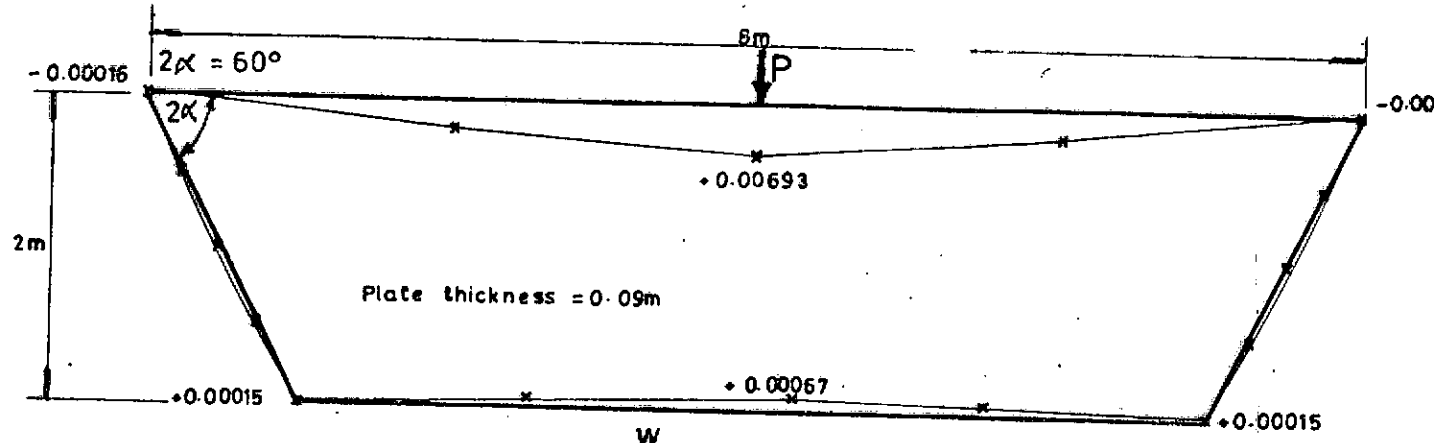

W
(a)

UNITS
DEFLECTION IN METR
STRESS IN KN/M2

TRANSVERSE DEFLECTED SHAPE OF BOX WITH LOAD AT CENTRE

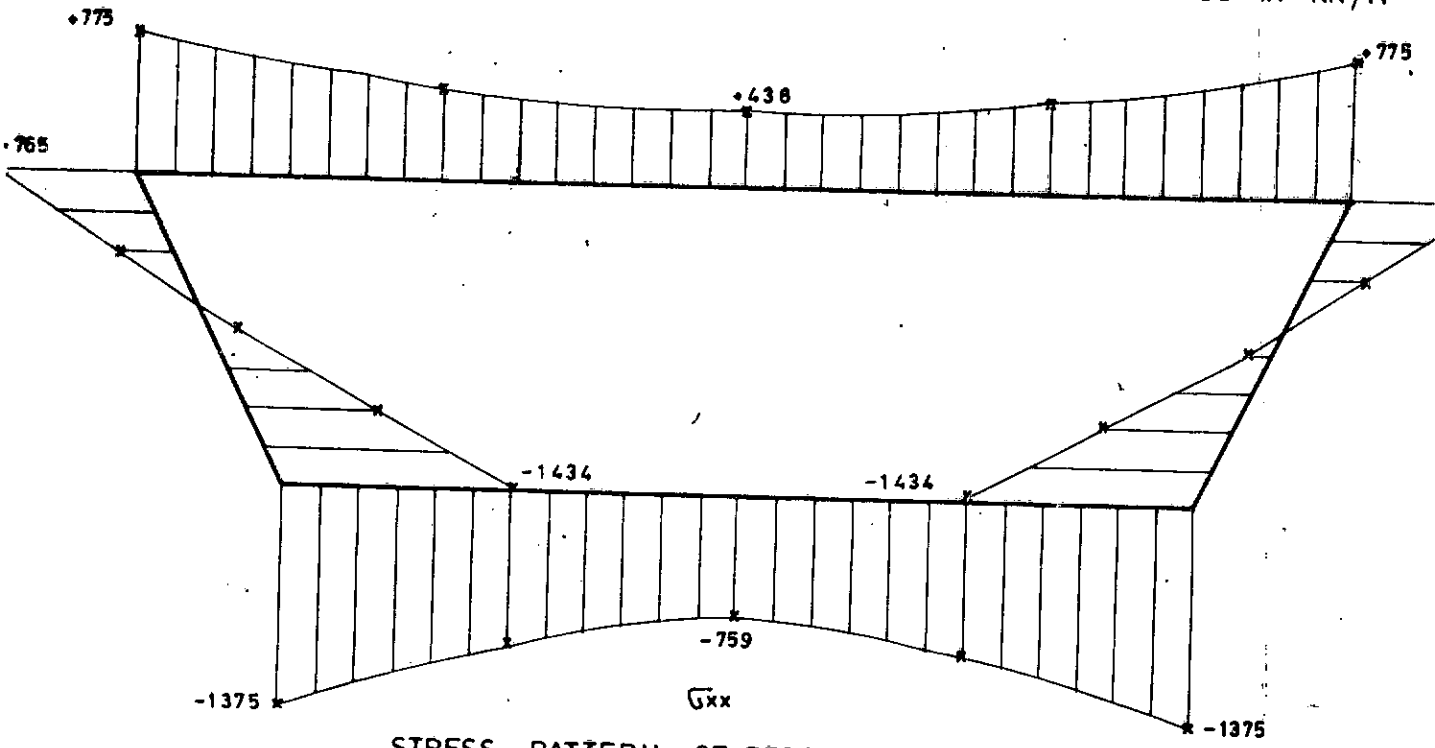

STRESS PATTERN OF DEFORMED BOX

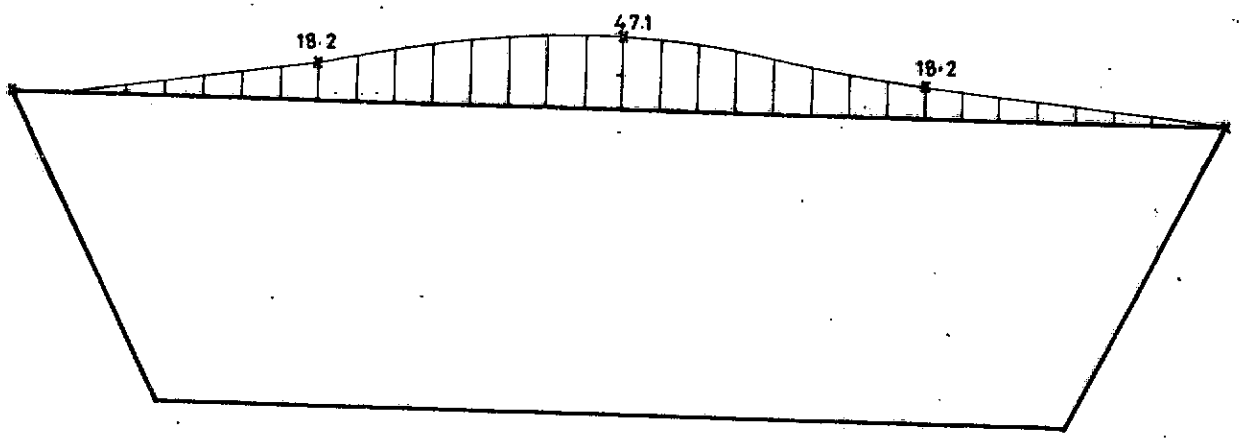

M_{yy} BENDING MOMENT PATTERN

FIG. 3—10

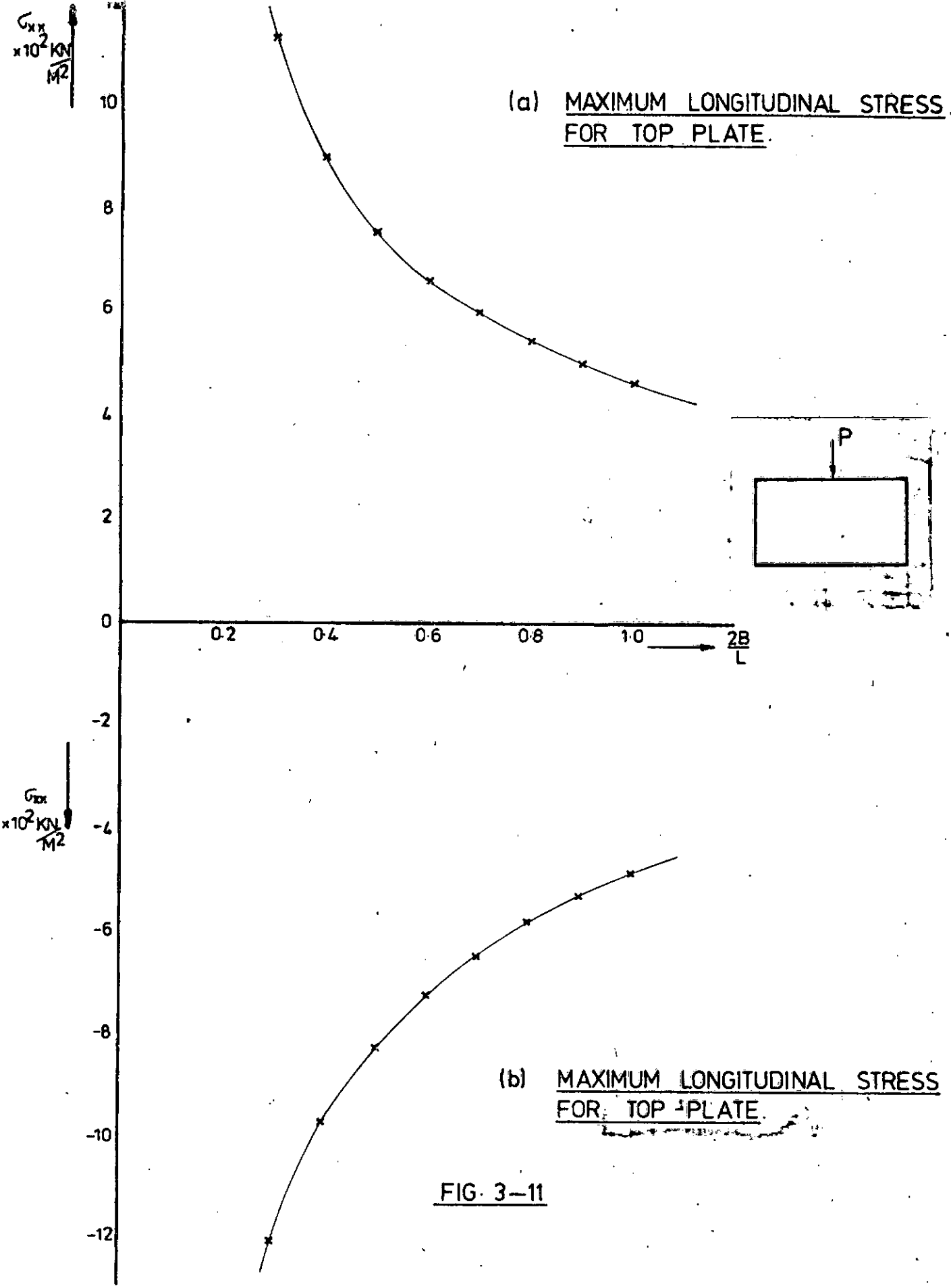
σ_{xx}
$\times 10^2$ KN/M^2
10
8
6
4
2
0
-2
-4
-6
-8
-10
-12
0·2
0·4
0·6
0·8
1·0
2B/L
P
(a) MAXIMUM LONGITUDINAL STRESS FOR TOP PLATE.
(b) MAXIMUM LONGITUDINAL STRESS FOR TOP PLATE.

FIG. 3–11

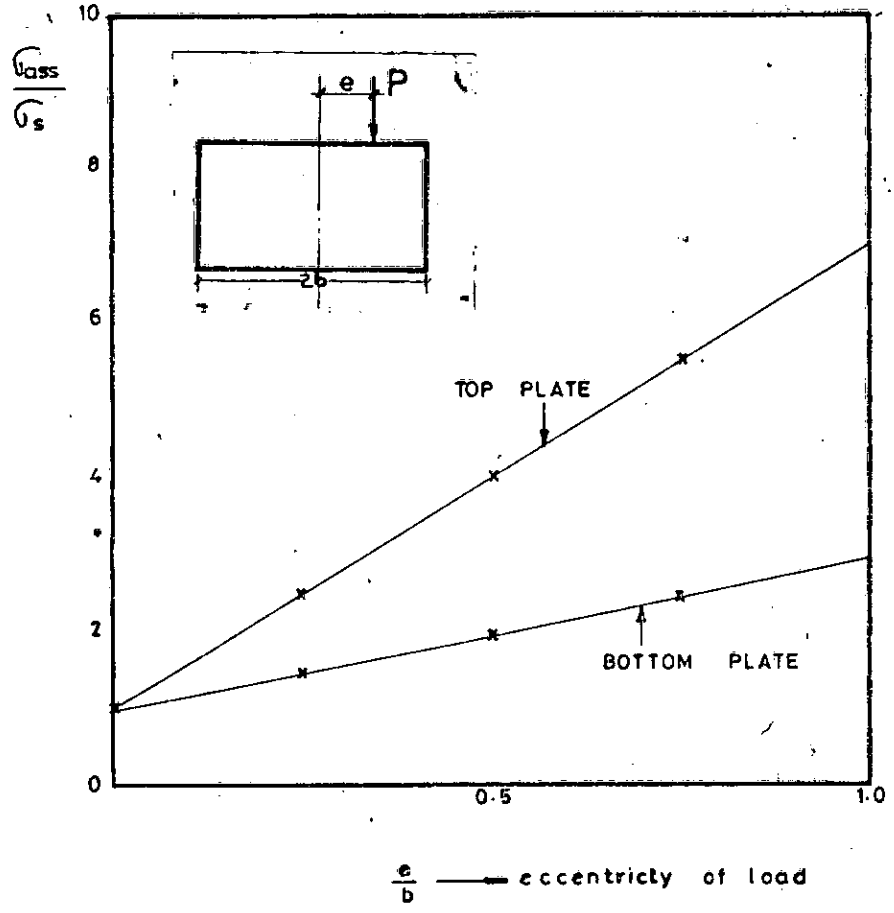
10
8
6
4
2
0
0.5
1.0
e
P
2b
TOP PLATE
BOTTOM PLATE
e/b ——— eccentricty of load

FIG. 3—12

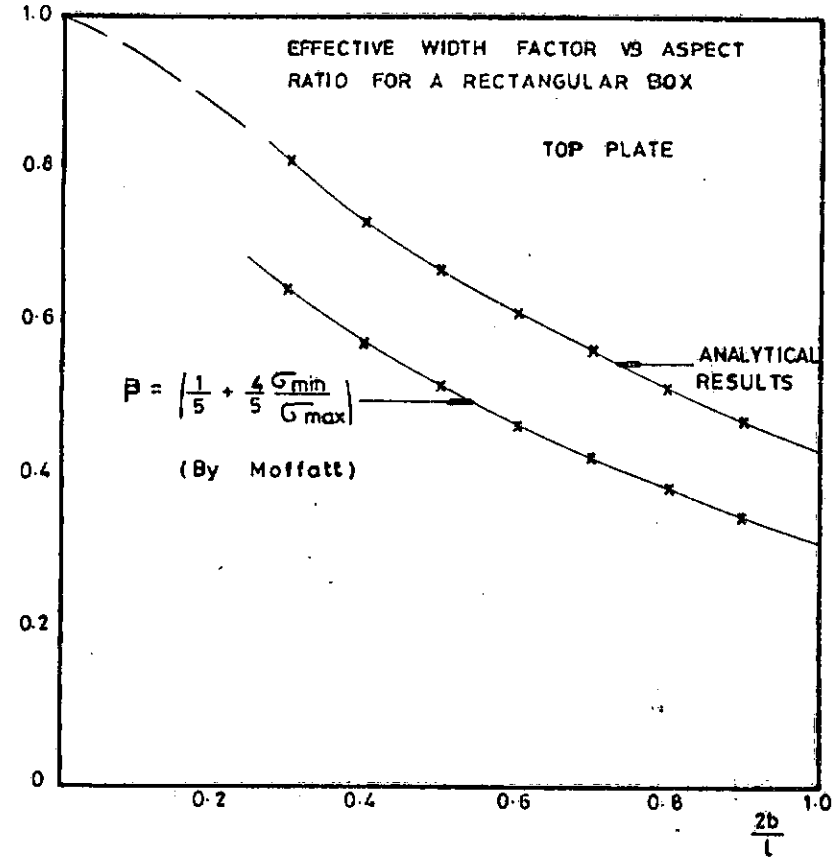
EFFECTIVE WIDTH FACTOR VS ASPECT RATIO FOR A RECTANGULAR BOX
TOP PLATE
ANALYTICAL RESULTS
$\beta = \left|\frac{1}{5} + \frac{4}{5}\frac{\sigma_{min}}{\sigma_{max}}\right|$
(By Moffatt)
1.0
0.8
0.6
0.4
0.2
0
0.2
0.4
0.6
0.8
1.0
$\frac{2b}{l}$

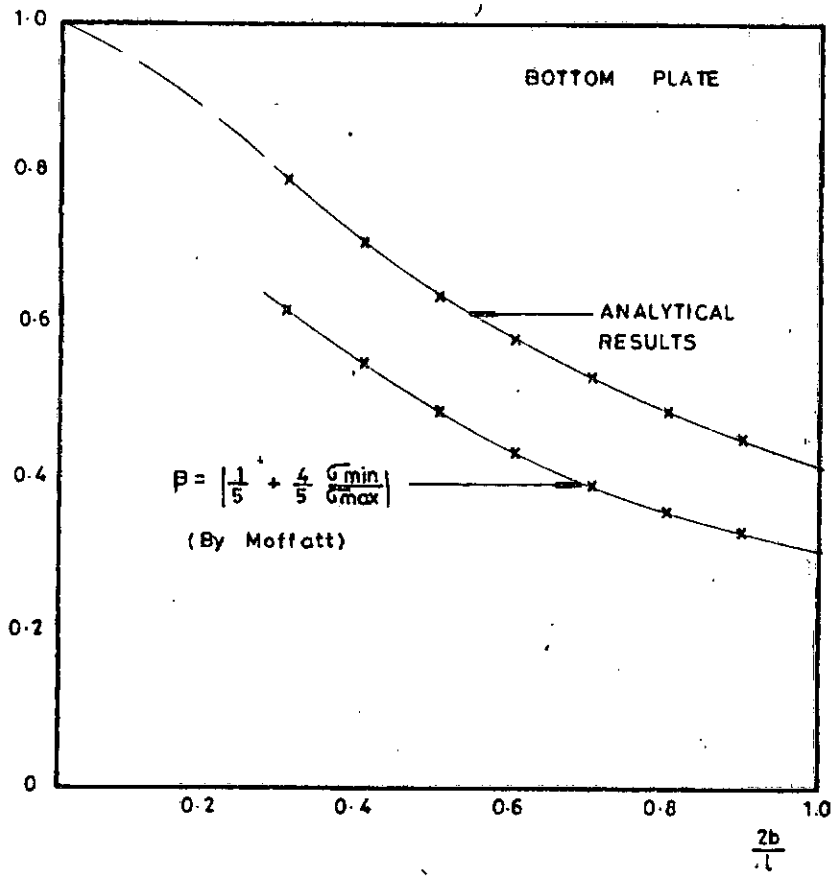
BOTTOM PLATE
ANALYTICAL RESULTS
$\beta = \left|\frac{1}{5} + \frac{4}{5}\frac{\sigma_{min}}{\sigma_{max}}\right|$
(By Moffatt)
1.0
0.8
0.6
0.4
0.2
0
0.2
0.4
0.6
0.8
1.0
$\frac{2b}{l}$

FIG. 3 – 13

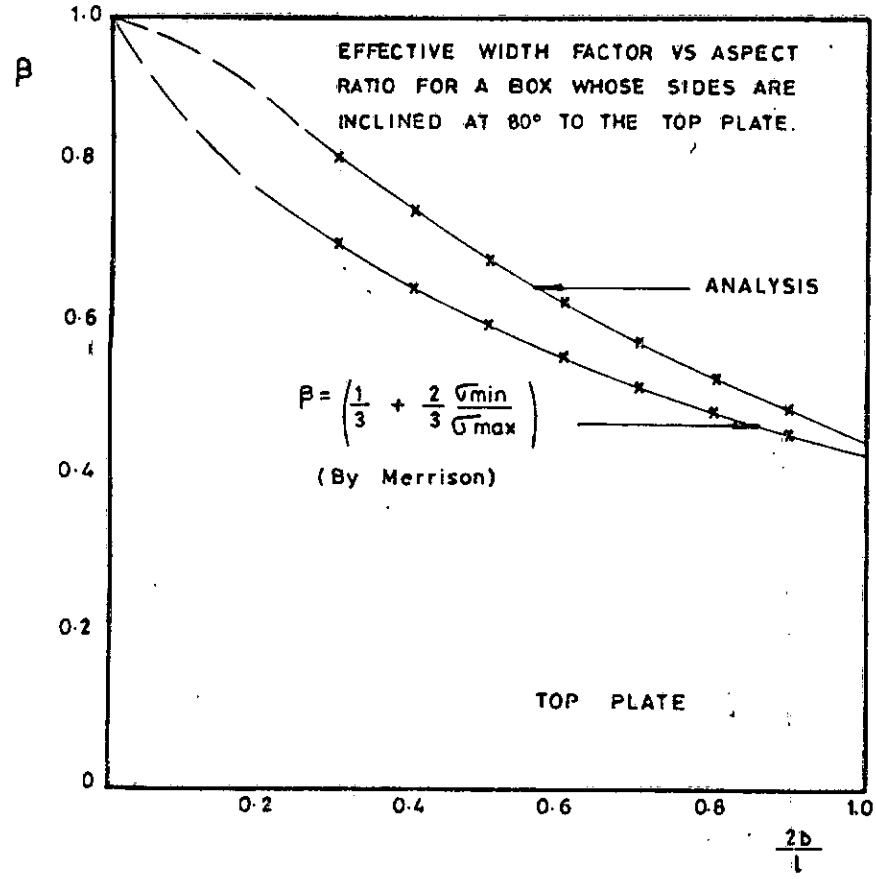
EFFECTIVE WIDTH FACTOR VS ASPECT RATIO FOR A BOX WHOSE SIDES ARE INCLINED AT 80° TO THE TOP PLATE.
β
1.0
0.8
0.6
0.4
0.2
0
ANALYSIS
β = (1/3 + 2/3 σmin/σmax)
(By Merrison)
TOP PLATE
0.2
0.4
0.6
0.8
1.0
2b/l

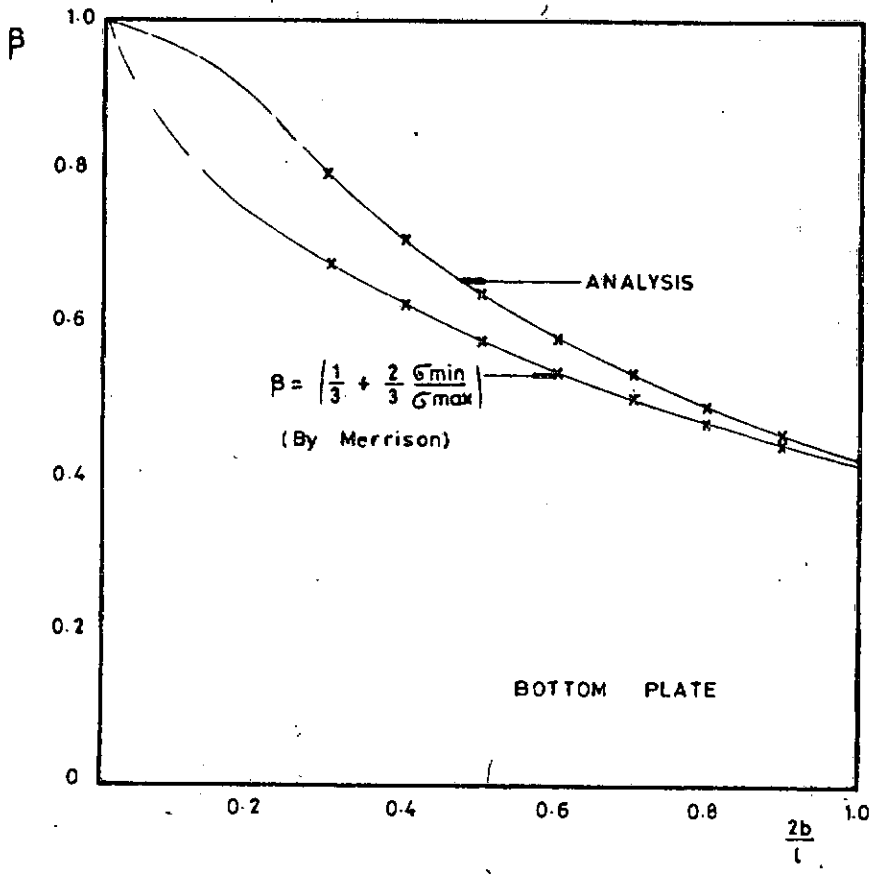
β
1.0
0.8
0.6
0.4
0.2
0
ANALYSIS
β = (1/3 + 2/3 σmin/σmax)
(By Merrison)
BOTTOM PLATE
0.2
0.4
0.6
0.8
1.0
2b/l

FIG. 3–14

other in tension. In a document titled "Criteria for Design of steel-concrete composite box girder Highway Bridges" prepared by Mattock et al, the recommendations in respect of shear lag reads as follows:

Tension Flanges

"In the case of simply supported spans, the bottom flange shall be considered completely effective in resisting bending if its width does not exceed one-fifth of the span length. If the width exceeds one-fifth of the span, an amount equal to one-fifth of the span only shall be considered effective".

Compression Flanges

In respect of compression flanges no specific recommendations appeared to have been made with regard to shear lag, although considerations of elastic stability were used in suggesting design criteria of these elements. Whichever methods are used in designing these elements, there will be need to predict stresses and deflexions at some stages of design. Shear lag consideration should therefore be applied to the compression flange as well whether it is stiffened against buckling or not.

The results of the analysis confirm the recommendations referred to in respect of tension flanges, however, in respect of compression flanges, the results show that shear lag effects are equally manifest in these components and effective widths of compression flanges are equally relevant in design. Figure 3.13/14shows the variation of effective width factors with aspect ratio ranging from 0 to 1.0.

Effective width factors obtained from this analysis were compared with values obtained by Moffatt and Dowling[25] and those recommended in the Merrison[24] report (Table 1). Values of effective width factors recommended in the Merrison report appear to be based on Moffatt and Dowling's works. There is some appreciable divergence between the results of the present analysis and the recommended values in the two works referred to. Although the top deck of the rectangular box girder section considered by Moffatt and Dowling is orthotropic as against the isotropic deck assumed in this analysis, it is believed that the two results should be comparable. Merrison's report gave a formula relating the variation of longitudinal stress across a flange with the effective width factor. This formula assumes a parabolic profile for the distribution of longitudinal flange stresses. Moffatt and Dowling on the other hand suggested a quartic variation of longitudinal stress across the flange width, also relating their own formula to effective width factor.

Based on these two formulae and applying the minimum and maximum longitudinal stresses obtained from this analysis, effective width factors were computed and compared with those directly obtained from

this analysis. Values obtained on the basis of Merrison's formula are only slightly lower than these analytical results, whilst Moffatt and Dowling's formula resulted in much lower values. In addition, effective width values obtained from the Moffatt and Dowling formula would appear not to tend to unity as aspect ratio tends to zero, a general feature already confirmed by many earlier authors of shear lag phenomenon[17,24]. The symmetrical pattern of stress in the flanges of a box-girder obtained from analytical results when dealing with a symmetrical loading in the transverse direction tends to reinforce a belief in the concept of effective width for box-girder design. However, an examination of the stress patterns resulting from the lack of symmetry of transverse loading for the cross-sectional configurations considered in this analysis tends to raise some doubts about the validity of effective width concepts when dealing with box-girders.

EFFECT OF ECCENTRICITY OF TRANSVERSE LOADING RELATIVE TO THE CROSS-SECTIONAL VERTICAL AXIS:

When a symmetrical box section is subjected to an eccentric loading, the resulting deformations are accompanied with distortion and warping of

the cross-section; these in turn give rise to warping longitudinal stresses which vary from tension to compression from one edge of a flange to the other. These stresses are not easily predicted by the approximate method of transformed section theory. An attempt to do this by using a Beam on Elastic Foundation analogy has been referred to in the introduction to this thesis. The B.E.F. analysis restricts itself to assymmetric corner loads on a box girder. For a single cell box girder this represents the extreme or worst case of unsymmetrical loading and should therefore predict the most severe longitudinal stresses associated with warping. However, as has been observed elsewhere in this thesis, the method of analysis is complex and is certainly difficult to accept as a valid basis of estimating these stresses. The question that must be answered is how important is the warping effect on longitudinal stress magnitudes or in designing for the worst stressed situation. Again reference must be made to "Criteria for Design of steel-concrete Composite Box Girder Highway Bridges" prepared by Mattock and others. In this document reference is made to warping stresses under Secondary Bending Stresses as follows:

"If the inclination of the web plates to the vertical is not greater than 1 to 4 (this corresponds to $2\alpha = 75^0\ 58'$)*, and the width of the bottom flange is not greater than 20 percent of the span, the transverse bending stresses resulting from distortion of the girder cross-section and from vibrations of the bottom plate, need not be considered. For structures in this category, transverse bending stresses due to supplementary loadings, such as utilities, shall not exceed 5000 psi".

---

*the amplification in the bracket is inserted by the author of this thesi

"For structures exceeding these limits, a detailed evaluation of the transverse bending stresses due to all causes shall be made. These stresses shall be limited to a maximum stress or range of stress of 20,000 psi".

Figure 3.19 shows the results for a box-girder section with top flange aspect ratio of 0.25 and bottom flange aspect ratio of 0.215 with side slopes of $2\alpha = 80^0$. The rate of growth of maximum edge stresses associated with warping effect with severity of load eccentricity is shown in Figure 3.12. It is observed from this result that growth of stress at flange plate edges has a linear relationship with eccentricity and that edge stresses under unsymmetric loading could be multiples of the maximum flange stresses for a symmetrical loading of the same magnitude. The obvious conclusion is that secondary bending stresses arising from warping and distortion should be considered and, depending on the possible mode of application of live load to a bridge deck, should be the governing condition of attaining permissible stresses. This result appears to suggest that effective width concept in design consideration may be irrelevant to box-girder response, especially where unsymmetrical loading of severe eccentricities is likely. This will most certainly be the case in respect of bridge structures where more often than not the traffic lanes will not be equally loaded at most times.

COMPARISON OF DISTORSION STRESSES WITH RESULTS OF B.E.F. ANALOGY

The B.E.F. analogy of Abdel-Samad et al gives many equations to be used in calculating displacements, warping and distortion stresses,

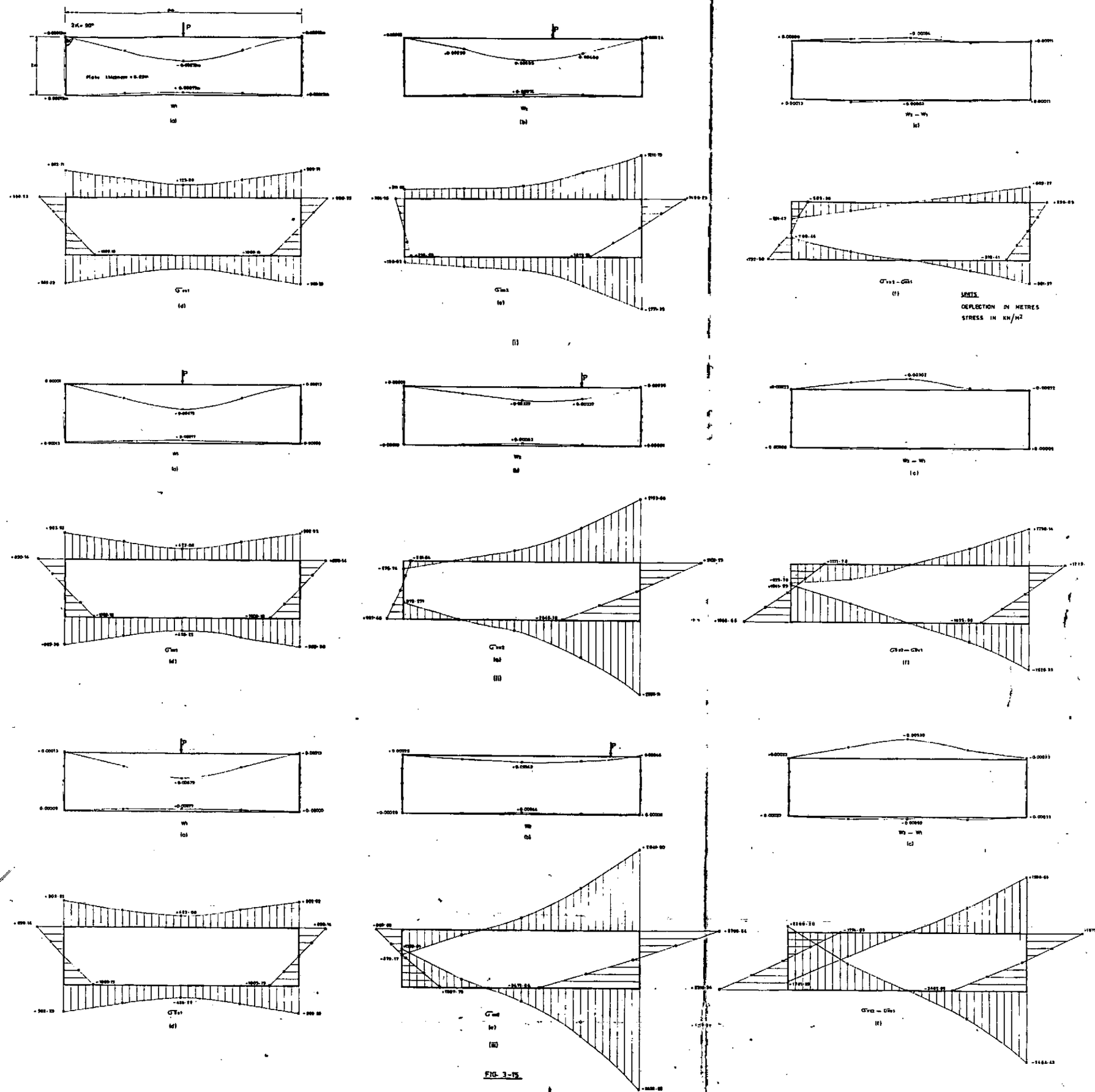
2K = 90°
P
W1
(a)
W2
(b)
W2 − W1
(c)
(d)
(e)
(f)
UNITS.
DEFLECTION IN METRES
STRESS IN KN/M2
(I)
(II)
(III)

FIG. 3-15

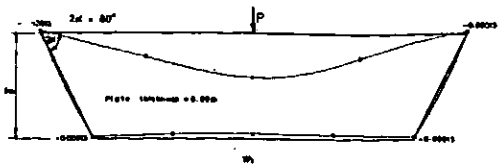

(a)

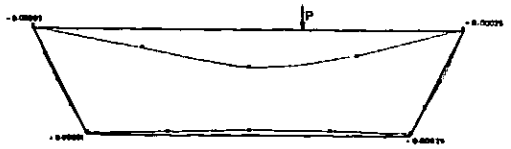

(b)

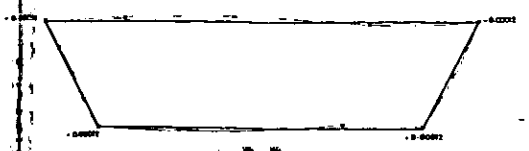

(c)

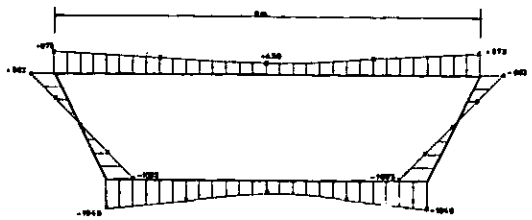

(d)

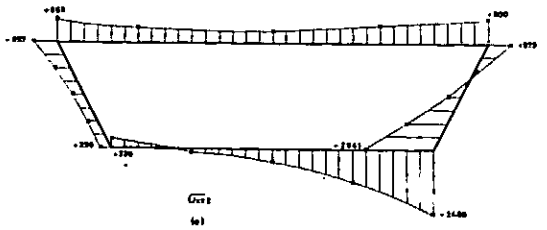

(e)

(i)

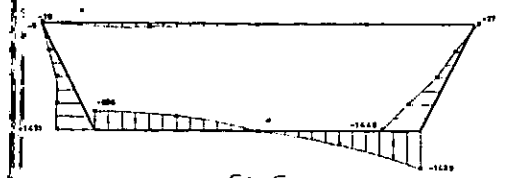

(f)

UNITS

DEFLECTION IN METRES

STRESS IN KN/M^2

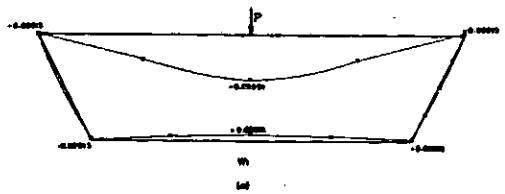

(a)

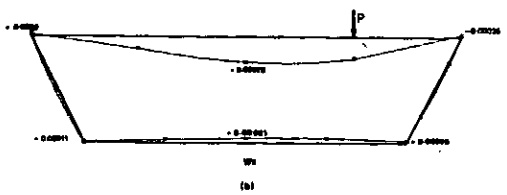

(b)

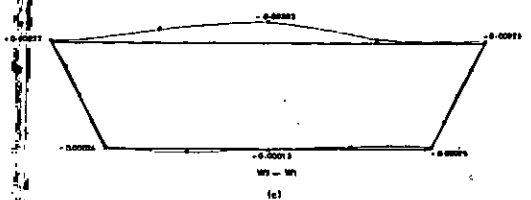

(c)

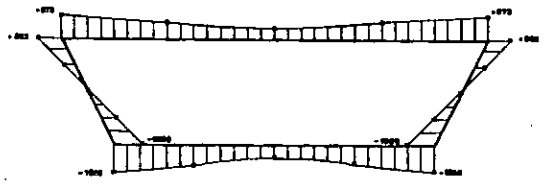

(d)

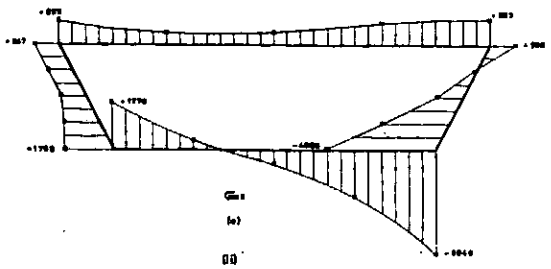

(e)

(ii)

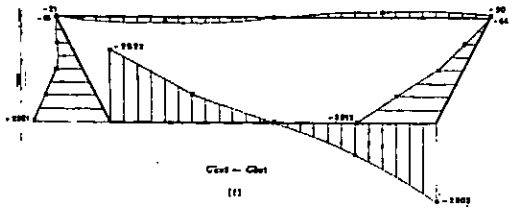

(f)

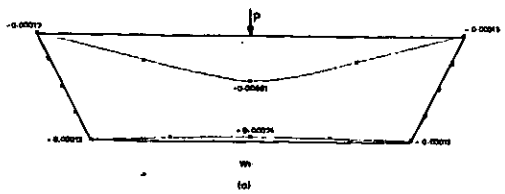

(a)

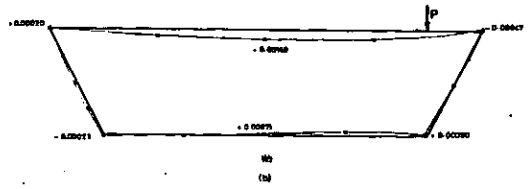

(b)

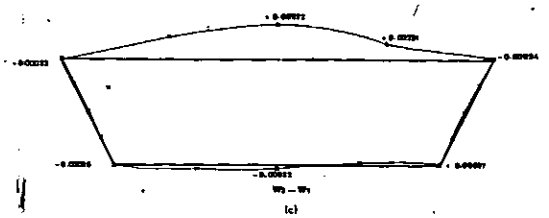

(c)

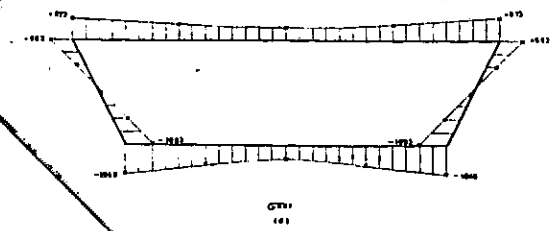

(d)

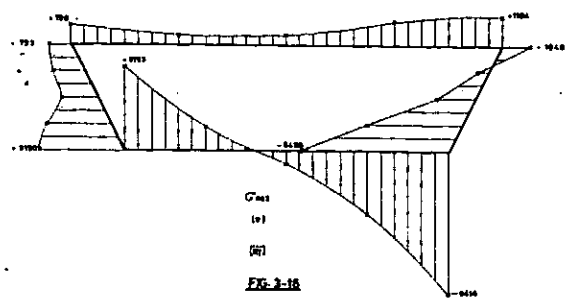

(e)

(iii)

FIG. 3-16

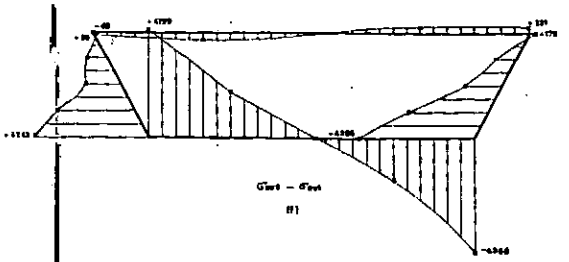

(f)

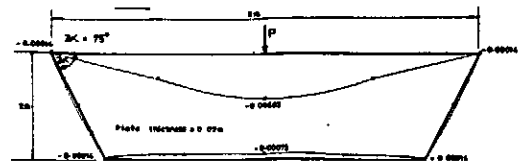

W_1

(a)

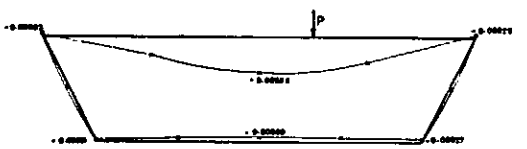

W_2

(b)

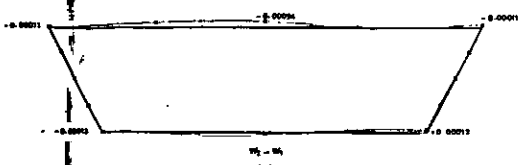

$W_2 - W_1$

(c)

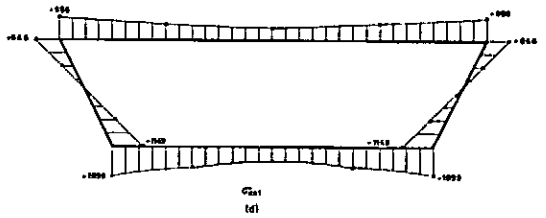

$\sigma_{\theta 1}$

(d)

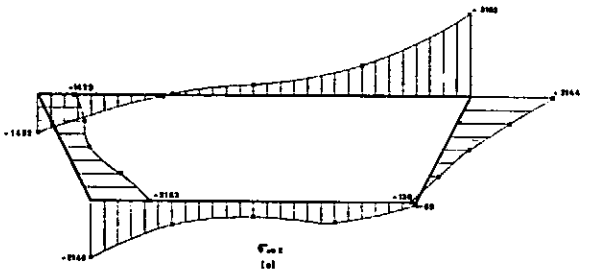

$\sigma_{\theta 2}$

(e)

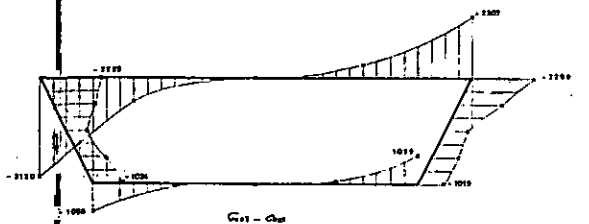

$\sigma_{\theta 2} - \sigma_{\theta 1}$

(f)

(I)

UNITS

DEFLECTION IN METRES

STRESS IN KN/M^2.

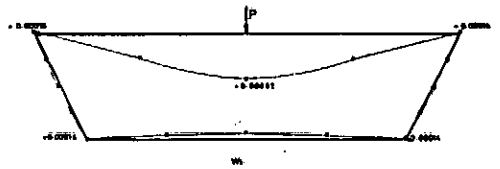

W_1

(a)

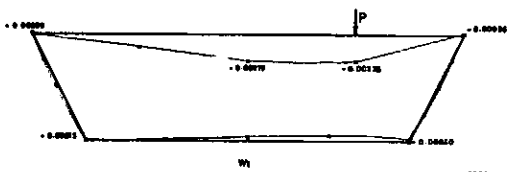

W_1

(b)

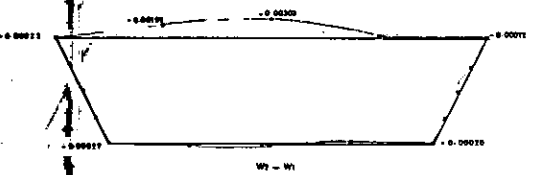

$W_2 - W_1$

(c)

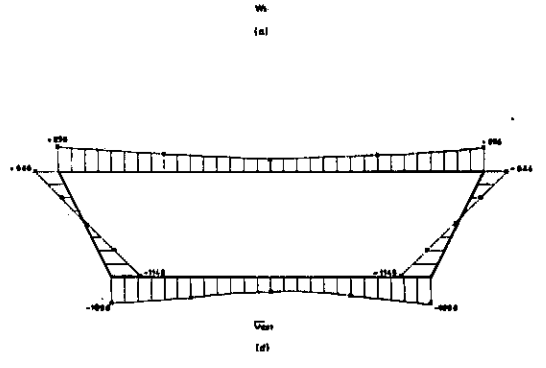

$\bar{\sigma}_{\theta 1}$

(d)

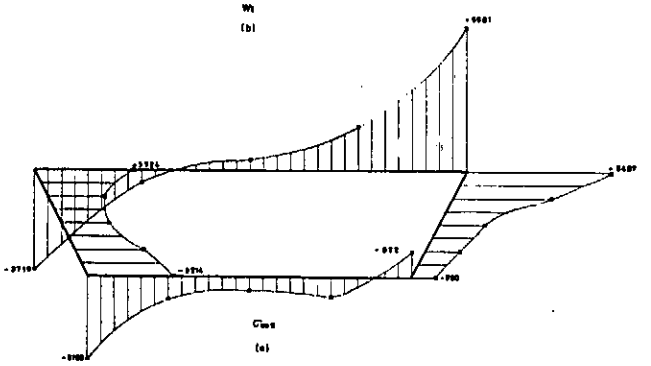

$\bar{\sigma}_{\theta 2}$

(e)

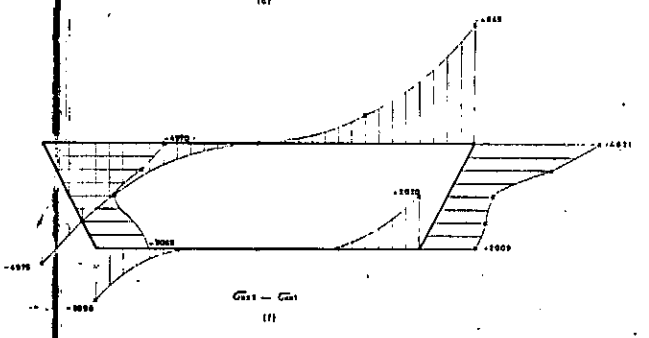

$\bar{\sigma}_{\theta 2} - \bar{\sigma}_{\theta 1}$

(f)

(II)

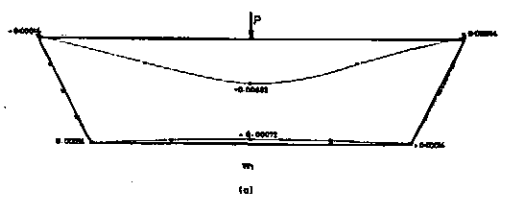

W_1

(a)

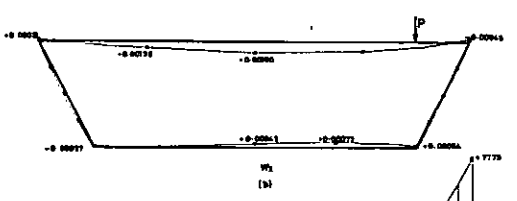

W_2

(b)

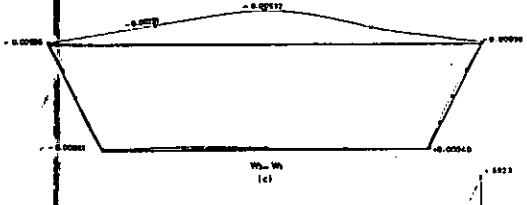

$W_2 - W_1$

(c)

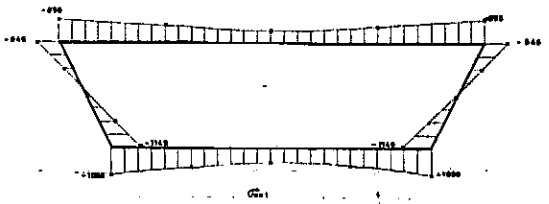

$\bar{\sigma}_{\theta 1}$

(d)

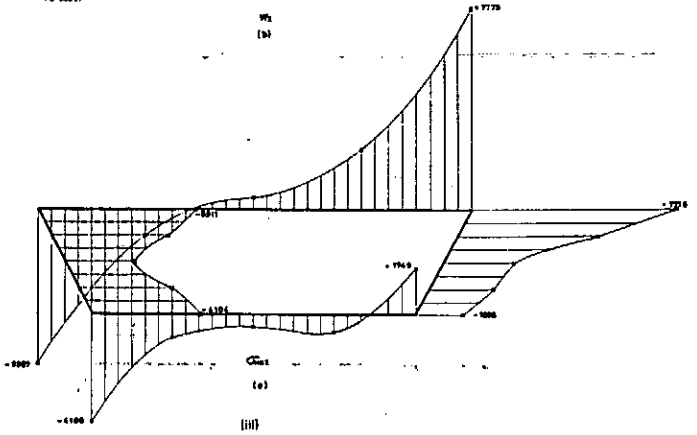

$\bar{\sigma}_{\theta 2}$

(e)

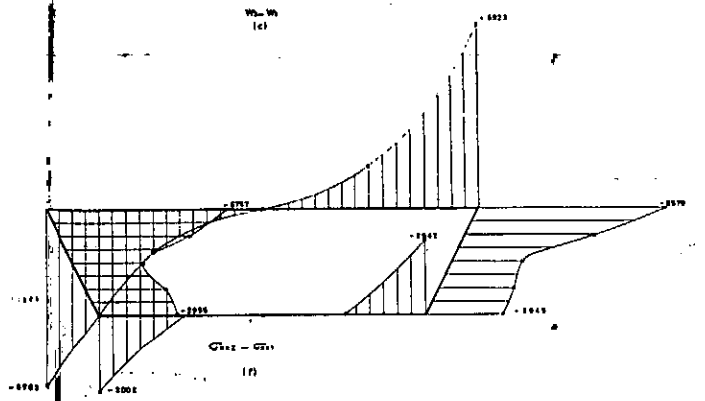

$\bar{\sigma}_{\theta 2} - \bar{\sigma}_{\theta 1}$

(f)

(III)

FIG. 3-17

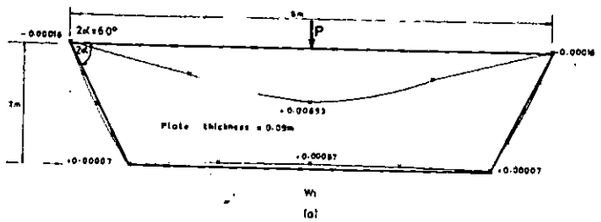

W_1

(a)

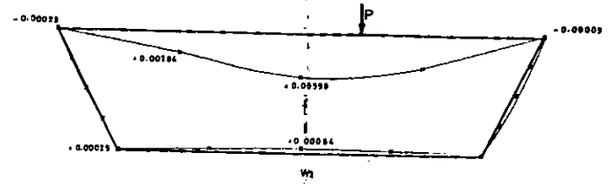

W_2

(b)

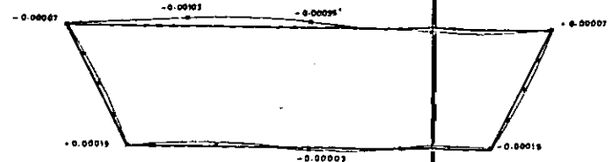

$W_2 - W_1$

(c)

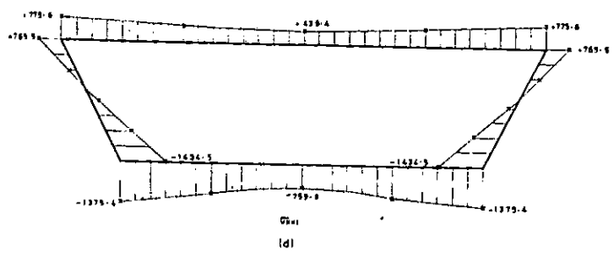

$\bar{G}_{xx1}$

(d)

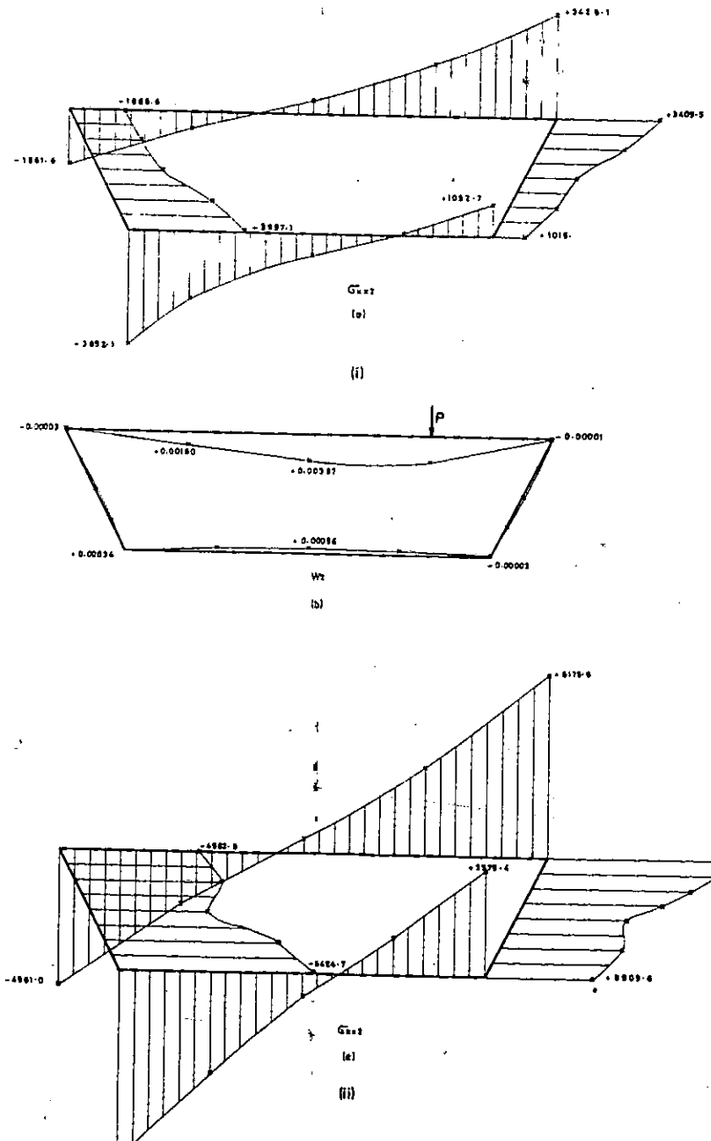

$\bar{G}_{xx2}$

(e)

(i)

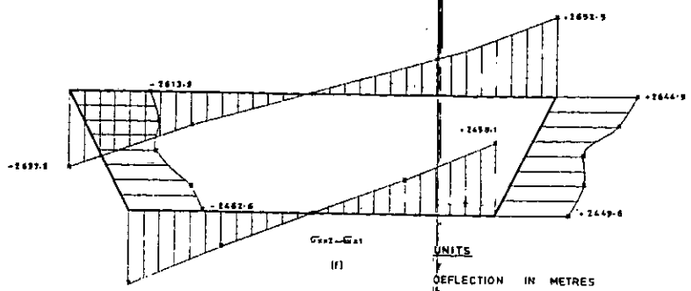

$\bar{G}_{xx2} - \bar{G}_{xx1}$

(f)

UNITS

DEFLECTION IN METRES

STRESS IN KN/M^2

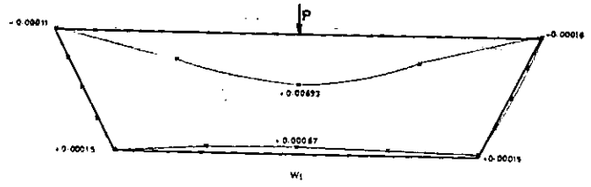

W_1

(a)

W_2

(b)

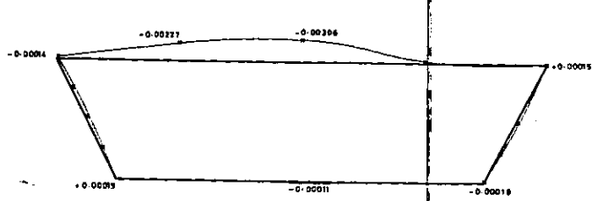

$W_2 - W_1$

(c)

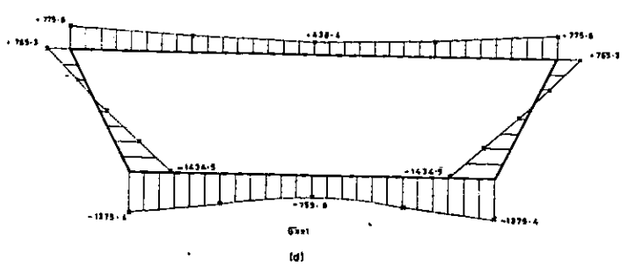

$\bar{G}_{xx1}$

(d)

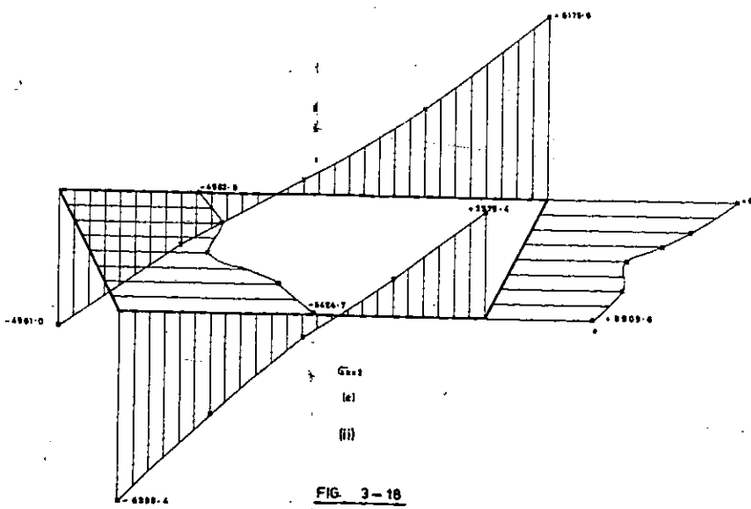

$\bar{G}_{xx2}$

(e)

(ii)

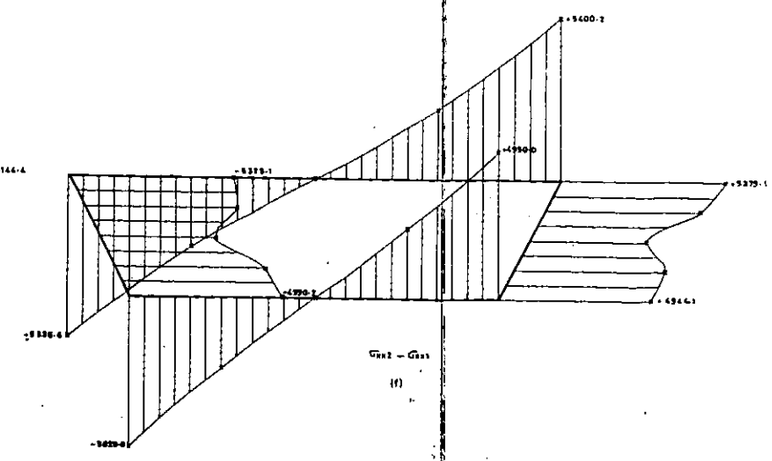

$\bar{G}_{xx2} - \bar{G}_{xx1}$

(f)

FIG. 3 – 18

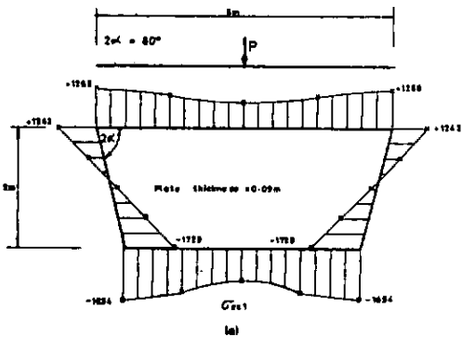

(a)

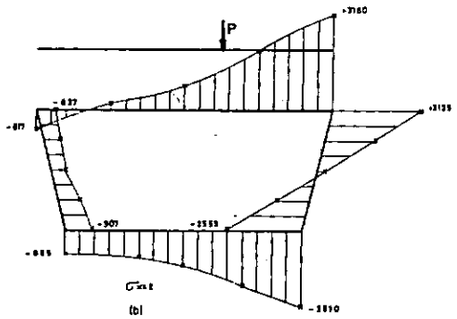

(b)

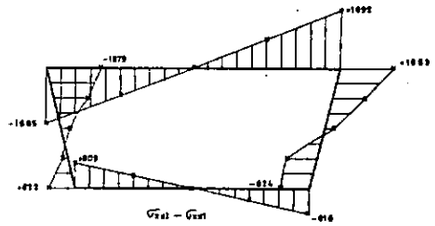

(c)

UNITS

DEFLECTION IN : METRES

STRESS IN KN / M²

(i)

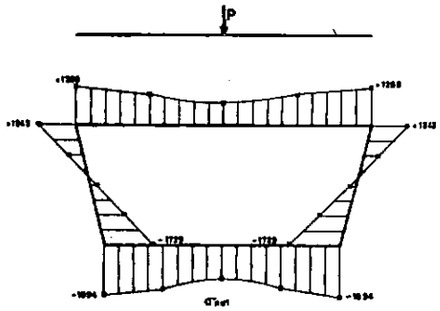

(a)

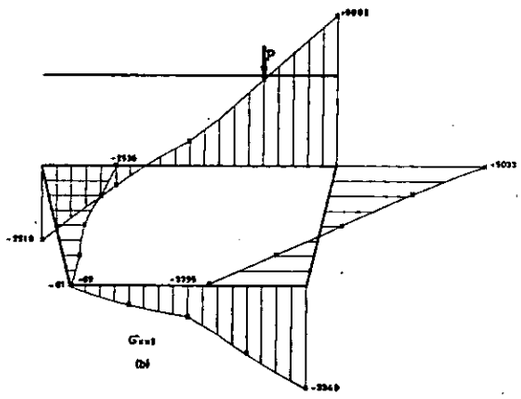

(b)

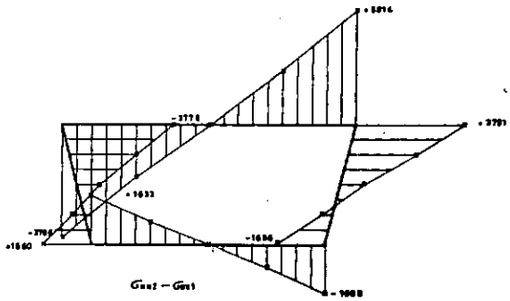

(c)

(ii)

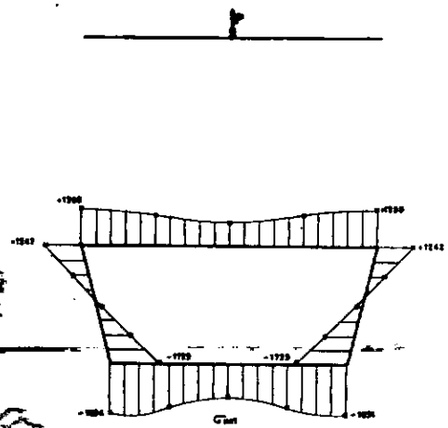

(a)

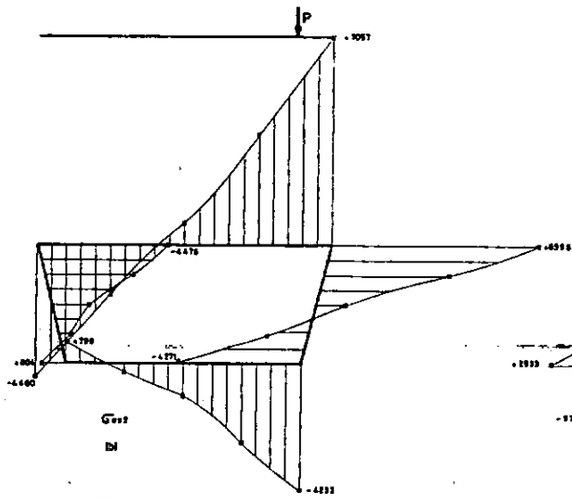

(b)

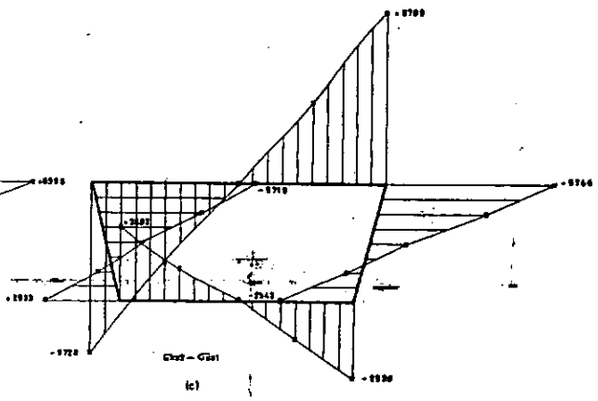

(c)

(iii)

FIG 3 – 19

shear stresses etc. A direct comparison between the results of the analysis presented in this thesis and those from the B.E.F. analogy is not possible because of differences in the geometry of the box sections assumed and the type of assymmetric loading applied in the two analyses. However, the distortional stresses calculated using the B.E.F. analogy formulae for a box section with a 60^0 side slope angle, one of the cross-sectional configurations used in this thesis, are $675KN/m^2$ at one edge of the top plate and $894KN/m^2$ at an edge of the bottom plate. The corresponding results from the more direct analytical method of this thesis are $1861KN/m^2$ and $1082KN/m^2$ respectively.

EFFECT OF BOX-GIRDER WEB SIDE SLOPE

Figure 3.20 shows the growth in longitudinal flange peak stress as a ratio of the longitudinal peak stress for symmetrical loading, with decreasing web slope (to the vertical) for different eccentricities of loading. For the symmetric loading, that is, zero eccentricity, web side slope only has a slight effect on longitudinal flange peak stress growth. However, when eccentricity of loading occurs, the longitudinal flange peak stress growth pattern with side slope exhibits instability (i.e it becomes oscillatory) when the web side slope is greater than about 15^0 to the vertical. The increase in longitudinal peak stress values over the corresponding longitudinal peak stress for symmetric loading being up to 55% for the worst eccentricity considered. Associated with this oscillatory variation of the peak longitudinal stress with side slope are regions where the peak stress value passes through zero magnitude. This would tend to suggest that there are critical angles for web side slope greater than 15^0 to the vertical where secondary bending effects

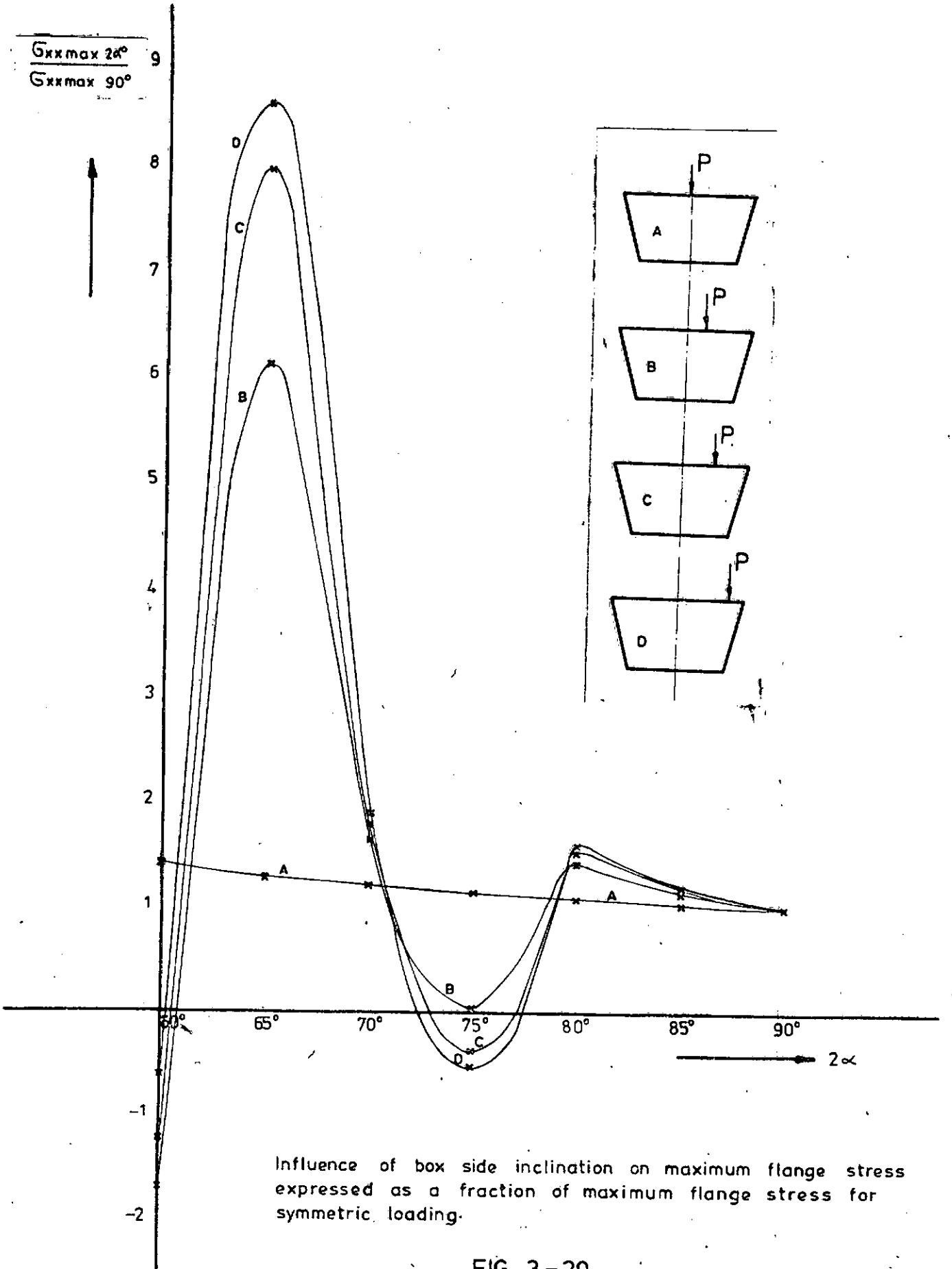

Influence of box side inclination on maximum flange stress expressed as a fraction of maximum flange stress for symmetric loading.

FIG. 3-20

are minimum. This will, of course, require further exhaustive studies before any firm conclusion can be reached. If this trend is confirmed in future studies, it would be possible to give a design guide on practical side slopes of the web of box-girders. The instability of the box-girder referred to in this section is generally characterised by the non-reversal of longitudinal stress in the box-girder webs.

ORTHOTROPY OF THE TOP AND BOTTOM FLANGES AND WEBS

The observations made in respect of effect of eccentricity of loading on longitudinal stresses may necessitate some rethinking about the arrangement of stiffeners in the longitudinal direction of the thin-plated elements of a steel box-girder. Severe eccentricities give rise to stress reversals in all the plate elements of a box-girder and cause increases of stress far greater than could be estimated from the symmetrical loading case. This implies that any of the plate element could be subjected to high edge stresses and therefore stiffening by the incorporation of longitudinal stiffeners should not be limited to the flanges alone. The arrangement of the stiffeners should be such as to compensate for the severe peak stresses to which these box-girder elements may be subjected due to severe eccentricities. The spacing of the stiffeners, following this conjecture, will not be uniform as recommended by Mattock and others but will vary in such a way as to give more stiffener influence at the corners of the box.

CHAPTER IV

EXPERIMENTAL PROGRAM

1. Introduction
2. Model Size and Material
3. Model Design and Fabrication
4. Test Set Up
5. Experimental Procedure.

4-1 INTRODUCTION:

The aim of the experiment is to examine the total response i.e. the general behaviour of a single cell box girder bridge, to a symmetric transverse loading.

The primary objectives are:-

(i) To study the deflexion profile of the box girder.

(ii) To study the stress patterns at various regions of the box girder.

(iii) To reach some conclusions that will help a designer appreciate the mode of response to transverse loading of the type of box girder tested, and also attempt some qualitative comparison between experimental response and analytical response.

Experimental tests were performed on a single span box girder model with its ends simply supported, under a two point symmetric loading arrangement (see Fig. 4-1).

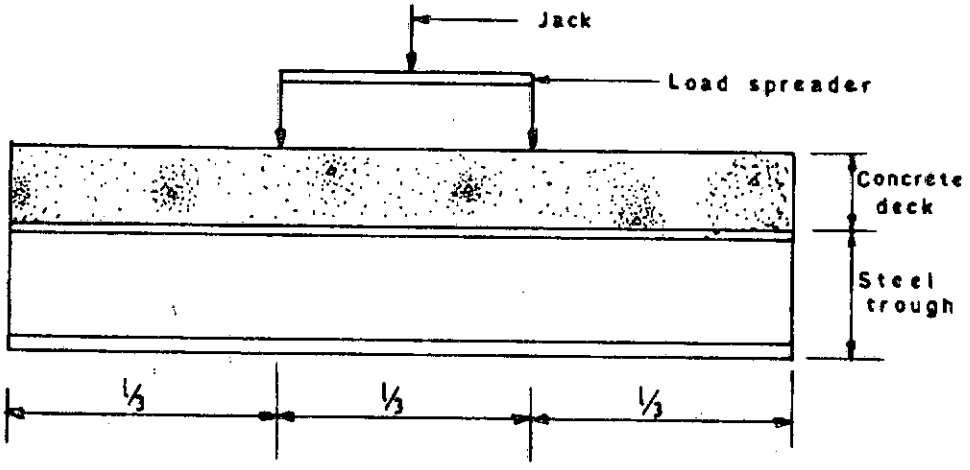

THE LOADING SYSTEM

FIG 4-1

4-2 MODEL SIZE AND MATERIAL

For an experimental investigation of this type, some of the considerations are, the ideal size for simulation of prototype behaviour and for easy handling, materials of fabrication for ease of construction of the model and scale effects.

The first two are usually dictated by the cost of manufacture and available laboratory facilities for testing, whilst the last has a bearing on the reliability of the model in simulating the response or performance of the prototype. Some reported results on structural scale model tests suggest that small scale models do simulate satisfactorily prototype behaviour.

The model used in this experimental programme is made up of a steel troughing supporting and interconnected to a reinforced concrete deck. This arrangement was dictated by consideration of ease of prefabrication. It is believed that the composite nature of the box girder test-specimen will not drastically alter its basic general response to transverse loading from that of a box girder, either wholly in steel or wholly in concrete. One additional advantage of the

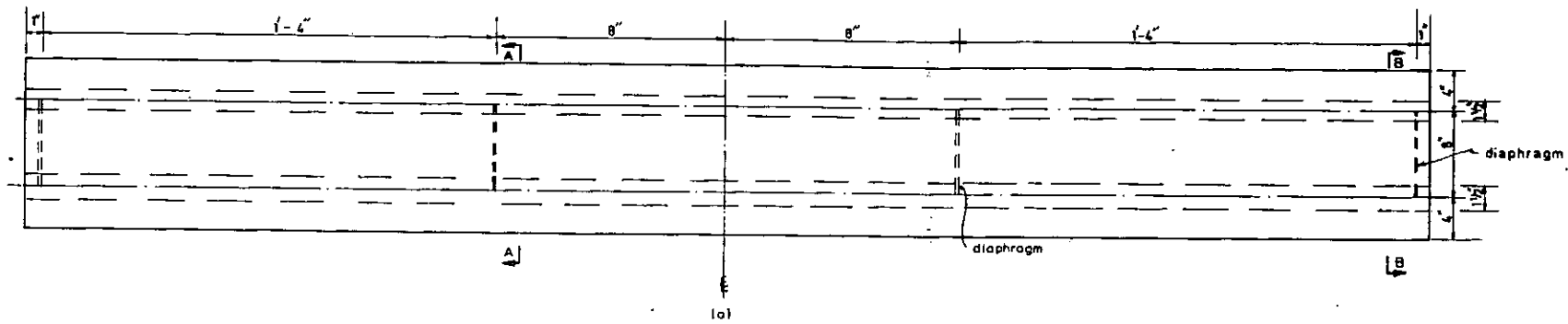

(a)

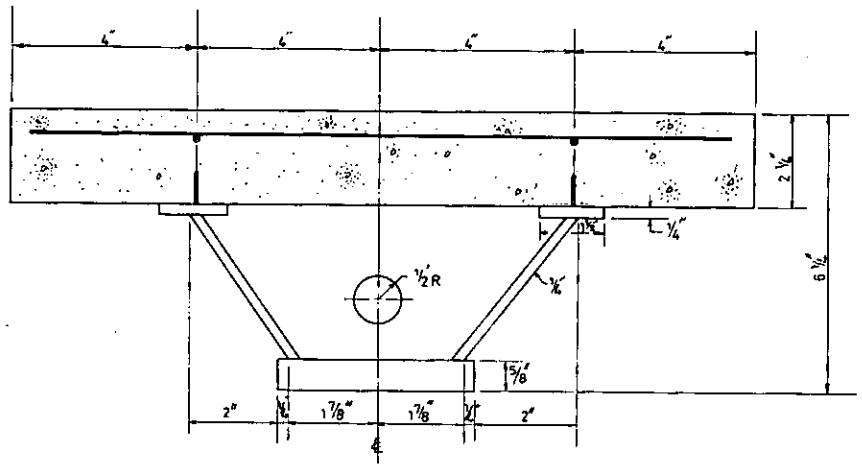

SECTION A-A (b)

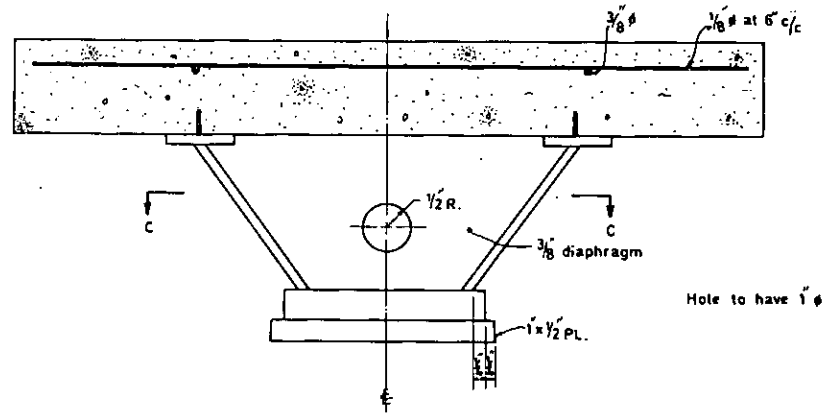

SECTION B-B (c)

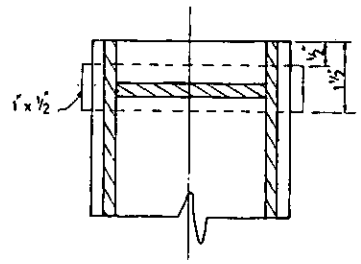

SECTION C-C (d)

BRIDGE MODEL DETAILS & DIMENSIONS (steel and concrete)

FIG. 4-2

POSITIONS OF DIAL GAUGES ACROSS THE SPAN

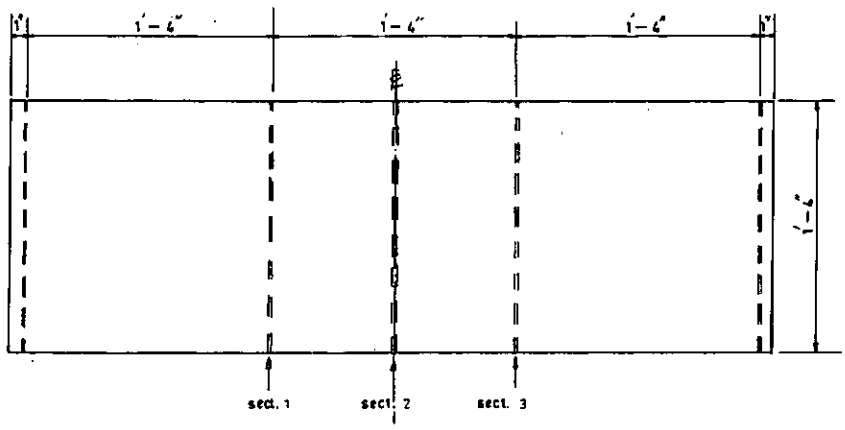

(a)

POSITIONS OF THE DIAL GAUGES AT EACH SECTION (1, 2 & 3)

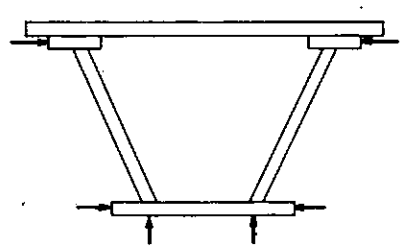

(b)

POSITIONS OF THE STRAIN GAUGES ACROSS THE SPAN.

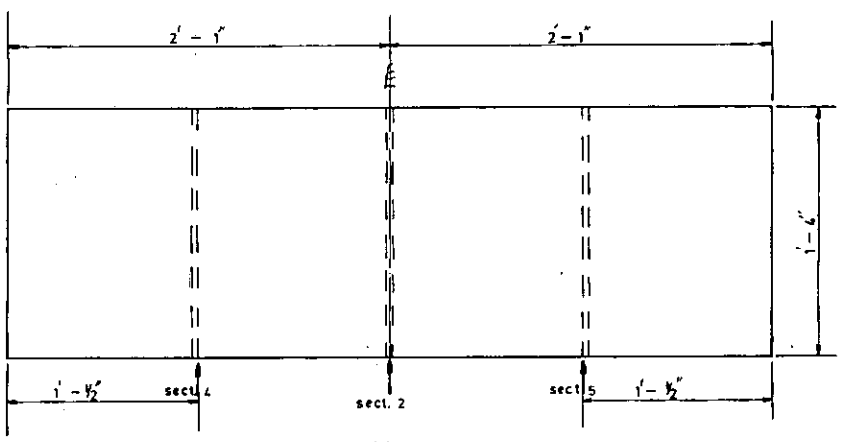

(c)

POSITIONS OF THE STRAIN ROSETTES AT SECTIONS 4 & 5.

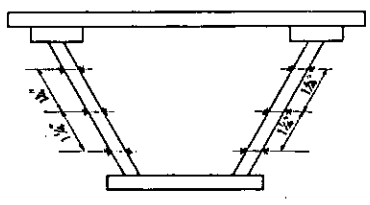

(d)

POSITIONS OF THE LINEAR GAUGES AT SECTION 2

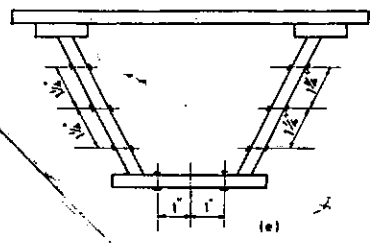

(e)

FIG. 4-3

Scale 1 : 2

predominant steel troughing of the box girder model is to enhance a degree of "elastic" behaviour under load.

The reinforced concrete deck is 4' 2" long by 1' 4" wide by $2\frac{1}{4}$" thick and projects beyond the edges of the prefabricated supporting steel troughing. Intermediate steel diaphragms were welded to the steel troughing as shown in Fig. 4-2. The concrete mix used for the deck is $1:1\frac{1}{2}:3$ with a water cement ration of 0.5. Ordinary portland cement was used for the concrete mix with fine sand and $\frac{3}{8}$" aggregates.

4-3 MODEL DESIGN AND FABRICATION:

The model is strictly a composite box girder bridge.

The steel portion of the box girder cross-section was prefabricated by Messrs Dorman Long Nigeria Limited by welding the various steel plate components together (Pl. 1)

After delivery from the shop floor, a single row of $1\frac{1}{4}$" high studs (shear connectors) was welded on to each of the top flanges of the box girder at a spacing of 3" from centre to centre.

First, the positions of the strain gauges and rosettes were marked. At the midspan cross-section, where pure bending is expected to occur as a result of the loading manner, three points were marked on each of the two side plates of the steel troughing. Three points were marked on each of the two side plates of the steel troughing. Three points were also marked on the bottom plate (see Fig.4-3e). These points are the locations of the linear gauges. The markings were done inside and outside the model. At the quarter span cross-section from one end of the test piece, where both bending and shearing would occur, three points each were marked on the inside and outside of a side plate. The same was done at the quarter span cross-section from the other end but here the markings were done on the second side plate (see Fig.4-3d). These are the locations of the strain rossettes. The surface around the marked points were then cleaned with emery cloth to remove scales and rusts in order to achieve good bond between the gauges and the rest piece. The gauges were then stuck on by means of tensol cement. The tensol cement was prepared by mixing together one part of component B (the hardner) to twenty-five (25) parts of A to obtain a quick setting and good bonding material.

Thin insulated wires (of different colours) with little electrical resistance were cut in equal lengths of about 5 feet for the electrical connection of the gauges in a measuring bridge circuit. A dummy guage was stuck on a steel plate to compensate for heat and temperature changes.

One end of each twin wire was soldered on to the leads of a strain gauge whilst the other end, after testing for electrical continuity using an avometer to ensure that the soldering had been properly done, was connected to the Data Recording System.

The strain rossettes were generally more difficult and delicate to handle and some of the strain gauge lead wires cut off after the soldering had been completed. As a result, not all the strain gauges functioned.

Manufacture of the Composite Box Girder - The concrete deck was cast in two stages. First, a wooden formwork measuring 4' 2" x $8\frac{3}{4}$" x $1\frac{1}{4}$" was made. In it was laid a wire mesh of $\frac{1}{8}$" diameter as nominal reinforcement. This formwork was used to cast a concrete slab which was later used to cover the top opening of the steel trough as a permanent part of the second stage shuttering. This was then left to cure for about four days before the second stage. This was done in order to minimise the problem of removal of the shuttering within the trough of the box girder.

For the second stage, a wooden formwork for the complete deck (4' 2" x 1' 4" x $2\frac{1}{4}$") was constructed from $\frac{5}{8}$" plywood. This was supported from the laboratory floor. The first slab, covering the top opening of the steel troughing was then centrally placed in the new formwork (see pl. 1).

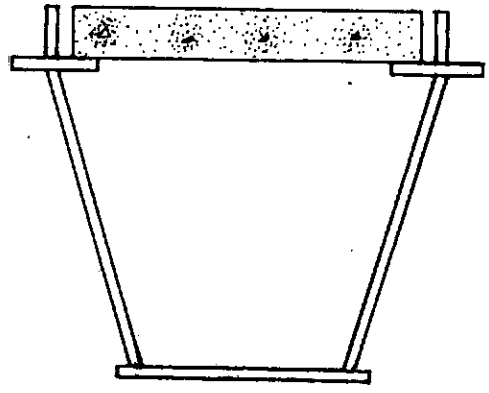

Two $\frac{3}{8}$" diameter mild steel bars were laid longitudinally at about 1" away from the shear connectors on top of the first stage concrete slab. $\frac{1}{8}$" diameter steel rods were then laid across these two longitudinal ones, at about 6" centre to centre. (Fig.4-4 pl.1).

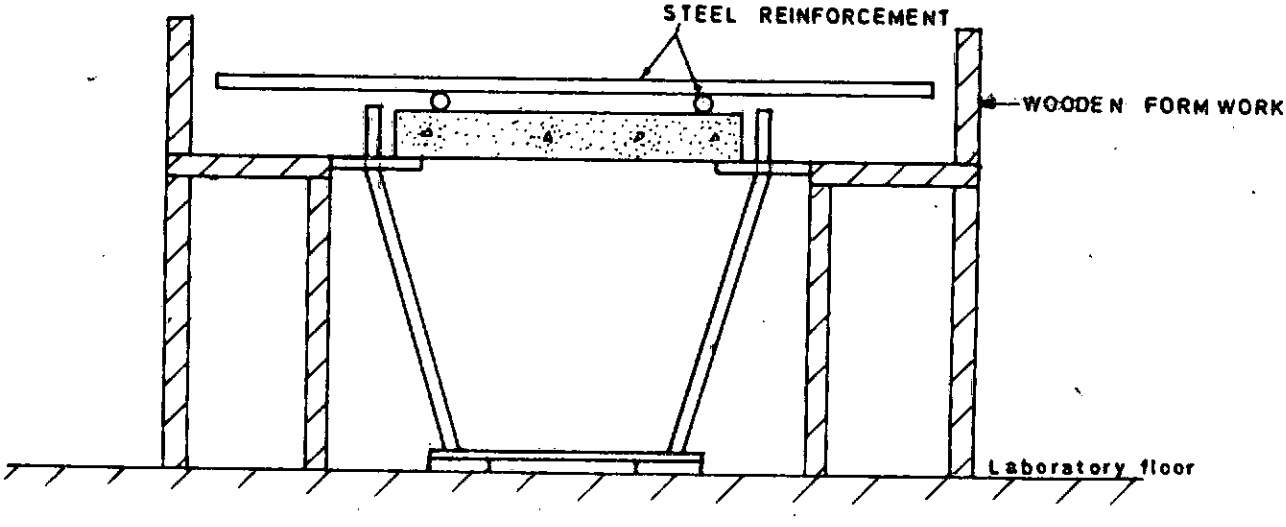

FIG 4-4

The concrete, after having been mixed in a Fredonis Wis Drum Mixer, was poured into the formwork, covering the first stage smaller slab,

embedding the shear connectors and the reinforcement. The wet concrete was gently vibrated with an electrically operated vibrator and the surface levelled. The cast concrete deck was left to cure for twenty eight days. The curing was effected by means of wet sack cloths placed over the specimen. After five days, the mould was struck off and the sackings were kept wet by watering daily for the 28-day curing period. After the curing period the ends of the box girder model were then supported on two short steel columns resting on the laboratory floor. Other instrumentations e.g. fixing of dial gauges, fixing of demec points etc., were then carried out and a frame for fixing dial gauges was errected round the box girder. The free ends of the wires from the linear strain gauges and strain rossettes were soldered on to blocks of multipin connectors which connected the wires to the Data Recording System.

The test piece rests directly on a fixed roller bearing at one end and a free roller bearing at the other. The base plate of each end roller bearing rests on a load cell placed on its short steel supporting column.

4-4 TEST SET UP:

The box girder model was placed under the test frame (see pl 2).

This frame is made of 2 - 8 feet high 8" x 4" rolled steel columns bolted to the laboratory strong floor at 6 feet centres with a 8" x 8" rolled steel joist cross-beam bolted to the steel columns. Fig. 4-5 shows the set up of the last piece within the loading frame. The loading jack was attached to the centre of the cross-beam as shown in Fig. 4-1.

PLATE 1

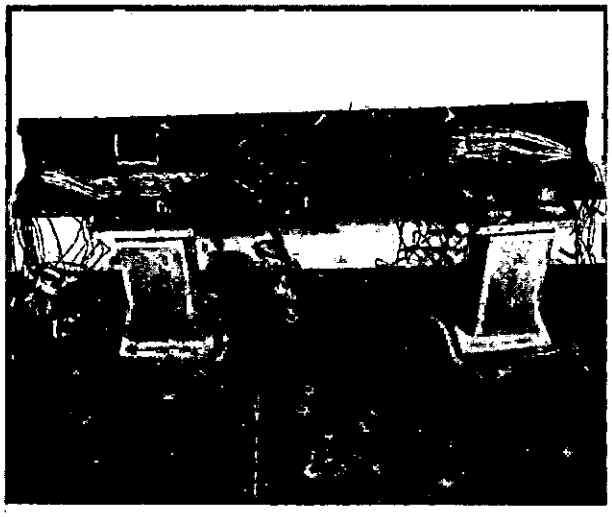

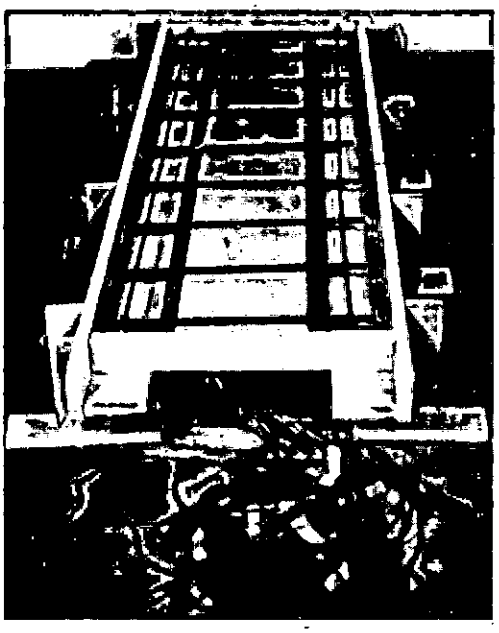

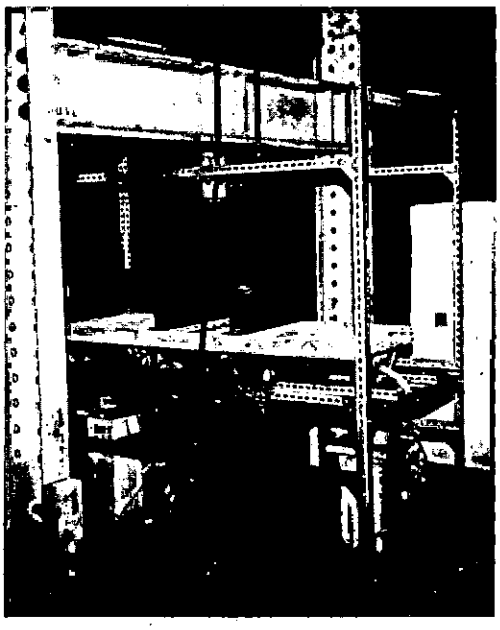

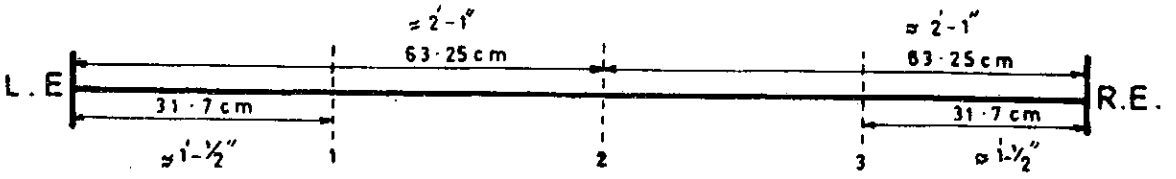

SECTION TO SHOW STRAIN GAUGE LOCATIONS

L.E = Left End

R.E = Right End

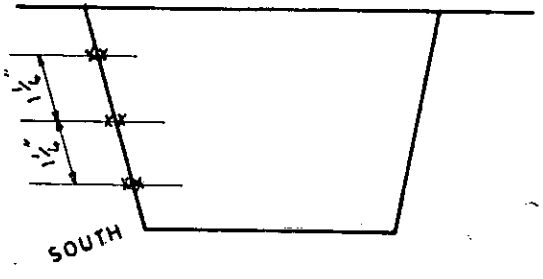

LEFT SECTION

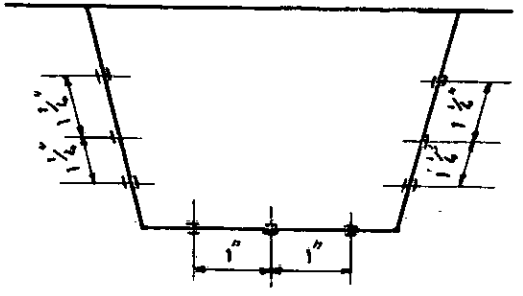

MIDDLE SECTION

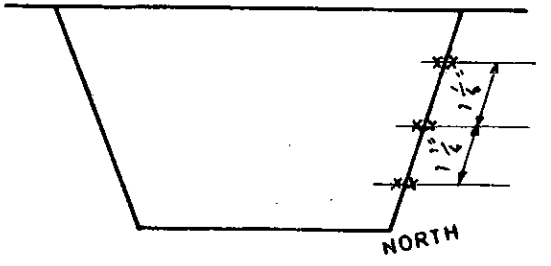

RIGHT SECTION

= LINEAR STRAIN GAUGE

XX STRAIN ROSETTES

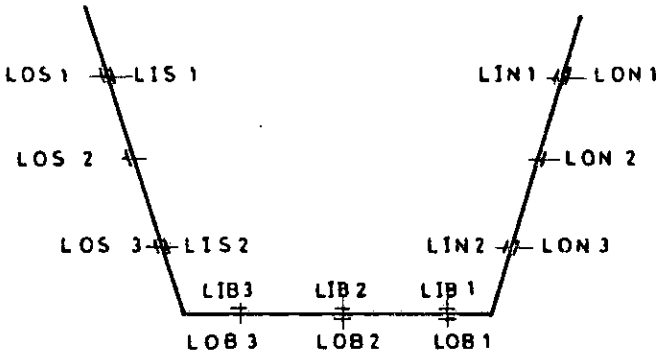

MIDDLE SECTION (Linear Gauges)

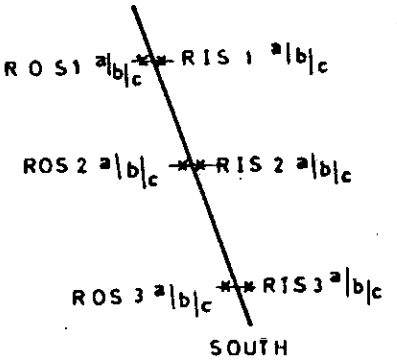

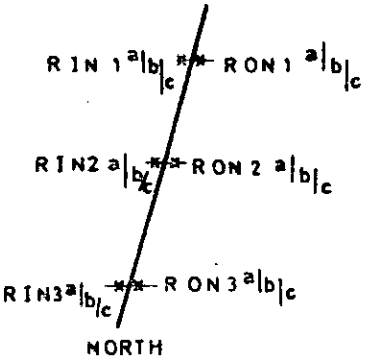

SIDE SECTIONS (Rosette Strain Gauges)

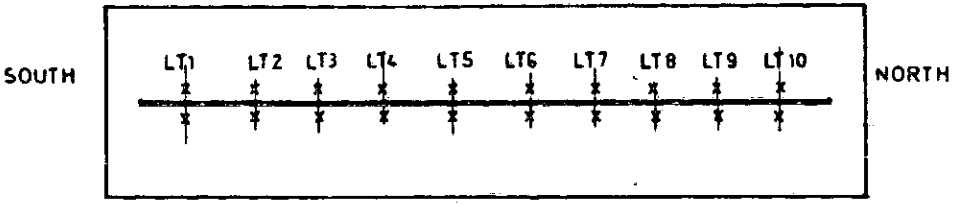

DECK (top) VIEW (LINEAR GAUGES)

LOCATION OF STRAIN ROSETTES AND LINEAR GAUGES

LABELLING OF GAUGES

KEY

L = Linear
R = Roselte
B = Bottom
I = Inside
O = Outside
N = North
S = South
T = Top
D = Dial
U = Upper
L' = Lower

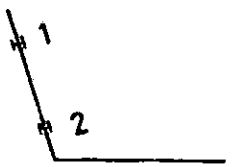

LINEAR

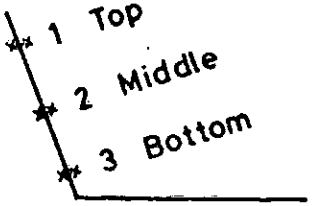

ROSETTE

For the linear case for example,

LIN1 = Top linear gauge on the Inside on the North side

LIS 2 = Bottom linear Inside gauge on South side

For the Rosette it would read like this:

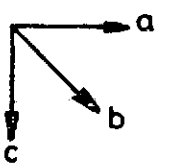

RIN3a = Inside Rosette Gauge at the bottom on the North side and in the direction 'a'

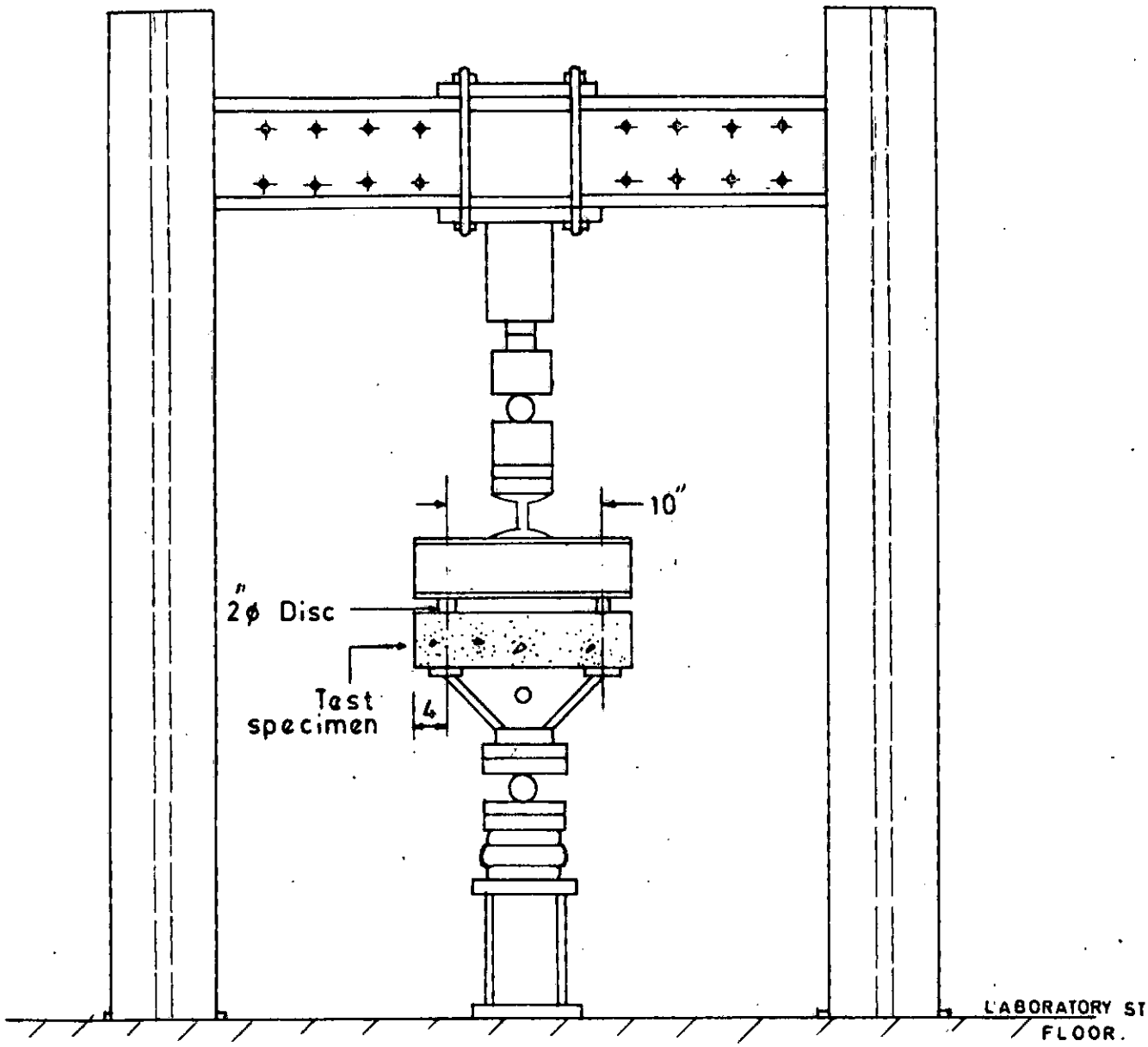

FIG 4-5

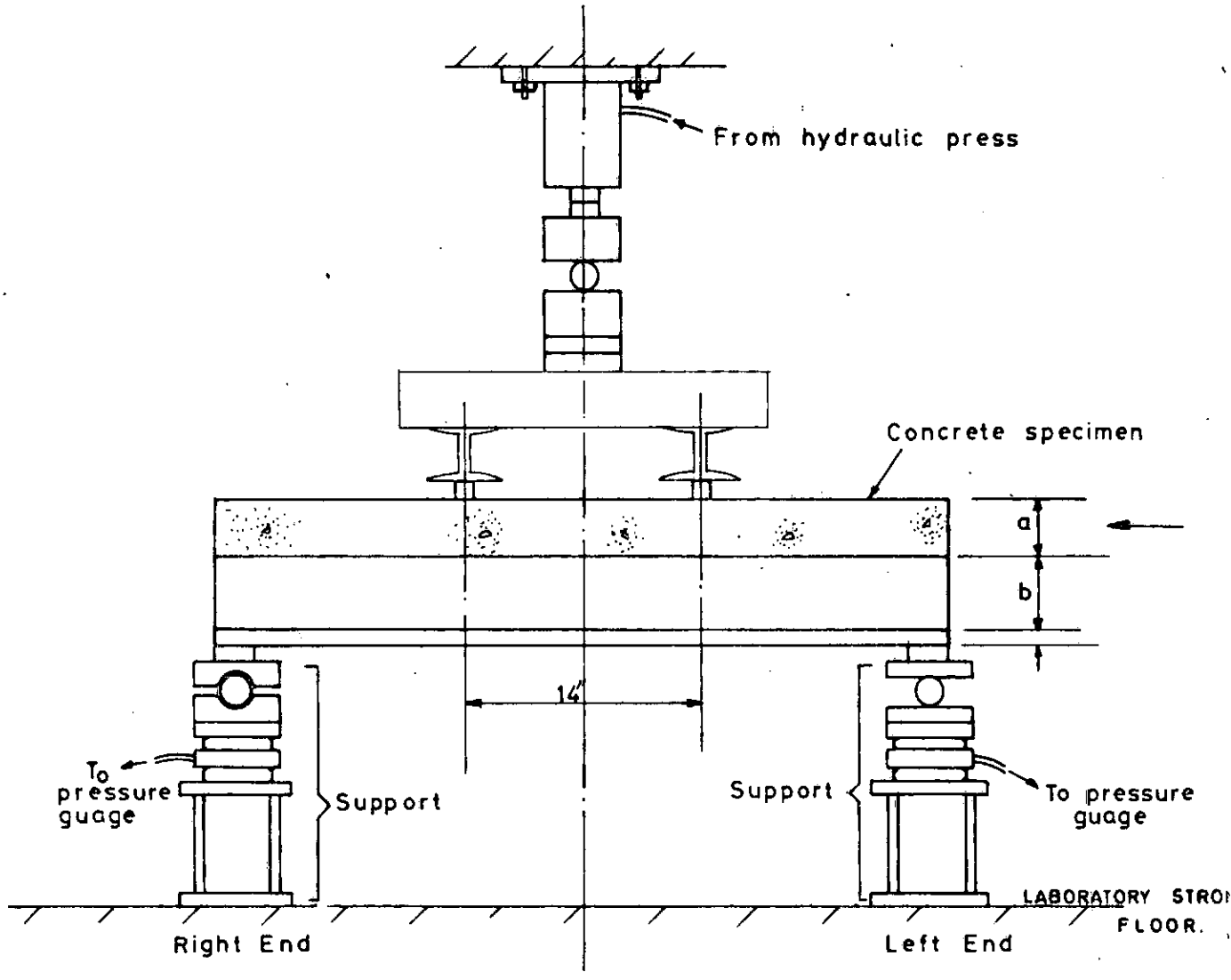
From hydraulic press
Concrete specimen
a
b
14"
To pressure guage
Support
Support
To pressure guage
LABORATORY STRON
FLOOR.
Right End
Left End

FIG 4-6

PLATE 2

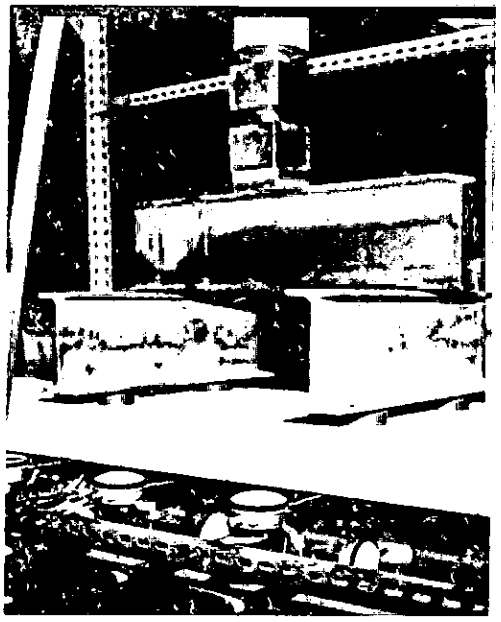

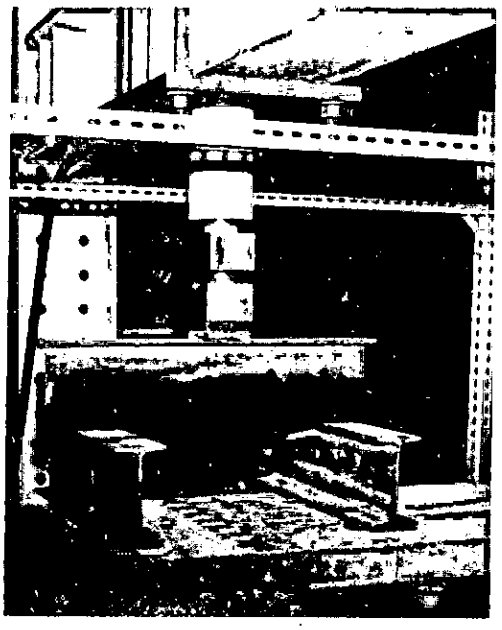

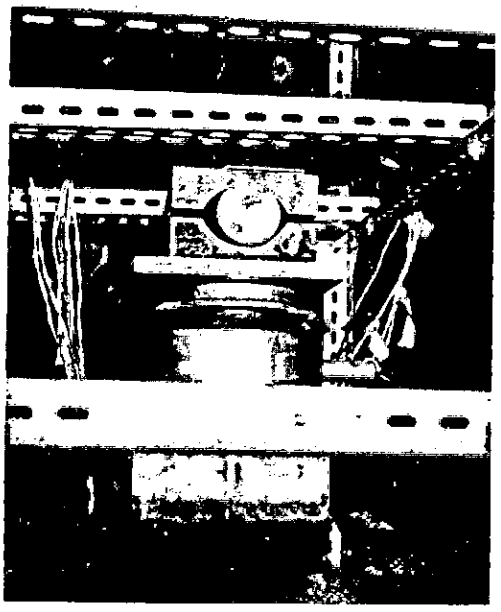

PLATE 3

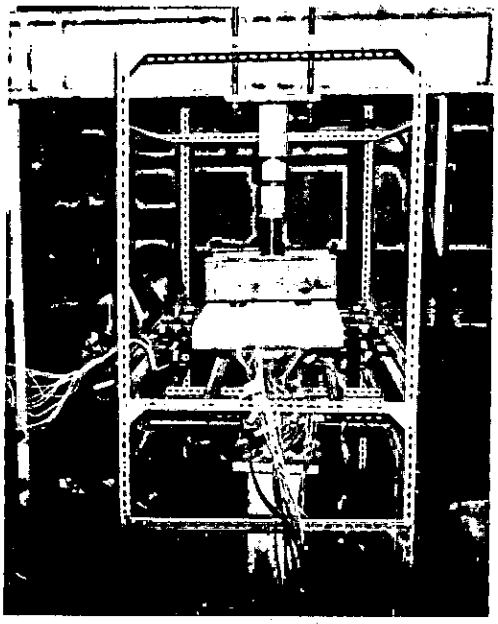

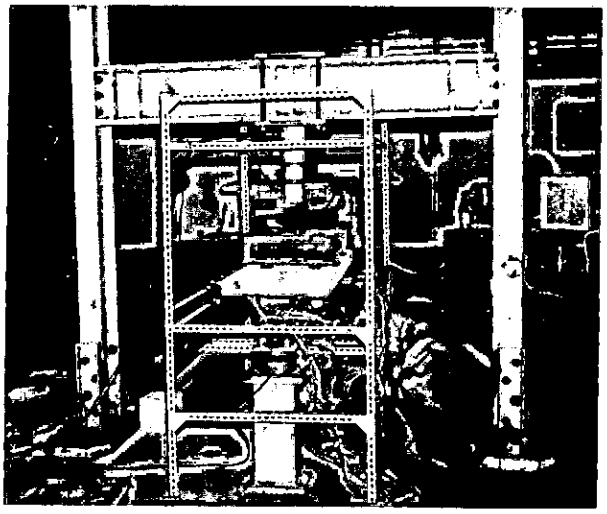

A smaller frame made of dexion angles was used to hold all the measuring dial gauges.

The frame was 5' 1" long by 2' 6½" wide by 5' 0" high.

Three sections of the test specimen carried the electrical resistance strain (ERS) gauges.

The midspan section and two sections at the third span points.

The ERS gauges were the Romulus type, the dial gauges were the John Bull type and the Data Recording System was the Transducer Meter Type 061 (made by Sangamo Controls Limited).

End Supports - One end support consists of a steel plate measuring 6½" x 6½" x ½" thick supporting a roller bearing system made up of a 2" diameter cylindrical steel roller sandwiched between two steel plates and seating within the two part-cylindrical identations of two 4½" x 4¾" x 1¼" steel plates. See Pl. 2.

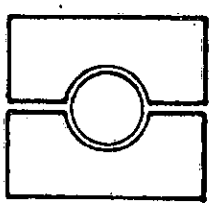

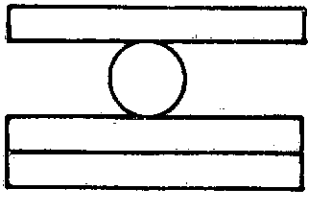

The other end is supported by means of an arrangement of three steel plates measuring $6\frac{1}{2}$" x $6\frac{1}{2}$" x $\frac{1}{2}$" thick and a 2" diameter cylindrical steel roller. Two plates were placed on top of a load cell which was placed on the short steel columns whilst the other acted as a bearing plate on the specimen with the roller sandwiched between them.

4-5 EXPERIMENTAL PROCEDURE:

Before the application of any load, the dial gauge readings were taken, the initial readings of the linear ERS gauges and strain rossettes were recorded. The pressure gauges of the load cells were set to the zero mark. See Pl. 3.

The whole arrangement of the test specimen and the location of points of application of the loads were carefully checked and adjusted to ensure a symmetrical two point loading. After this, the load was applied in an increasing manner by means of a hydraulic jack in steps of about 600lb.

At each stage of loading, all linear strain gauge, strain rossette and dial gauge readings were recorded.

4-6 DISCUSSION OF EXPERIMENTAL RESULTS

Figures 4-7 and 4-8 give the results of the experimental programme. Whilst deflexion results are reliable, strain gauge readings are rather erratic. This was thought to be due largely to drift in the strain gauges and to the instability of the strain measuring device. For example the data recording system was not precise, the needle of the bridge was always oscilliating. The device for balancing the resistances in the bridge was manually operated and it took some time between zeroing, loading and reading, probably causing overheating of the gauges. The results of the strain gauges in the rossettee group. Notwithstanding these set-backs, some attempts are made to interprete the linear gauge results.

DEFLEXIONS

Figure 4-7 shows the deflexion characteristic of the testpiece for the loading system applied. These results are related to the theoretical deflexions that would be obtained using the transformed section theory. It is obvious from Figure 4-7b that measured deflexions are much smaller than would be expected from the transformed section theory. It should be noted that the plate elements of the experimental tests piece are much thicker than would be required for a linear scale model of a steel box-girder prototype; this is dictated by the constraints of constructing extremely thin plates into a box section. On the whole the box section is shown to be much more flexurally stiffer than would be supposed from simple beam bending

TABLE 2

KN/M^2

LOAD KN	LT1	LT2	LT3	LT4	LT5	LT6	LT7	LT8	LT9	LT10
5.40	2835	1554	1785	1339	987	1911	2436	2583	2100	2638
8.00	2224	2142	2352	1612	924	2331	2381	1615	2121	1870
10.6	5355	4893	5754	3321	2814	2250	3111	3421	4263	4683
13.3	6006	5124	4384	4282	2289	4641	4851	4901	4473	5801
15.9	6195	4452	3276	3360	2793	4893	4187	3444	4586	4641
18.5	6478	5271	5061	4641	2898	3754	4460	3780	4990	5570
21.0	1764	1318	1365	672	756	2331	2239	2126	2163	1722

TABLE 3 KN/M^2

LOAD KN	LON1	LON2	LON3	LOB1	LOB2	LOB3	LOS1	LOS2	LOS3
5.40	10,500	14,700	20,800	20,450	18,770	22,970	7,970	10,876	12,070
8.00	14,700	25,200	30,920	50,820	36,330	44,730	12,030	16,030	30,600
10.6	42,000	49,140	57,720	67,200	54,390	63,420	42,120	55,000	65,000
13.3	15,240	22,460	27,650	29,850	27,650	28,150	17,340	22,340	24,600
15.9	24,070	34,860	43,860	47,250	45,150	50,190	21,700	34,490	41,490
18.5	35,100	42,610	59,560	60,140	61,320	63,420	23,730	38,220	65,520
21.0	48,300	58,120	63,630	61,530	52,710	67,200	27,280	49,770	61,740

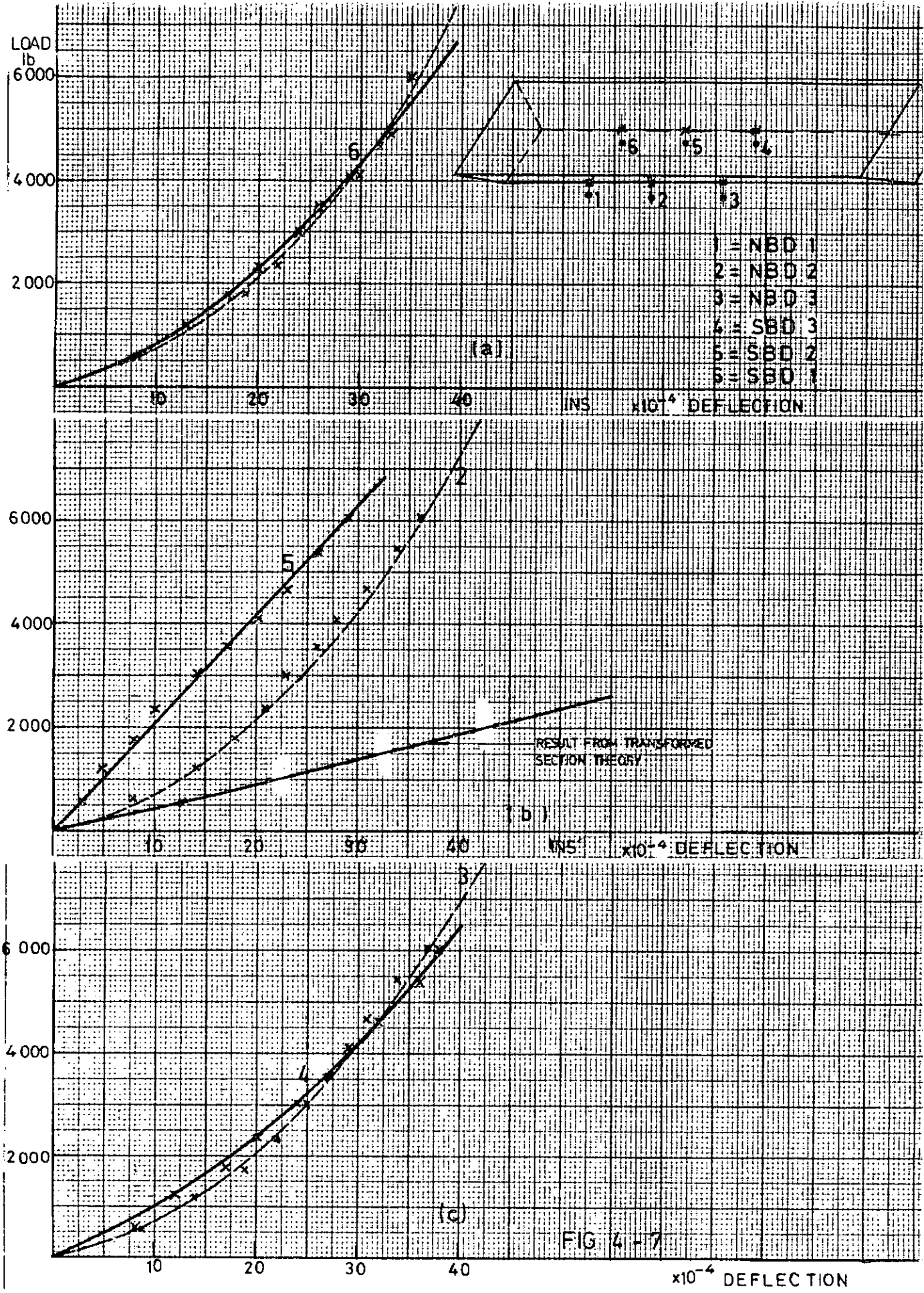
LOAD
lb
6 000
4 000
2 000
6
1
2
3
4
5
1 = NBD 1
2 = NBD 2
3 = NBD 3
4 = SBD 3
5 = SBD 2
6 = SBD 1
(a)
10
20
30
40
INS
×10⁻⁴ DEFLECTION
6000
4000
2000
5
2
3
RESULT FROM TRANSFORMED SECTION THEORY
(b)
10
20
30
40
INS
×10⁻⁴ DEFLECTION
6 000
4 000
2 000
3
4
(c)
10
20
30
40
×10⁻⁴ DEFLECTION

FIG 4-7

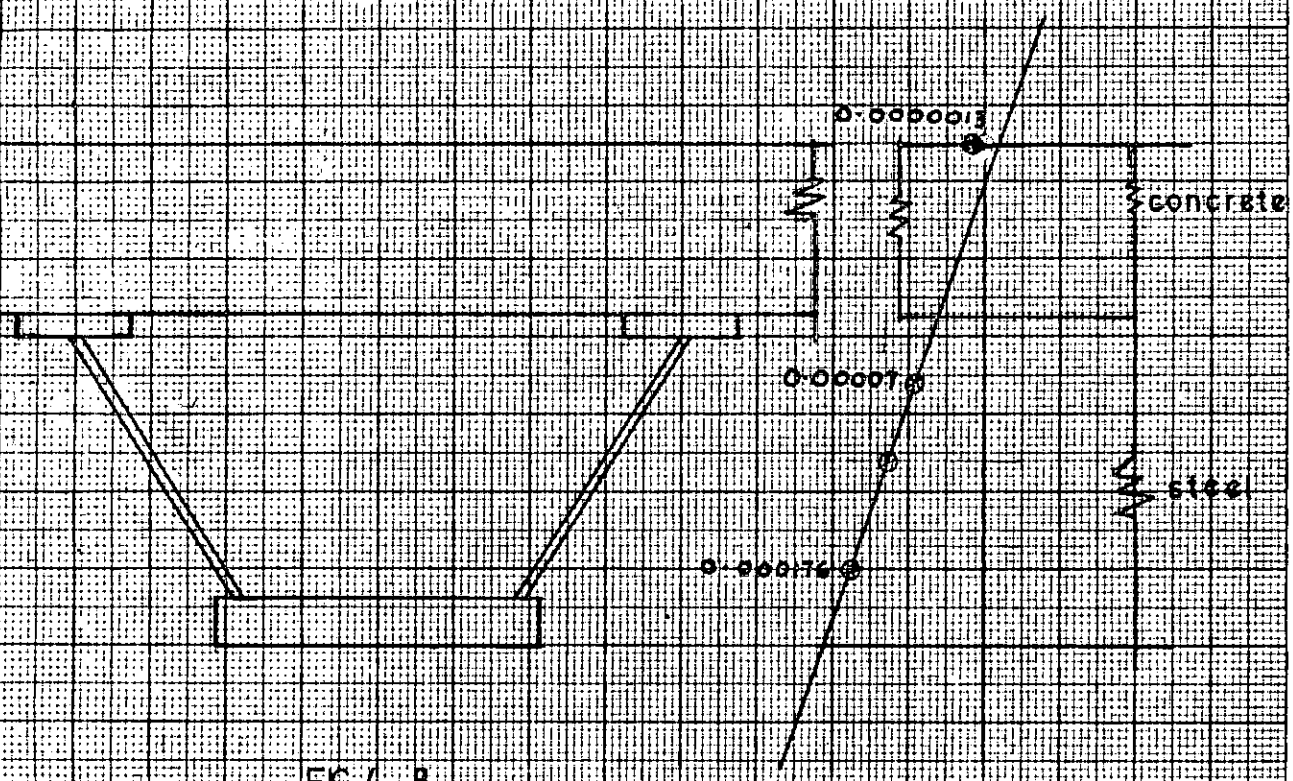

FIG 4-8

theory. The none-linearity of most of the deflexion profiles with load is thought to be due to the inelastic behaviour of the concrete deck.

STRAINS

Figure 4-8 shows the strain behaviour across the top concrete flange and over the cross-section. Although the concrete strains as measured by ERS gauges are tensile, they none-the-less demonstrate the shear lag effect across the wide concrete flange. The 'elastic' properties of the concrete used are not fully known. For example, the Poisson's ratio for the concrete is not known. In the absence of an obvious cause, the tensile nature of the extreme top fibre concrete strains is thought to be due to the general erratic behaviour of the measuring system. Figure 4-8 shows the strain distribution across the depth of the section at a load of 5·4 KN The strain distribution is linear across the steel section but not co-linear across the entire section. None-co-linearity of strain over girder depth has been recorded by various workers as a characteristic of composite beams where there is interface discontinuity of materials and interaction is ensured by means of some mechanical form of shear connection. This tendency is usually accompanied with interface slip. Although an attempt was made to measure interface slip in this test, no measurable slip seemed to have occured.

CHAPTER V

GENERAL RECOMMENDATIONS

A careful study of the proposals put forward in the report of the Committee of Inquiry into the Basis of Design and Method of Erection of Steel Box Girder Bridges under Merrison reveals two interesting features as follows:

1. Loads and forces to be considered in design are to be estimated using appropriate partial load factors and strength factors.

2. Recommendations on Global analysis of the super-structure emphasised the use of elastic methods of analysis in estimating relevant moments, shears and deflexions.

Because the behaviour of box girders is still not fully understood, it is not feasible to use a collapse method concept in their designs; also theoretical studies of elasitc behaviour of this type of structure have shown that only the elastic method of analysis is sufficiently understood to help unravel the complex behaviour of the interacting plate assembly forming the box. Recommendations on method of analysis as contained in the report seem to be based on three procedures:

1. The use of the transformed section theory in predicting longitudinal stresses due to symmetrical loading allowing for shear lag effects in the flanges of box girders.

2. The estimation of longitudinal torsional warping stresses in the vicinity of intermediate supports and at the loaded section under the HB vehicle and knife edge load using the elastic relation for torsional bending.

3. The estimation of additional longitudinal distorsional warping stresses of the section due to applied torque and employing the results of the Beam on Elastic Foundation analogy referred to earlier. In any design effort at least two of these three procedures will have to be employed to predict total stresses due to applied loading. From the results of the present analysis, the following recommendations are suggested for adoption in the design of box girder bridges.

1. The loads, forces and permissible stresses to be considered should be so factored as to correspond to assumed working loads and stresses, since reliance is put on elastic methods in estimating the response to loads of an assumed design section.

2. That unified approach to the analysis of box girder bridges be adopted instead of two or three combined approaches none of which is exact or capable of giving global picture of response. The method of analysis presented here and similar methods (e.g. Goldberg and Leve's displacements method) are not too complex to employ in the design of this complex structure. The HB vehicle and knife Edge Load are representable in mathematical form, using Fourier expansion and the solution of "Edge-connected Composite Plates" subjected to bending presented in the thesis.

3. Effective width factors should only be used where torsional couples are small. Where torsional couples due to the HB vehicle and Knife Edge load are large, the effective width concept is no longer appropriate. A torsional couple could be considered small if the additional longitudinal stress due to it is not more than 25% of the permissible stress.

4. Although the present analysis has not examined the influence of diaphragms, it is suggested that the full torsional effect of the loads referred to in 3 above be allowed for in design.

5. Where effective width factors are relevant to design, the recommendations in this thesis (Table 1) or those in the Merrison report may be quite adequate.

6. The side slope of the inclined webs of box girders be not greater than 15^0 to the vertical. Future studies may help in answering nagging questions about the instability of longitudinal stress values with web side slope.

7. Longitudinal flange stiffeners may be evenly spaced where torsional effects are minimal, for example, when the bridge deck is not very wide and the loads are not likely to be at the extreme edges of the top flange. However, where torsional effects are likely to be pronounced, stiffeners should be provided in both flange and web with such spacing as to ensure greater stiffener effect at the corners of the box.

8. These recommendations should be applied in conjuction with recommendations in Codes of Practice as they relate to buckling in steel plates, creep and shrinkage in concrete.

NOTATIONS

$2b$	=	Width of top plate of box girder
$2c$	=	Length of slanting sides of box girder
$2d$	=	Width of bottom plate of box girder
w	=	Transverse deflection in z- direction
x,y	=	Rectangular co-ordinate axes for plate
P	=	Applied Load
E,μ,ν	=	Modulus of Elasticity, Shearing Modulus of Elasticity and Poisson's ratio.
M_{xx}	=	Bending moment in the x- direction
M_{yy}	=	Bending moment in y- direction
M_{xy}	=	Twisting moment about plane x-y.
Q_{xx}	=	Shearing Force Per Unit Length parallel to the y axes
Q_{yy}	=	Shearing Force Per Unit Length parallel to the x axes
V_{xx}	=	Kirchoff Shearing Stress normal to edge x- axis
V_{yy}	=	Kirchoff Shearing Stress normal to y- axis
σ_{xx}	=	Normal Stress in x- direction
σ_{yy}	=	Normal Stress in y- direction
σ_{xy}	=	Shearing Stress in the xy plane
u	=	Displacement in x direction for any point in the mid-plane of the plate.
v	=	Displacement in y- direction for any point in the mid-plane of the plate.

$A_n^{(i)}, B_n^{(i)}$
$C_n^{(i)}, D_n^{(i)}$ = Superposition coefficients with respect to the bending field.

$\bar{A}_n^{(i)}, \bar{B}_n^{(i)}$
$\bar{C}_n^{(i)}, \bar{D}_n^{(i)}$ = Superposition coefficients with respect to the extensional field

D = Flexural Ridigidity of Plate = $\frac{Et^3}{12(1-\nu^2)}$

ϵ = Small increment in length

η = Distance of point load from the x- axis measured in the y- direction

ξ = Distance of point load from the y- axis measured in the x- direction

ℓ = Length of span

2α = The angle which a slanting plate makes with the top plat

N_{xx} = Internal plate force per unit length in the x direction (Membrane Force)

N_{yy} = Membrane force per unit length in the y- direction

N_{xy} = Membrane shearing force in the plane x-y

W^0 = Transverse deflection field due to the applied load

W^* = The superimposed transverse deflection field

ϕ_i = Stress function

$f(x)$ = Function of x

$g(y)$ = Function of y

t = Thickness of Plate

P1	=	$-(3-\nu)/(1-\nu)$
P2	=	$-2.0/(1+\nu)$
P3	=	$-(1-\nu)/(1+\nu)$
P4	=	$t^2/12$
P5	=	$t^2(1+\nu)/12.(1-\nu)$
P6	=	$2/(1-\nu)$
P7	=	$-2\nu/(1+\nu)$
P8	=	λ^2
P33	=	$(1+\nu)/(1-\nu)$
P44	=	$2/(1-\nu^2).(1-\nu)$
P_u	=	Harmonic component of ~~Ultimate~~ Load
n	=	Number of the harmonic or number of half-waves in the x- direction.
λ	=	Coefficient parameter
β	=	Effective width factor

REFERENCES:

1. E.N. Wright, Abdel-Samad & Arthur Robinson,
"B.E.F. Analogy for the Analysis of Box Girders"
Journal of the Structural Div. Proc. of American Society
of Civil Engineers - July, 1968.

2. "Progress Report on Steel Box Girder Bridges"
by sub-committee on Box Girders of the ASCE-AASIIO - April, 1971

3. David Malcolm & Richard Redwood
"Shear Lag in Stiffened Box Girders"
Journal of Structural Div. of A.S.C.E. - July, 1970.

4. Abdel-Samad, Sana R. Wright, Richard Robinson,
"Analysis of Box Girders with Diaphragms"
Journal of Structural Div. - October, 1968.

5. Denison Campbell-Allen & Raymond J.L. Wedgwood,
"Need for Diaphragms in Concrete Box Girders"
Journal of Structural Div. - March, 1971

6. O.C. Zienkiewicz and J. Kai Cheving
"The finite element method for Analysis of Elastic
and Orthotropic Slabs"
Journal of Structural Div. A.S.C.E. - August, 1964.

7. Constancio Miranda & Keshavan Nair,
"Finite Beams on Elastic Foundations"
Journal of Structural Div. A.S.C.E. - April, 1966.

8. J. Dundurs & M.G. Samuchin
"Transmission of Concentrated forces into Prismatic Shells"
International Journal of Solid and Structures - 1971
Vol. 7, pp. 1627-164.

9. J.R. Yalaki, A.S.D. Wang
"Analysis of a Box made of Elastic Orthotropic Plates"
International Journal of Solids and Structures - 1972.

10. A.R. Cusens & Y.C. Loo
"Applications of the Finite Strip Method in the
Analysis of Concrete Box Bridges"

11. Ernest Grube
"Die Genan Membranentheorie der prismatischen Faltiverke" (in German

12. Michael S. Troisky & Abdul K. Azad
"Bending and Torsion in Orthotropic Deck Box Girder"
Journal of Structural Div. A.S.C.E. - September, 1972.

13. Dennis E. Myers & Peter B. Cooper
"Box Girder Model Studies"
Journal of Structural Div. A.S.C.E.

14. Goldberg and Leve
"Theory of Prismatic Folded Plate Structure"
International Ass. for Bridge & Structrual Engrg. Publication - 1957

15. Zanoni Edward "Model Studies of a Folded Plate Structure"
Thesis presented to Lehigh Univ at Bethlerem Pa. in 1962 in
partial fulfilment of the requirements for the degree of M.Sc.

16. "Trends in the Design of Steel Box Girder Bridges"
from Progress Report by Sub-Committee on B.G. Bridges.
Journal of Structural Div. of A.S.C.E. - June, 1967.

17. A.O. Adekola
"The Dependence of Shear Lag on Partial Interaction in
Composite Beams" from International Journal of Solids
Structures, 1974, Vol.10, pp. 389 - 400.

18. Sokolnikoff & Redheffer
"Mathematics of Physics and Modern Engineering"
Published by McGraw-Hill Book Company.

19. Timoshenko and Winowsky-Krieger
"Theory of Plates and Shells"
Published by McGraw-Hill Book Company.

20. Timoshenko and Goodier "Theory of Elasticity"
Published by McGraw-Hill Book Company.

21. Borodich, "Theory of Elasticity".

22. Sokolnikoff, "Mathematical Theory of Elasticity"

23. DeFries-Skene and Scordelis
"Direct Stiffness Solution for Folded Plates"
Journal of Structural Division. Proceeding of A.S.C.E.
Vol. 90 - August, 1964.

24. A.W. Merrison et al
"Inquiry into the design and erection of Steel Box Girder Bridges" Report of Committee - Appendix 1. 1973.

25. Moffatt K.R., and Dowling P.J.
"Shear Lag in Steel Box Girder Bridges"
The Structural Engineer, Journal of the I.S.E., Vol.53 No. 10.

APPENDIX: COMPUTER PROGRAMME LISTING.

```
// JOB JC1200 SOMOLU
// OPTION LINK
// EXEC FFORTRAN
      FUNCTION SIMUL(N1,AA,X,EPS,INDIC,NRC)
      IMPLICIT REAL*8(A-H,O-Z)
      REAL *8 AA,X,EPS,SIMUL
      DIMENSION IROW(32),JCOL(32),JORD(32),Y(32),AA(NRC,NRC),X(32)
      MAX=N1
      IF(INDIC.GE.0) MAX=N1+1
C
C     IS N1 LAGER THAN 32
      IF (N1.LE.32) GO TO 5
      WRITE(3,250)
      SIMUL=0.
      RETURN
C     BEGIN ELIMINATION PROCEDURE
C
    5 DETER=1.
      DO 18 K=1,N1
      KM1=K-1
C
C     SEARCH FOR THE PIVOT ELEMENT
      PIVOT=0.
      DO 11 I=1,N1
      DO 11 J=1,N1
C
C     SCAN IROW AND JCOL ARRAYS FOR INVALID PIVOT SUBSCRIPTS
C
      IF(K.EQ.1) GO TO 9
      DO 8 ISCAN = 1,KM1
      DO 8 JSCAN =1,KM1
      IF(I.EQ.IROW(ISCAN)) GO TO 11
      IF(J.EQ.JCOL(ISCAN))GO TO 11
    8 CONTINUE
    9 IF(DABS(AA(I,J)).LE.DABS(PIVOT)) GO TO 11
      PIVOT = AA(I,J)
      IROW(K)=I
      JCOL(K) = J
   11 CONTINUE
C
C     INSURE THAT SELECTED PIVOT IS LARGER THAN EPS
C
      IF(DABS(PIVOT).GT.EPS) GO TO 13
      SIMUL=0.
      RETURN
C     UPDATE THE DETERMINANT  VALUE
C
   13 IROWK = IROW(K)
      JCOLK = JCOL(K)
      DETER = DETER*PIVOT
C
C     NORMALIZE PIVOT ROW ELEMENTS
C
      DO 14 J=1, MAX
   14 AA(IROWK,J) = AA(IROWK,J)/PIVOT
C     CARRY OUT ELIMINATION AND DEVELOP INVERSE
```

```
C
      AA(IROWK,JCOLK) = 1./PIVOT
      DO 18 I=1,N1
      AAIJCK =AA(I,JCOLK)
       IF(I .EQ. IROWK) GO TO 18
      AA(I,JCOLK)=-AAIJCK/PIVOT
      DO 17 J=1,MAX
   17 IF(J.NE.JCOLK) AA(I,J)=AA(I,J)-AAIJCK*AA(IROWK,J)
   18 CONTINUE
C
C     ORDER SOLUTION VALUES (IF ANY) AND CREATE JORD ARRAY
C
      DO 20 I=1,N1
      IROWI=IROW(I)
      JCOLI = JCOL(I)
      JORD(IROWI) = JCOLI
   20 IF(INDIC.GE.0) X(JCOLI)=AA(IROWI,MAX)
C     ADJUST SIGN OF DETERMINANT
C
      INTCH = 0
      NM1 = N1-1
      DO 22 I=1,NM1
      IP1 =I+1
      DO 22 J=IP1,N1
      IF(JORD(J).GE.JORD(I)) GO TO 22
      JTEMP=JORD(J)
      JORD(J) = JORD(I)
      JORD(I) = JTEMP
      INTCH =INTCH + 1
   22 CONTINUE
      IF(INTCH/2*2.NE.INTCH) DETER=-DETER
C     IF INDIC IS POSITIVE RETURN WITH RESULTS
   24 IF(INDIC.LE.0) GO TO 26
      SIMUL =DETER
      RETURN
C
C     IF INDIC IS NEGATIVE OR ZERO UNSCRAMBLE THE INVERSE FIRST BY ROWS
   26 DO 28 J=1,N1
      DO 27 I=1,N1
      IROWI = IROW(I)
      JCOLI = JCOL(I)
   27 Y(JCOLI) =AA(IROWI,J)
      DO 28 I=1,N1
   28 AA(I,J) = Y(I)
C     THEN BY COLUMNS
      DO 30 I=1,N1
      DO 29 J=1,N1
      IROWJ =IROW(J)
      JCOLJ = JCOL(J)
   29 Y(IROWJ) = AA(I,JCOLJ)
      DO 30 J=1,N1
   30 AA(I,J) = Y(J)
C     RETURN FOR INDIC NEGATIVE OR ZERO
      RETURN
C     FORMAT FOR OUTPUT STATEMENT
  250 FORMAT(10HON TOO BIG)
      END
```

```
C
      IMPLICIT REAL*8(A-H,O-Z)
      REAL *8 AA,X,EPS,SIMUL
      DIMENSION PSI1(10),PSI2(10),PSI3(10),PSI4(10),SH1(10),
     1CH1(10),CCCTH1(10),SH2(10),CH2(10),SH3(10),CH3(10),
     2SH4(10),CH4(10),CCCTH4(10),F0(10),F1(10),G0(10),G1(10),RB(32),
     3X(32),AA(33,33),SINA(10),BB(32,1),CCCTH2(10),SSH4(10),SSH1(10),
     4CCH1(10),SSH2(10),CCH2(10),CCH4(10),CH11(10),SH11(10),CH22(10),
     5SH22(10),CH33(10),SH33(10),PSI11(10),PSI22(10),PSI33(10),PSI12(1
     6,SH12(10),CH12(10),B1(10),B2(10),D11(10),D2(10),SINP(10)
      REAL MKYT1,MKYT12,MKYT0,MKYT42,MKYT4,MKYS1,MKYS12,MKYS0,MKYS22,
     1MKYS2,MKYB2,MKYB22,MKYB0,MKYB32,MKYB3,MKYS3,MKYS32,MKYS00,MKYS42
     2MKYS4,MYT1,MYT12,MYT0,MYT42,MYT4,MYS1,MYS12,MYS0,MYS22,MYS2,MYB2
     3MYB22,MYB0,MYB32,MYB3,MYS3,MYS32,MYS00,MYS42,MYS4
    1 READ(1,100) N1,INDIC,EPS
      WRITE (3,604)N1,INDIC,EPS
  604 FORMAT(10X,2(I2,5X),F14.9)
C     CALCULATING AND PRINTING OF AUGMENTED MATRIX AA
C
      MAX =N1
      IF(INDIC.GE.0)MAX=N1+1
      P=2.0E+2
      SP=20.0
      W=2.0*P/SP
      W=-W
      PYE=3.141592654
      EPS1=0.5*SP
      ES=210.0E+9
      EC=21.0E+9
      POIS=0.3

      T=0.09
      B=2.5
      ALPHA=19.0*PYE/36.0
      DO 112 KC=1,7
      ALPHA=ALPHA-(PYE/36.0)
      SINC=DSIN(ALPHA)
      COSC=DSQRT(1.0-SINC*SINC)
      C=1.0/SINC
      D1=B-(2.0*COSC/SINC)
      COI=ES/(1.0-POIS*POIS)
      D=COI*T*T*T/12.0
      IP=2
C
C

      ETA=-B/4.0
      DO 111 K=1,5
      ETA=ETA+B/4.0
      IF(ETA-B)4,111,4
    4 WK1=0.0
      AVKSXT=0.0
      AVKSXB=0.0
      WK1=0.0
      WK12=0.0
      WK0=0.0
```

```
WK42=0.0
WK4=0.0
WKS1=0.0
WKS12=0.0
WKS0=0.0
WKS22=0.0
WKS2=0.0
WK2=0.0
WKB22=0.0
WKB0=0.0
WKB32=0.0
WK3=0.0
WKS3=0.0
WKS32=0.0
WKS00=0.0
WKS42=0.0
WKS4=0.0
TKX1=0.0
TKX0=0.0
TKX42=0.0
TKX4=0.0
TKX12=0.0
SKX1=0.0
SKX12=0.0
SKX0=0.0
SKX22=0.0
SKX2=0.0
BKX2=0.0
BKX22=0.0
BKX0=0.0
BKX32=0.0
BKX3=0.0
SKX3=0.0
SKX32=0.0
SKX00=0.0
SKX42=0.0
SKX4=0.0
TKY1=0.0
TKY12=0.0
TKY0=0.0
TKY42=0.0
TKY4=0.0
SKY1=0.0
SKY12=0.0
SKY0=0.0
SKY22=0.0
SKY2=0.0
BKY2=0.0
BKY22=0.0
BKY0=0.0
BKY32=0.0
BKY3=0.0
SKY3=0.0
SKY32=0.0
SKY00=0.0
SKY42=0.0
```

```
      SKY4=0.0
      MKYT1=0.0
      MKYT12=0.0
      MKYT0=0.0
      MKYT42=0.0
      MKYT4=0.0
      MKYS1=0.0
      MKYS12=0.0
      MKYS0=0.0
      MKYS22=0.0
      MKYS2=0.0
      MKYB2=0.0
      MKYB22=0.0
      MKYB0=0.0
      MKYB32=0.0
      MKYB3=0.0
      MKYS3=0.0
      MKYS32=0.0
      MKYS00=0.0
      MKYS42=0.0
      MKYS4=0.0
C
      E=0.0
      EA=0.0
      DO 98 N=1,IP
      EA=EA+1.0
      E=2.0*EA-1.0
      ANDA=E*PYE/SP
      PSI1(N)=B*ANDA
      PSI2(N)=C*ANDA
      PSI3(N)=D1*ANDA
      A1=DEXP(PSI1(N))
      A2=DEXP(-PSI1(N))
      SH1(N)=0.5*(A1-A2)
      CH1(N)=0.5*(A1+A2)
      A1=DEXP(PSI2(N))
      A2=DEXP(-PSI2(N))
      SH2(N)=0.5*(A1-A2)
      CH2(N)=0.5*(A1+A2)
      A1=DEXP(PSI3(N))
      A2=DEXP(-PSI3(N))
      SH3(N)=0.5*(A1-A2)
      CH3(N)=0.5*(A1+A2)
      P1=-(3.0-POIS)/(1.0+POIS)
      P2=-2.0/(1.0+POIS)
      P3=-(1.0-POIS)/(1.0+POIS)
      P4=T*T/12.0
      P5=T*T*(1.0+POIS)/(12.0*(1.0-POIS))
      P6=2.0/(1.0-POIS)
      P7=-2.0*POIS/(1.0+POIS)
      P8=ANDA*ANCA
      P33=(1.0+POIS)/(1.0-POIS)
      P44=2.0/((1.0-POIS*POIS)*(1.0-POIS))
      P88=ANDA*ANCA*ANDA
      P89=T*T*T
      P72=-P88*P89/(12.0*(1.0-POIS)*(1.0-POIS))
```

```
P74=(1.0-POIS)
P70=ES*ANDA*SINA(N)/(B*(1.0+POIS))
P71=ES*ANDA*SINA(N)/(D1*(1.0+POIS))
AN=B-ETA
A1=DEXP(ANDA*(B-ETA))
A2=DEXP(-ANDA*(B-ETA))
SSH1(N)=0.5*(A1-A2)
CCH1(N)=0.5*(A1+A2)
CCCTH1(N)=CCH1(N)/SSH1(N)
AN1=B+ETA
A1=DEXP(ANDA*(B+ETA))
A2=DEXP(-ANDA*(B+ETA))
SSH2(N)=0.5*(A1-A2)
CCH2(N)=0.5*(A1+A2)
CCCTH2(N)=CCH2(N)/SSH2(N)
PSI4(N)=2.0*B*ANDA
A1=DEXP(PSI4(N))
A2=DEXP(-PSI4(N))
SSH4(N)=0.5*(A1-A2)
CCH4(N)=0.5*(A1+A2)
CCCTH4(N)=CCH4(N)/SSH4(N)
PSI12(N)=1.5*B*ANDA
A1=DEXP(PSI12(N))
A2=DEXP(-PSI12(N))
SH12(N)=0.5*(A1-A2)
CH12(N)=0.5*(A1+A2)
PSI11(N)=B*ANDA/2.0
PSI22(N)=C*ANDA/2.0
PSI33(N)=D1*ANDA/2.0
A1=DEXP(PSI11(N))
A2=DEXP(-PSI11(N))
SH11(N)=0.5*(A1-A2)
CH11(N)=0.5*(A1+A2)
A1=DEXP(PSI22(N))
A2=DEXP(-PSI22(N))
SH22(N)=0.5*(A1-A2)
CH22(N)=0.5*(A1+A2)
A1=DEXP(PSI33(N))
A2=DEXP(-PSI33(N))
SH33(N)=0.5*(A1-A2)
CH33(N)=0.5*(A1+A2)
C1=CH1(N)
S1=SH1(N)
C2=CH2(N)
S2=SH2(N)
C3=CH3(N)
S3=SH3(N)
C11=CH11(N)
S11=SH11(N)
C22=CH22(N)
S22=SH22(N)
C33=CH33(N)
S33=SH33(N)
P111=PSI11(N)
P122=PSI22(N)
P133=PSI33(N)
```

```
      P11=PSI1(N)
      P12=PSI2(N)
      P13=PSI3(N)
      S41=P4*P8*SH1(N)
      C41=P4*P8*CH1(N)
      S42=P4*P8*SH2(N)
      C42=P4*P8*CH2(N)
      S43=P4*P8*SH3(N)
      C43=P4*P8*CH3(N)
      S51=P5*P8*SH1(N)
      C51=P5*P8*CH1(N)
      S52=P5*P8*SH2(N)
      C52=P5*P8*CH2(N)
      S53=P5*P8*SH3(N)
      C53=P5*P8*CH3(N)
      SINA(N)=DSIN(ANDA*EPS1)
      F1(N)=W*SSH1(N)*SINA(N)/(2.0*ANDA*ANDA*ANDA*SSH4(N)*D)
      F0(N)=W*SSH2(N)*SINA(N)/(2.0*ANDA*ANDA*ANDA*SSH4(N)*D)
      G1(N)=ANDA*(B-ETA)*CCCTH1(N)-(1.0+PSI4(N)*CCCTH4(N))
      G0(N)=ANDA*(B+ETA)*CCCTH2(N)-(1.0+PSI4(N)*CCCTH4(N))
C     SET UP RIGHT HAND SIDE
C
C     FOR   THE  CASE  OF  TOTAL  DISPLACEMENT  FIELDS  FOR  TOP  PLAT
C
      DO 200 NN = 1,32
  200 BB(NN,1) =0.0
      BB(1,1)=ANDA*F0(N)*(P4*G0(N)-P5)
      BB(6,1)=F0(N)*(G0(N)+1.0)
      BB(25,1)=-ANDA*F1(N)*(P4*G1(N)-P5)
      BB(30,1)=-F1(N)*(1.0+G1(N))
C
      DO 300 NN=1,32
  300 RB(NN)=BB(NN,1)
      DO 400 M=1,33
      DO 500 MM=1,33
  500 AA(M,MM) = 0.0
  400 CONTINUE
C
C
      AA(1,1)=S41
      AA(1,2)=C41
      AA(1,3)=-(C51-S41*P11)
      AA(1,4)=-(S51-C41*P11)
      AA(1,5)=S42*COSC
      AA(1,6)=-C42*COSC
      AA(1,7)=(C52-S42*P12)*COSC
      AA(1,8)=-(S52-C42*P12)*COSC
      AA(1,21)=S2*SINC
      AA(1,22)=-C2*SINC
      AA(1,23)=-(P12*S2+P2*C2)*SINC
      AA(1,24)=(P12*C2+P2*S2)*SINC
      AA(2,5)=-S42*SINC
      AA(2,6)=C42*SINC
      AA(2,7)=-(C52-S42*P12)*SINC
      AA(2,8)=(S52-C42*P12)*SINC
      AA(2,17)=S1
```

```
AA(2,18)=C1
AA(2,19)=P11*S1+P2*C1
AA(2,20)=P11*C1+P2*S1
AA(2,21)=S2*COSC
AA(2,22)=-C2*COSC
AA(2,23)=-(P12*S2+P2*C2)*COSC
AA(2,24)=(P12*C2+P2*S2)*COSC
AA(3,5)=C2*SINC
AA(3,6)=-S2*SINC
AA(3,7)=-P12*C2*SINC
AA(3,8)=P12*S2*SINC
AA(3,17)=C1
AA(3,18)=S1
AA(3,19)=P11*C1+P1*S1
AA(3,20)=P11*S1+P1*C1
AA(3,21)= C2*COSC
AA(3,22)=-S2*COSC
AA(3,23)=-(P12*C2+P1*S2)*COSC
AA(3,24)=(P12*S2+P1*C2)*COSC
AA(4,1)=C1
AA(4,2)=S1
AA(4,3)=P11*C1
AA(4,4)=P11*S1
AA(4,5)=C2*COSC
AA(4,6)=-S2*COSC
AA(4,7)=-P12*C2*COSC
AA(4,8)=P12*S2*COSC
AA(4,21)=-C2*SINC
AA(4,22)= S2*SINC
AA(4,23)= (P12*C2+P1*S2)*SINC
AA(4,24)=-(P12*S2+P1*C2)*SINC
AA(5,17)=S1
AA(5,18)=C1
AA(5,19)=P11*S1
AA(5,20)=P11*C1
AA(5,21) = S2
AA(5,22)=-C2
AA(5,23)=-P12*S2
AA(5,24) = P12*C2
AA(6,1)=S1*ANDA
AA(6,2)=C1*ANDA
AA(6,3)=(C1+P11*S1)*ANDA
AA(6,4)=(S1+P11*C1)*ANDA
AA(6,5)=+S2*ANDA
AA(6,6)=-C2*ANDA
AA(6,7)=-(C2+P12*S2)*ANDA
AA(6,8)=+(S2+P12*C2)*ANDA
AA(7,1)=C1
AA(7,2)=S1
AA(7,3)=(P6*S1+P11*C1)
AA(7,4)=(P6*C1+P11*S1)
AA(7,5)=-C2
AA(7,6)=S2
AA(7,7)=(P6*S2+P12*C2)
AA(7,8)=-(P6*C2+P12*S2)
AA(8,17)=C1
```

```
AA(8,18)=S1
AA(8,19)=(P11*C1+P3*S1)
AA(8,20)=(P11*S1+P3*C1)
AA(8,21)=C2
AA(8,22) = -S2
AA(8,23) = -(P12*C2+P3*S2)
AA(8,24)=(P12*S2+P3*C2)
AA(9,5)= S42*COSC
AA(9,6)=C42*COSC
AA(9,7)=-(C52-S42*P12)*COSC
AA(9,8)=-(S52-C42*P12)*COSC
AA(9,9)=-S43
AA(9,10)=C43
AA(9,11) = -(C53-S43*P13)
AA(9,12)=(S53-C43*P13)
AA(9,21)= +S2*SINC
AA(9,22)= +C2*SINC
AA(9,23)= (P12*S2+P2*C2)*SINC
AA(9,24)= +(P12*C2+P2*S2)*SINC
AA(10,5)=S42*SINC
AA(10,6)=C42*SINC
AA(10,7)=-(C52-S42*P12)*SINC
AA(10,8)=-(S52-C42*P12)*SINC
AA(10,21) = -S2*COSC
AA(10,22)=-C2*COSC
AA(10,23)=-(P12*S2+P2*C2)*COSC
AA(10,24)= -(P12*C2+P2*S2)*COSC
AA(10,25)=S3
AA(10,26)=-C3
AA(10,27)=-(P13*S3+P2*C3)
AA(10,28)=P13*C3+P2*S3
AA(11,5)=-C2*SINC
AA(11,6)=-S2*SINC
AA(11,7)=-P12*C2*SINC
AA(11,8)=-P12*S2*SINC
AA(11,21)=-C2*COSC
AA(11,22)=-S2*COSC
AA(11,23)=-(P12*C2+P1*S2)*COSC
AA(11,24)=-(P12*S2+P1*C2)*COSC
AA(11,25)=C3
AA(11,26)=-S3
AA(11,27)=-(P13*C3+P1*S3)
AA(11,28)=P13*S3+P1*C3
AA(12,5)=-C2*COSC
AA(12,6)=-S2*COSC
AA(12,7)=-P12*C2*COSC
AA(12,8)=-P12*S2*COSC
AA(12,9)=C3
AA(12,10)=-S3
AA(12,11)=-P13*C3
AA(12,12)=P13*S3
AA(12,21)= C2*SINC
AA(12,22)= S2*SINC
AA(12,23)= (P12*C2+P1*S2)*SINC
AA(12,24)= (P12*S2+P1*C2)*SINC
AA(13,21) = +S2
```

```
AA(13,22)=C2
AA(13,23)=P12*S2
AA(13,24) = P12*C2
AA(13,25) = S3
AA(13,26)=-C3
AA(13,27)=-P13*S3
AA(13,28) = P13*C3
AA(14,5)= S2*ANDA
AA(14,6)= C2*ANDA
AA(14,7)=(C2+P12*S2)*ANDA
AA(14,10)=-C3*ANDA
AA(14,11)=-(C3+P13*S3)*ANDA
AA(14,12)=+(S3+P13*C3)*ANDA
AA(15,5)=C2
AA(15,6)= S2
AA(15,7)= (P6*S2+P12*C2)
AA(15,8)=(P6*C2+P12*S2)
AA(15,9) = -C3
AA(15,10)= S3
AA(15,11)=(P6*S3+P13*C3)
AA(15,12)=-(P6*C3+P13*S3)
AA(16,21)=C2
AA(16,22) = S2
AA(16,23) = (P12*C2+P3*S2)
AA(16,24)=(P12*S2+P3*C2)
AA(16,25)=C3
AA(16,26) = -S3
AA(16,27) = -(P13*C3+P3*S3)
AA(16,28)=P13*S3+P3*C3
AA(17,9)= S43
AA(17,10)=C43
AA(17,11)=-(C53-S43*P13)
AA(17,12)=-(S53-C43*P13)
AA(17,13)=-S42*COSC
AA(17,14)=C42*COSC
AA(17,15)=-(C52-S42*P12)*COSC
AA(17,16)= (S52-C42*P12)*COSC
AA(17,29)= S2*SINC
AA(17,30)=-C2*SINC
AA(17,31)=-(S2*P12+P2*C2)*SINC
AA(17,32)= (C2*P12+P2*S2)*SINC
AA(18,13)= S42*SINC
AA(18,14)=-C42*SINC
AA(18,15)=(C52-S42*P12)*SINC
AA(18,16)=-(S52-C42*P12)*SINC
AA(18,25)=-S3
AA(18,26)=-C3
AA(18,27)=-(P13*S3+P2*C3)
AA(18,28)=-(P13*C3+P2*S3)
AA(18,29)= S2*COSC
AA(18,30)=-C2*COSC
AA(18,31)=-(P12*S2+P2*C2)*COSC
AA(18,32)= (P12*C2+P2*S2)*COSC
AA(19,29)= C2*COSC
AA(19,30)=-S2*COSC
AA(19,31)=-(P12*C2+P1*S2)*COSC
```

```
AA(19,32)= (P12*S2+P1*C2)*COSC
AA(19,13)=-C2*SINC
AA(19,14)= S2*SINC
AA(19,15)= P12*C2*SINC
AA(19,16)=-P12*S2*SINC
AA(19,25)=-C3
AA(19,26)=-S3
AA(19,27)=-(P13*C3+P1*S3)
AA(19,28)=-(P13*S3+P1*C3)
AA(20,9)=C3
AA(20,10)= S3
AA(20,11)= P13*C3
AA(20,12)=P13*S3
AA(20,13)=-C2*COSC
AA(20,14)= S2*COSC
AA(20,15)= P12*C2*COSC
AA(20,16)=-P12*S2*COSC
AA(20,29)=-C2*SINC
AA(20,30)= S2*SINC
AA(20,31)= (P12*C2+P1*S2)*SINC
AA(20,32)=-(P12*S2+P1*C2)*SINC
AA(21,25) = +S3
AA(21,26)=C3
AA(21,27)=P13*S3
AA(21,28) = P13*C3
AA(21,29) = S2
AA(21,30)=-C2
AA(21,31)=-P12*S2
AA(21,32) = P12*C2
AA(22,9)= S3*ANDA
AA(22,10)= C3*ANDA
AA(22,11)=(C3+P13*S3)*ANDA
AA(22,12)= (S3+P13*C3)*ANDA
AA(22,13)= +S2*ANDA
AA(22,14)= -C2*ANDA
AA(22,15)=-(C2+P12*S2)*ANDA
AA(22,16)= +(S2+P12*C2)*ANDA
AA(23,9)=C3
AA(23,10)=+S3
AA(23,11)= (P6*S3+P13*C3)
AA(23,12)=(P6*C3+P13*S3)
AA(23,13)=-C2
AA(23,14)= S2
AA(23,15)= (P6*S2+P12*C2)
AA(23,16)=-(P6*C2+P12*S2)
AA(24,25)=C3
AA(24,26) = S3
AA(24,27) = (P13*C3+P3*S3)
AA(24,28)=(P13*S3+P3*C3)
AA(24,29)=C2
AA(24,30) = -S2
AA(24,31) = -(P12*C2+P3*S2)
AA(24,32)=(P12*S2+P3*C2)
AA(25,1)=-S41
AA(25,2)=C41
AA(25,3)=-(C51-S41*P11)
```

```
AA(25,4)=(S51-C41*P11)
AA(25,13)=-S42*COSC
AA(25,14) = -C42*COSC
AA(25,15)= (C52-S42*P12)*COSC
AA(25,16)=+(S52-C42*P12)*COSC
AA(25,29)= S2*SINC
AA(25,30)= C2*SINC
AA(25,31)= (P12*S2+P2*C2)*SINC
AA(25,32)= (P12*C2+P2*S2)*SINC
AA(26,13)=S42*SINC
AA(26,14)= C42*SINC
AA(26,15)=-(C52-S42*P12)*SINC
AA(26,16)=-(S52-C42*P12)*SINC
AA(26,17)= S1
AA(26,18)=-C1
AA(26,19)=-(P11*S1+P2*C1)
AA(26,20)=+(P11*C1+P2*S1)
AA(26,29)= S2*COSC
AA(26,30)= C2*COSC
AA(26,31)= (P12*S2+P2*C2)*COSC
AA(26,32)= (P12*C2+P2*S2)*COSC
AA(28,13)= C2*COSC
AA(28,14)= S2*COSC
AA(28,15)= P12*C2*COSC
AA(28,16)= P12*S2*COSC
AA(28,29)= C2*SINC
AA(28,30)= S2*SINC
AA(28,31)= (P12*C2+P1*S2)*SINC
AA(28,32)= (P12*S2+P1*C2)*SINC
AA(27,13)= C2*SINC
AA(27,14)= S2*SINC
AA(27,15)= P12*C2*SINC
AA(27,16)= P12*S2*SINC
AA(27,29)=-C2*COSC
AA(27,30)=-S2*COSC
AA(27,31)=-(P12*C2+P1*S2)*COSC
AA(27,32)=-(P12*S2+P1*C2)*COSC
AA(27,17)=-C1
AA(27,18)= S1
AA(27,19)= (P11*C1+P1*S1)
AA(27,20)=-(P11*S1+P1*C1)
AA(28,1)=C1
AA(28,2)=-S1
AA(28,3)=-P11*C1
AA(28,4)=P11*S1
AA(29,17)=S1
AA(29,18)=-C1
AA(29,19)=-P11*S1
AA(29,20)=P11*C1
AA(29,29) = S2
AA(29,30)=C2
AA(29,31)=P12*S2
AA(29,32) = P12*C2
AA(30,1)=-S1*ANCA
AA(14,9)=+S3*ANCA
AA(
```

```
      AA(30,3)=(C1+P11*S1)*ANDA
      AA(30,4)=-(S1+P11*C1)*ANDA
      AA(30,13)=-S2*ANDA
      AA(30,14)=-C2*ANDA
      AA(30,15)=-(C2+P12*S2)*ANDA
      AA(30,16)=-(S2+P12*C2)*ANDA
      AA(31,1) = -C1
      AA(31,2) = S1
      AA(31,3) = (P6*S1+P11*C1)
      AA(31,4) = -(P6*C1+P11*S1)
      AA(31,13) = C2
      AA(31,14) = S2
      AA(31,15) = (P6*S2+P12*C2)
      AA(31,16) = (P6*C2+P12*S2)
      AA(32,17)=C1
      AA(32,18)=-S1
      AA(32,19)=-(P11*C1+P3*S1)
      AA(32,20)=(P11*S1+P3*C1)
      AA(32,29)=C2
      AA(32,30) = S2
      AA(32,31) = (P12*C2+P3*S2)
      AA(32,32)=(P12*S2+P3*C2)
C
      DO 2112 I=1,32
 2112 AA(I,33)=BB(I,1)
C
C     CALL SIMUL
      DETER=SIMUL(32,AA,X,EPS,INDIC,33)
C
C     PRINTING OF SOLUTIONS
      IF(INDIC.GE.0) GO TO 38
    7 WRITE(3,202)DETER
      WRITE(3,40)((AA(I,J),J=1,8),I=1,32)
      WRITE(3,40)((AA(I,J),J=9,16),I=1,32)
      WRITE(3,40)((AA(I,J),J=17,24),I=1,32)
      WRITE(3,40)((AA(I,J),J=25,32),I=1,32)
      GO TO 98
   38 WRITE(3,203) DETER,N1
      WRITE(3,208)(X(I),I=1,8)
      WRITE(3,208)(X(I),I=9,16)
      WRITE(3,208)(X(I),I = 17,24)
      WRITE(3,208)(X(I),I=25,32)
      WO12=F1(N)*(G1(N)*SH12(N)+PSI12(N)*CH12(N))*SINA(N)
      WO22=FO(N)*(GO(N)*SH11(N)+PSI11(N)*CH11(N))*SINA(N)
      W1=ANDA*(X(1)*CH1(N)+X(2)*SH1(N)+X(3)*PSI1(N)*CH1(N)+X(4)*PSI1(N)
     1SH1(N))*SINA(N)
      WT42=((ANDA*(X(1)*CH11(N)-X(2)*SH11(N)-X(3)*PSI11(N)*CH11(N)+X(4)
     1PSI11(N)*SH11(N)))+(F1(N)*(G1(N)*SH11(N)+PSI11(N)*CH11(N))))*SINA
     2(N)
      WT12=ANDA*(X(1)*CH11(N)+X(2)*SH11(N)+X(3)*PSI11(N)*CH11(N)+X(4)*
     1PSI11(N)*SH11(N))*SINA(N)
      WTO=((ANDA*X(1))+(F1(N)*(G1(N)*SH1(N)+PSI1(N)*CH1(N))))*SINA(N)
      W4=ANDA*(X(1)*CH1(N)-X(2)*SH1(N)-X(3)*PSI1(N)*CH1(N)+X(4)*PSI1(N)
     1SH1(N))*SINA(N)
      WS1=ANDA*(X(5)*CH2(N)+X(6)*SH2(N)+X(7)*PSI2(N)*CH2(N)+X(8)*PSI2(N
     1*SH2(N))*SINA(N)
```

```
      WS12=ANDA*(X(5)*CH22(N)+X(6)*SH22(N)+X(7)*PSI22(N)*CH22(N)+X(8)*
     1PSI22(N)*SH22(N))*SINA(N)
      WS0=ANDA*X(5)*SINA(N)
      WS22=ANDA*(X(5)*CH22(N)-X(6)*SH22(N)-X(7)*PSI22(N)*CH22(N)+X(8)*
     1PSI22(N)*SH22(N))*SINA(N)
      WS2=ANDA*(X(5)*CH2(N)-X(6)*SH2(N)-X(7)*PSI2(N)*CH2(N)+X(8)*PSI2(N
     1*SH2(N))*SINA(N)
      W2=ANDA*(X(9)*CH3(N)+X(10)*SH3(N)+X(11)*PSI3(N)*CH3(N)+X(12)*PSI3
     1N)*SH3(N))*SINA(N)
      WB22=ANDA*(X(9)*CH33(N)+X(10)*SH33(N)+X(11)*PSI33(N)*CH33(N)+X(12
     1*PSI33(N)*SH33(N))*SINA(N)
      WB0=ANDA*X(9)*SINA(N)
      WB32=ANDA*(X(9)*CH33(N)-X(10)*SH33(N)-X(11)*PSI33(N)*CH33(N)+X(12
     1*PSI33(N)*SH33(N))*SINA(N)
      W3=ANDA*(X(9)*CH3(N)-X(10)*SH3(N)-X(11)*PSI3(N)*CH3(N)+X(12)*PSI3
     1N)*SH3(N))*SINA(N)
      WS3=ANDA*(X(13)*CH2(N)+X(14)*SH2(N)+X(15)*PSI2(N)*CH2(N)+X(16)*PS
     12(N)*SH2(N))*SINA(N)
      WS32=ANDA*(X(13)*CH22(N)+X(14)*SH22(N)+X(15)*PSI22(N)*CH22(N)+X(1
     1)*PSI22(N)*SH22(N))*SINA(N)
      WS00=ANDA*X(13)*SINA(N)
      WS42=ANDA*(X(13)*CH22(N)-X(14)*SH22(N)-X(15)*PSI22(N)*CH22(N)+X(1
     1)*PSI22(N)*SH22(N))*SINA(N)
      WS4=ANDA*(X(13)*CH2(N)-X(14)*SH2(N)-X(15)*PSI2(N)*CH2(N)+X(16)*
     1PSI2(N)*SH2(N))*SINA(N)
      T10=0.5*B
      IF(ETA-T10)11,12,12
   11 WT12=WT12+W022
      GO TO 10
   12 WT12=WT12+W012
   10 CONTINUE
      TSEX1=ES*SINA(N)*P8*(-X(17)*SH1(N)-X(18)*CH1(N)+X(19)*(P7*CH1(N)-
     1PSI1(N)*SH1(N))+X(20)*(P7*SH1(N)-PSI1(N)*CH1(N)))/(1.0+POIS)
      TSEX12=ES*SINA(N)*P8*(-X(17)*SH11(N)-X(18)*CH11(N)+X(19)*(P7*CH11
     1(N)-PSI11(N)*SH11(N))+X(20)*(P7*SH11(N)-PSI11(N)*CH11(N)))/(1.0+
     2POIS)
      TSEX0=-ES*SINA(N)*P8*X(18)/(1.0+POIS)
      TSEX42=ES*SINA(N)*P8*(X(17)*SH11(N)-X(18)*CH11(N)+X(19)*(P7*CH11(
     1)-PSI11(N)*SH11(N))-X(20)*(P7*SH11(N)-PSI11(N)*CH11(N)))/(1.0+POI
     2)
      TSEX4=ES*SINA(N)*P8*(X(17)*SH1(N)-X(18)*CH1(N)+X(19)*(P7*CH1(N)-
     1PSI1(N)*SH1(N))-X(20)*(P7*SH1(N)-PSI1(N)*CH1(N)))/(1.0+POIS)
      SSEX1=ES*SINA(N)*P8*(-X(21)*SH2(N)-X(22)*CH2(N)+X(23)*(P7*CH2(N)-
     1PSI2(N)*SH2(N))+X(24)*(P7*SH2(N)-PSI2(N)*CH2(N)))/(1.0+POIS)
      SSEX12=ES*SINA(N)*P8*(-X(21)*SH22(N)-X(22)*CH22(N)+X(23)*(P7*CH22
     1(N)-PSI22(N)*SH22(N))+X(24)*(P7*SH22(N)-PSI22(N)*CH22(N)))/(1.0+
     2POIS)
      SSEX0=-ES*SINA(N)*P8*X(22)/(1.0+POIS)
      SSEX22=ES*SINA(N)*P8*(X(21)*SH22(N)-X(22)*CH22(N)+X(23)*(P7*CH22
     1(N)-PSI22(N)*SH22(N))-X(24)*(P7*SH22(N)-PSI22(N)*CH22(N)))/(1.0+
     2POIS)
      SSEX2=ES*SINA(N)*P8*(X(21)*SH2(N)-X(22)*CH2(N)+X(23)*(P7*CH2(N)-
     1PSI2(N)*SH2(N))-X(24)*(P7*SH2(N)-PSI2(N)*CH2(N)))/(1.0+POIS)
      BSEX2=ES*SINA(N)*P8*(-X(25)*SH3(N)-X(26)*CH3(N)+X(27)*(P7*CH3(N)-
     1PSI3(N)*SH3(N))+X(28)*(P7*SH3(N)-PSI3(N)*CH3(N)))/(1.0+POIS)
      BSEX22=ES*SINA(N)*P8*(-X(25)*SH33(N)-X(26)*CH33(N)+X(27)*(P7*CH33
```

```
1(N)-PSI33(N)*SH33(N))+X(28)*(P7*SH33(N)-PSI33(N)*CH33(N)))/(1.0+
2POIS)
 BSEX0=-ES*SINA(N)*P8*X(26)/(1.0+POIS)
 BSEX32=ES*SINA(N)*P8*(X(25)*SH33(N)-X(26)*CH33(N)+X(27)*(P7*CH33
1(N)-PSI33(N)*SH33(N))-X(28)*(P7*SH33(N)-PSI33(N)*CH33(N)))/(1.0+
2POIS)
 BSEX3=ES*SINA(N)*P8*(X(25)*SH3(N)-X(26)*CH3(N)+X(27)*(P7*CH3(N)-
1PSI3(N)*SH3(N))-X(28)*(P7*SH3(N)-PSI3(N)*CH3(N)))/(1.0+POIS)
 SSEX3=ES*SINA(N)*P8*(-X(29)*SH2(N)-X(30)*CH2(N)+X(31)*(P7*CH2(N)-
1PSI2(N)*SH2(N))+X(32)*(P7*SH2(N)-PSI2(N)*CH2(N)))/(1.0+POIS)
 SSEX32=ES*SINA(N)*P8*(-X(29)*SH22(N)-X(30)*CH22(N)+X(31)*(P7*CH2
1(N)-PSI22(N)*SH22(N))+X(32)*(P7*SH22(N)-PSI22(N)*CH22(N)))/(1.0+
2POIS)
 SSEX00=-ES*SINA(N)*P8*X(30)/(1.0+POIS)
 SSEX42=ES*SINA(N)*P8*(X(29)*SH22(N)-X(30)*CH22(N)+X(31)*(P7*CH22
1(N)-PSI22(N)*SH22(N))-X(32)*(P7*SH22(N)-PSI22(N)*CH22(N)))/(1.0+
2POIS)
 SSEX4=ES*SINA(N)*P8*(X(29)*SH2(N)-X(30)*CH2(N)+X(31)*(P7*CH2(N)-
1PSI2(N)*SH2(N))-X(32)*(P7*SH2(N)-PSI2(N)*CH2(N)))/(1.0+POIS)
 TSEY1=ES*SINA(N)*P8*(X(17)*SH1(N)+X(18)*CH1(N)+X(19)*(P11*SH1(N)+
1P2*CH1(N))+X(20)*(P11*C1+P2*S1))/(1.0+POIS)
 TSEY12=ES*SINA(N)*P8*(X(17)*S11+X(18)*C11+X(19)*(P111*S11+P2*C11
1+X(20)*(P111*C11+P2*S11))/(1.0+POIS)
 TSEY0=ES*SINA(N)*P8*(X(18)          +X(19)*P2)/(1.0+POIS)
 TSEY42=ES*SINA(N)*P8*(-X(17)*S11+X(18)*C11+X(19)*(P111*S11+P2*C1
1-X(20)*(P111*C11+P2*S11))/(1.0+POIS)
 TSEY4=ES*SINA(N)*P8*(-X(17)*S1+X(18)*C1+X(19)*(P11*S1+P2*C1)-X(2
1*(P11*C1+P2*S1))/(1.0+POIS)
 SSEY1=ES*SINA(N)*P8*(X(21)*S2+X(22)*C2+X(23)*(P12*S2+P2*C2)+X(24
1(P12*C2+P2*S2))/(1.0+POIS)
 SSEY12=ES*SINA(N)*P8*(X(21)*S22+X(22)*C22+X(23)*(P122*S22+P2*C22
1X(24)*(P122*C22+P2*S22))/(1.0+POIS)
 SSEY0=ES*SINA(N)*P8*(X(22)+X(23)*P2)/(1.0+POIS)
 SSEY22=ES*SINA(N)*P8*(-X(21)*S22+X(22)*C22+X(23)*(P122*S22+P2*C22
1-X(24)*(P122*C22+P2*S22))/(1.0+POIS)
 SSEY2=ES*SINA(N)*P8*(-X(21)*S2+X(22)*C2+X(23)*(P12*S2+P2*C2)-X(24
1*(P12*C2+P2*S2))/(1.0+POIS)
 BSEY2=ES*SINA(N)*P8*(X(25)*S3+X(26)*C3+X(27)*(P13*S3+P2*C3)+X(28
1*(P13*C3+P2*S3))/(1.0+POIS)
 BSEY22=ES*SINA(N)*P8*(X(25)*S33+X(26)*C33+X(27)*(P133*S33+P2*C33
1+X(28)*(P133*C33+P2*S33))/(1.0+POIS)
 BSEY0=ES*SINA(N)*P8*(X(26)+X(27)*P2)/(1.0+POIS)
 BSEY32=ES*SINA(N)*P8*(-X(25)*S33+X(26)*C33+X(27)*(P133*S33+P2*C33
1-X(28)*(P133*C33+P2*S33))/(1.0+POIS)
 BSEY3=ES*SINA(N)*P8*(-X(25)*S3+X(26)*C3+X(27)*(P13*S3+P2*C3)-X(28
1*(P13*C3+P2*S3))/(1.0+POIS)
 SSEY3=ES*SINA(N)*P8*(X(29)*S2+X(30)*C2+X(31)*(P12*S2+P2*C2)+X(32)
1*(P12*C2+P2*S2))/(1.0+POIS)
 SSEY32=ES*SINA(N)*P8*(X(29)*S22+X(30)*C22+X(31)*(P122*S22+P2*C22)
1+X(32)*(P122*C22+P2 *S22))/(1.0+POIS)
 SSEY00=ES*SINA(N)*P8*(X(30)+X(31)*P2)/(1.0+POIS)
 SSEY42=ES*SINA(N)*P8*(-X(29)*S22+X(30)*C22+X(31)*(P122*S22+P2*C22
1-X(32)*(P122*C22+P2*S22))/(1.0+POIS)
 SSEY4=ES*SINA(N)*P8*(-X(29)*S2+X(30)*C2+X(31)*(P12*S2+P2*C2)-X(32
1*(P12*C2+P2*S2))/(1.0+POIS)
 MYT1=P72*(X(1)*P74*CH1(N)+X(2)*P74*S1+X(3)*(2.0*S1+P74*P3)*C1)+
```

```
1X(4)*(2.0*C1+P74*P11*S1))*SINA(N)
 MYT12=P72*(X(1)*P74*C11+X(2)*P74*S11+X(3)*(2.0*S11+P74*P111*C11)-
1X(4)*(2.0*C11+P74*P111*S11))*SINA(N)-D*(2.0*P8*S11*FO(N)+P8*FO(N)
2(GO(N)*P74*S11+P111*P74*C11))*SINA(N)
 MYTO=P72*(X(1)*P74+X(4)*2.0)*SINA(N)-D*(2.0*P8*S1*FC(N)+P8*FO(N
1)*(GO(N)*P74*S1+P74*P11*C1))*SINA(N)
 MYT42=P72*(X(1)*P74*C11-X(2)*P74*S11-X(3)*(2.0*S11+P74*P111*C11)-
1X(4)*(2.0*C11+P74*P111*S11))*SINA(N)-D*(2.0*P8*S11*F1(N)+P8*F1(N)
2(G1(N)*P74*S11+P74*P111*C11))*SINA(N)
 MYT4=P72*(X(1)*P74*C1-X(2)*P74*S1-X(3)*(2.0*S1+P74*P11*C1)+X(4)*
1.0*C1+P74*P11*S1))*SINA(N)
 MYS1=P72*(X(5)*P74*C2-X(6)*P74*S2-X(7)*(2.0*S2+P74*P12*C2)+X(8)*
1.0*C2+P74*P12*S2))*SINA(N)
 MYS12=P72*(X(5)*P74*C22-X(6)*P74*S22-X(7)*(2.0*S22+P74*P122*C22)-
1X(8)*(2.0*C22+P74*P122*S22))*SINA(N)
 MYSO=P72*(X(5)*P74+X(8)*2.0)*SINA(N)
 MYS2 =P72*(X(5)*P74*C2+X(6)*P74*S2+X(7)*(2.0*S2+P74*P12*C2)+X(8)*
1(2.0*C2+P74*P12*S2))*SINA(N)
 MYS22=P72*(X(5)*P74*C22+X(6)*P74*S22+X(7)*(2.0*S22+P74*P122*C22)-
1X(8)*(2.0*C22+P74*P122*S22))*SINA(N)
 MYB2=P72*(X(9)*P74*C3-X(10)*P74*S3-X(11)*(2.0*S3+P74*P13*C3)+X(12
1*(2.0*C3+P74*P13*S3))*SINA(N)
 MYB22=P72*(X(9)*P74*C33-X(10)*P74*S33-X(11)*(2.0*S33+P74*P133*C33
1+X(12)*(2.0*C33+P74*P133*S33))*SINA(N)
 MYBO=P72*(X(9)*P74+X(12)*2.0)*SINA(N)
 MYB32=P72*(X(9)*P74*C33+X(10)*P74*S33+X(11)*(2.0*S33+P74*P133*C33
1+X(12)*(2.0*C33+P74*P133*S33))*SINA(N)
 MYB3=P72*(X(9)*P74*C3+X(10)*P74*S3+X(11)*(2.0*S3+P74*P13*C3)+X(12
1*(2.0*C3+P74*P13*S3))*SINA(N)
 MYS3=P72*(X(13)*P74*C2-X(14)*P74*S2-X(15)*(2.0*S2+P74*P12*C2)+X(
116)*(2.0*C2+P74*P12*S2))*SINA(N)
 MYS32=P72*(X(13)*P74*C22-X(14)*P74*S22-X(15)*(2.0*S22+P74*P122*C2
1)+X(16)*(2.0*C22+P74*P122*S22))*SINA(N)
 MYSOO=P72*(X(13)*P74+X(16)*2.0)*SINA(N)
 MYS42=P72*(X(13)*P74*C22+X(14)*P74*S22+X(15)*(2.0*S22+P74*P122*C2
1)+X(16)*(2.0*C22+P74*P122*S22))*SINA(N)
 MYS4=P72*(X(13)*P74*C2+X(14)*P74*S2+X(15)*(2.0*S2+P74*P12*C2)+X(1
1)*(2.0*C2+P74*P12*S2))*SINA(N)
 AVSXT=P70*(-X(18)*S1-X(19)*(P3*S1+P11*C1))
 AVSXB=P71*(-X(26)*S3-X(27)*(P3*S3+P13*C3))
 WK4=WK4+W4
 WK42=WK42+WT42
 WKO=WKO+WTO
 WK12=WK12+WT12
 WK1=WK1+W1
 WKS1=WKS1+WS1
 WKS12=WKS12+WS12
 WKSO=WKSO+WSO
 WKS22=WKS22+WS22
 WKS2=WKS2+WS2
 WKB22=WKB22+WB22
 WKBO=WKBO+WBO
 WKB32=WKB32+WB32
 WKS3=WKS3+WS3
 WKS32=WKS32+WS32
 WKSOO=WKSOO+WSOO
```

```
WKS42=WKS42+WS42
WKS4=WKS4+WS4
TKX4=TKX4+TSEX4
TKX0=TKX0+TSEX0
TKX1=TKX1+TSEX1
TKX12=TKX12+TSEX12
WK2=WK2+W2
WK3=WK3+W3
TKX42=TKX42+TSEX42
SKX1=SKX1+SSEX1
SKX12=SKX12+SSEX12
SKX0=SKX0+SSEX0
SKX22=SKX22+SSEX22
SKX2=SKX2+SSEX2
BKX2=BKX2+BSEX2
BKX22=BKX22+BSEX22
BKX0=BKX0+BSEX0
BKX32=BKX32+BSEX32
BKX3=BKX3+BSEX3
SKX3=SKX3+SSEX3
SKX32=SKX32+SSEX32
SKX00=SKX00+SSEX00
SKX42=SKX42+SSEX42
SKX4=SKX4+SSEX4
TKY42=TKY42+TSEY42
TKY4=TKY4+TSEY4
TKY0=TKY0+TSEY0
TKY1=TKY1+TSEY1
TKY12=TKY12+TSEY12
SKY1=SKY1+SSEY1
SKY12=SKY12+SSEY12
SKY0=SKY0+SSEY0
SKY22=SKY22+SSEY22
SKY2=SKY2+SSEY2
BKY2=BKY2+BSEY2
BKY22=BKY22+BSEY22
BKY0=BKY0+BSEY0
BKY32=BKY32+BSEY32
BKY3=BKY3+BSEY3
SKY3=SKY3+SSEY3
SKY32=SKY32+SSEY32
SKY00=SKY00+SSEY00
SKY42=SKY42+SSEY42
SKY4=SKY4+SSEY4
MKYT1=MKYT1+MYT1
MKYT12=MKYT12+MYT12
MKYT0=MKYT0+MYT0
MKYT42=MKYT42+MYT42
MKYT4=MKYT4+MYT4
MKYS1=MKYS1+MYS1
MKYS12=MKYS12+MYS12
MKYS0=MKYS0+MYS0
MKYS22=MKYS22+MYS22
MKYS2=MKYS2+MYS2
MKYB2=MKYB2+MYB2
MKYB22=MKYB22+MYB22
```

```
      MKYBO=MKYBO+MYBO
      MKYB32=MKYB32+MYB32
      MKYB3=MKYB3+MYB3
      MKYS3=MKYS3+MYS3
      MKYS32=MKYS32+MYS32
      MKYSOO=MKYOO+MYSOO
      MKYS42=MKYS42+MYS42
      MKYS4=MKYS4+MYS4
      AVKSXB=AVKSXB+AVSXB
      AVKSXT=AVKSXT+AVSXT
      EFWT=AVKSXT/TKX1
      EFWB=AVKSXB/BKX2
   98 CONTINUE
C
      WRITE(3,511)WK4,WK42,WKO,WK12,WK1
      WRITE(3,512)WKS1,WKS12,WKSO,WKS22,WKS2
      WRITE (3,513) WK2,WKB22,WKBO,WKB32,WK3
      WRITE(3,514)WKS3,WKS32,WKSOO,WKS42,WKS4
      WRITE(3,611)TKX1,TKX12,TKXO,TKX42,TKX4
      WRITE(3,612)SKX1,SKX12,SKXO,SKX22,SKX2
      WRITE(3,613)BKX2,BKX22,BKXO,BKX32,BKX3
      WRITE(3,614)SKX3,SKX32,SKXOO,SKX42,SKX4
      WRITE(3,711)TKY1,TKY12,TKYO,TKY42,TKY4
      WRITE(3,712)SKY1,SKY12,SKYO,SKY22,SKY2
      WRITE(3,713)BKY2,BKY22,BKYO,BKY32,BKY3
      WRITE(3,714)SKY3,SKY32,SKYOO,SKY42,SKY4
      WRITE(3,211) MKYT1,MKYT12,MKYTO,MKYT42,MKYT4
      WRITE(3,212) MKYS1,MKYS12,MKYSO,MKYS22,MKYS2
      WRITE(3,213) MKYB2,MKYB22,MKYBO,MKYB32,MYB3
      WRITE(3,214) MKYS3,MKYS32,MKYSOO,MKYS42,MKYS4
C
  111 CONTINUE
  112 CONTINUE
C
 1144 FORMAT(/1X,2(4X,F12.5))
 1000 FORMAT(/3X,'ANGLE=',F12.5)
 4444 FORMAT(/1X,'AVKSXT=',F12.5,6X,'AVKSXB=',F12.5)
  511 FORMAT(/1X,'WK4  =',F12.5,2X,'WK42 =',F12.5,2X,'WKO  =',F12.5,2X
     1'WK12 =',F12.5,2X,'WK1  =',F12.5)
  512 FORMAT(/1X,'WKS1 =',F12.5,2X,'WKS12=',F12.5,2X,'WKSO =',F12.5,2X
     1'WKS22=',F12.5,2X,'WKS2 =',F12.5)
  513 FORMAT(/1X,'WK2  =',F12.5,2X,'WKB22=',F12.5,2X,'WKBO =',F12.5,2X
     1'WKB32=',F12.5,2X,'WK3  =',F12.5)
  514 FORMAT(/1X,'WKS3 =',F12.5,2X,'WKS32=',F12.5,2X,'WKSOO=',F12.5,2X
     1'WKS42=',F12.5,2X,'WKS4 =',F12.5)
  611 FORMAT(/1X,'TKX1 =',F16.5,2X,'TKX12=',F16.5,2X,'TKXO =',F16.5,2X
     1'TKX42=',F16.5,2X,'TKX4 =',F16.5)
  612 FORMAT(/1X,'SKX1 =',F16.5,2X,'SKX12=',F16.5,2X,'SKXO =',F16.5,2X
     1'SKX22=',F16.5,2X,'SKX2 =',F16.5)
  613 FORMAT(/1X,'BKX2 =',F16.5,2X,'BKX22=',F16.5,2X,'BKXO =',F16.5,2X
     1'BKX32=',F16.5,2X,'BKX3 =',F16.5)
  614 FORMAT(/1X,'SKX3 =',F16.5,2X,'SKX32=',F16.5,2X,'SKXOO=',F16.5,2X
     1'SKX42=',F16.5,2X,'SKX4 =',F16.5)
  211 FORMAT(/1X,'MKYT1=',F12.5,2X,'MKYT12=',F12.5,2X,'MKYTO=',F12.5,2
     1'MKYT42=',F12.5,2X,'MKYT4=',F12.5)
  212 FORMAT(/1X,'MKYS1=',F12.5,2X,'MKYS12=',F12.5,2X,'MKYSO=',F12.5,2
```

```
     1'MKYS22=',F12.5,2X,'MKYS2=',F12.5)
  213 FORMAT(/1X,'MKYB2=',F12.5,2X,'MKYB22=',F12.5,2X,'MKYBO=',F12.5,2
     1'MKYB32=',F12.5,2X,'MKYB3=',F12.5)
  214 FORMAT(/1X,'MKYS3=',F12.5,2X,'MKYS32=',F12.5,2X,'MKYSCO=',F12.5,
     12X,'MKYS42=',F12.5,2X,'MKYS4=',F12.5)
  711 FORMAT(/1X,'TKY1=',F16.5,2X,'TKY12=',F16.5,2X,'TKYO=',F16.5,2X,
     1'TKY42=',F16.5,2X,'TKY4=',F16.5)
  712 FORMAT(/1X,'SKY1=',F16.5,2X,'SKY12=',F16.5,2X,'SKYO=',F16.5,2X,
     1'SKY22=',F16.5,2X,'SKY2=',F16.5)
  713 FORMAT(/1X,'BKY2=',F16.5,2X,'BKY22=',F16.5,2X,'BKYO=',F16.5,2X,
     1'BKY32=',F16.5,2X,'BKY3=',F16.5)
  714 FORMAT(/1X,'SKY3=',F16.5,2X,'SKY32=',F16.5,2X,'SKYOO=',F16.5,2X,
     1'SKY42=',F16.5,2X,'SKY4=',F16.5)
   40 FORMAT(1H1,8(3X,F12.5))
  100 FORMAT(I2,I2,F14.9)
  202 FORMAT(F14.8)
  203 FORMAT(F14.8,3X,I2)
  208 FORMAT(1H,8(3X,F12.5))
  406 FORMAT(//2X,2(5X,F16.5))
      STOP
      END
/*
//  EXEC LNKEDT
//  EXEC
32 1    000005
/*
/&
```